THE IMPACT AND REBOUND OF A

SMALL DROP STRIKING

A HOT SURFACE

THE IMPACT AND REBOUND OF A

SMALL WATER DROP STRIKING A

HOT SURFACE

BY

DENIS MICHAEL HARVEY, B.Sc., M.Sc.

A Thesis

Submitted to the Faculty of Graduate Studies

in Partial Fulfilment of the Requirements

for the Degree

Doctor of Philosophy

McMaster University

March 1967

DOCTOR OF PHILOSOPHY(1967)   McMASTER UNIVERSITY
(Chemical Engineering)   Hamilton, Ontario.

TITLE: The Impact and Rebound of a Small Water Drop
    Striking a Hot Surface

AUTHOR: Denis Michael Harvey, B.Sc. (Honours) Queen's University

           M.Sc.   Queen's University

SUPERVISOR: Professor T.W. Hoffman

NUMBER OF PAGES: xii, 268

SCOPE AND CONTENTS:

   Water drops at their boiling point were projected
through a steam atmosphere to strike a surface which was
varied in temperature from 300 to 900 degrees Fahrenheit.
A high-speed motion picture study of the collision process
showed that, except at low surface temperatures, the drop
flattened out on impact and rebounded in a state of
oscillation. Measurements of the change in drop diameter
on collision indicated that the amount of evaporation due
to heat transfer from the surface was extremely small except
when the drop extensively wetted the surface. Solution of
a mathematical model of the initial impact dynamics and
models of heat transfer through a vapour film beneath the
drop and by direct liquid-surface contact confirmed
experimental observations.

Dedication

To the Experimentalist, for the
courageous optimism with which he
wages his struggle against the
perversity of natural phenomena.

Acknowledgement

INDEX

ILLUSTRATIONS   Page

INTRODUCTION

When a small liquid drop strikes a very hot surface it flattens out and bounces away again without wetting the surface. During this impact the drop is separated from the surface by a thin film of vapour which minimizes the transfer of heat from the surface to the drop. As the temperature is lowered, depending on the surface conditions and the impact velocity, the drop may break through this film and wet the surface. Then the amount of heat transfer is much greater.

This phenomenon is of importance in the analysis of the problem of cooling very hot surfaces, a problem arising in continuous casting and certain other metal working processes. It is also of interest in mist flow cooling in nuclear reactors where the possibility of burnout occurs. In an Atomized Suspension Technique (25) reactor and other spray systems it is of interest to know what occurs when spray drops strike the walls. The phenomenon is also of some importance in understanding basic boiling phenomena.

Drops of approximately 1/2 millimeter in size were projected with velocities of from 1 to 10 feet per second at surfaces ranging in temperature from 300 to 800 degrees Fahrenheit. The impact was photographed using a high-speed motion camera. The drops were caught on rebound in a pan

1

filled with silicone oil, allowing a size comparison before and after impact which in turn indicated the amount of heat transfer that occurred.

SUMMARY

The study of the impact of a small drop on a very hot surface is of importance in the analysis of the problem of cooling of very hot surfaces and is of some importance in understanding basic boiling phenomena.

At the commencement of this study, the only work that had been reported on this problem was the investigation by Savic (1,2) of the impact of large drops on a wetted surface, where the surface tension of the drop was not an important factor. An investigation by Wachters was reported in 1965 on the impact of 2 millimeter drops on a very hot surface.

In this study, water drops at their boiling point were projected at a surface which was varied in temperature from 300 to 900 degrees Fahrenheit. An original technique was developed to project these drops, of diameter from 300 to 700 microns, at velocities of from 1 to 10 feet per second.

A high-speed motion picture study of the impact showed that, except at low surface temperatures, the drop flattened out on impact and rebounded in a state of oscillation. The drops were caught on rebound in an oil-filled pan. A measure of the drop diameter before and after collision allowed an estimate of the amount of evaporation and therefore the amount of heat transfer. A mathematical model of the initial impact of the drop was proposed, solved, and compared with experimental results. Two models of heat transfer were

Review of the Work of Previous Investigators

Introduction

When a liquid at its boiling point is heated on a hot surface, bubbles of vapour will be generated at the surface and will rise to the top of the liquid. The formation of bubbles in the liquid itself requires that the liquid be "superheated" to a temperature considerably above its boiling point. It can be shown that the pressure inside a bubble due to surface tension forces is proportional to the inverse of its radius. Therefore, a high vapour pressure and consequently high degree of superheat is necessary for bubble formation. However, there usually exists on the surface a number of "ready-made" bubbles, typically small amounts of gas trapped in roughness depressions in the surface. Nucleation will occur preferentially at these sites because a lower degree of superheat is required. This nucleation at an interface is referred to as heterogeneous nucleation. Nucleation in the free liquid phase is referred to as homogeneous nucleation.

As the temperature of the surface is progressively increased, the rate of heat transfer continues to increase, as does the number of bubble generating sites. As the surface temperature continues to increase it is observed that the bubbling phenomenon passes from one of discrete bubbles to one more of vapour jets as successive bubbles

coalesce. At a certain temperature, called the critical heat-flux temperature, the rate of heat transfer begins to decrease with increasing temperature. This is caused by a layer of vapour which separates and insulates the liquid from the surface. This layer of vapour is at first quite unstable, covering only small patches of the surface. Formation of this vapour layer is periodic or oscillatory in nature, a phenomenon which has been shown to arise out of the instability of vapour-jet up-flows and liquid down-flows onto the surface (26). As the surface temperature is further increased progressively more of the surface is covered by the vapour film. The rate of heat transfer reaches a minimum at a surface temperature where essentially all the surface is covered by this film, with at best only transitory contact between the liquid and the surface. This temperature marks the beginning of film boiling which is characterized by a stable film with regular generation of vapour bubbles at the liquid-vapour interface. Beyond this point the rate of heat transfer increases with increasing surface temperature.

These three regions of surface temperature are called respectively the "nucleate", "transition" and "film" boiling regimes.

When a small drop at its boiling point collides with a surface at a temperature above its boiling point, the dynamics of the collision and the amount of vaporization of the drop that occurs will depend on whether or not the

drop wets or sticks to the surface. If the drop wets the surface an appreciable amount of heat will be conducted into the drop, possibly causing nucleate boiling. If the drop does not wet the surface, such as occurs when the surface temperatures is high, the amount of heat transfer is very small. The drop is then insulated from the surface by a layer of vapour underneath, and the collision of the drop with the surface is elastic, like the bounce of a rubber ball.

A.   Dynamics of Impact

        Consider a liquid drop at its boiling point colliding
with a hot surface in an atmosphere of its own vapour.
If it is spherical and is not vibrating on approach it
may be completely characterized by the definition of its
diameter and velocity, and its properties: surface tension,
viscosity, density and temperature. The dynamics of the
collision will be determined by the viscous, surface and
inertial forces which act during the collision. If the
relative magnitude of these forces is the same for two
collisions then the physical appearance of the collisions
will be the same, differing only in time scale.

        If the collision is not influenced by surface
tension or viscous forces between the drop and the surface
in collision, then the relative magnitude of the inertial
and viscous forces affecting the collision may be character-
ized by the drop Reynolds Number, $\frac{DV\rho}{\mu}$. Similarly the rela-
tive magnitude of the inertial and surface tension forces
may be characterized by the drop Weber Number, $\frac{\rho DV^2}{\sigma}$.

        When the drop does not wet the surface it spreads
out to form a disc shape. The disc shape then contracts,
thrusting a column of fluid up from its center, away from
the surface. The drop eventually leaves the surface as a
vertical elongated body. The liquid leaving the surface
first has a higher velocity than the later fluid so that
the column continues to elongate as it moves away from

the surface. The surface tension forces act to restore the spherical shape and in so doing set the drop into violent vibration or may cause the drop to break into several parts.

When the drop partially wets the surface the rebound is irregular. If the drop completely wets the surface it does not leave the surface except as spray formed by violent nucleate boiling.

The first attempt at a mathematical description of the process of impact was made by Savic and Boult (1). They assumed in their solution that the surface tension forces were virtually negligible and could be neglected. By assuming the top of the drop to be a section of a sphere they were able to solve the LaPlace Equation for potential flow of the drop liquid spreading on the surface. Generally, the larger the Weber Number the more accurate this solution will be.

Experimentally, they were able to photograph the impact of large drops with a surface using a high-speed camera. In all cases the drop completely wetted the surface. The agreement between the model and their results appeared reasonable.

According to their model the initial impact pressure under the drop is extremely large. This arises from the assumption that there is no vapour underneath the drop and that the drop liquid meets no resistance until it contacts the surface. In actual fact the drainage of vapour

out from underneath the drop will cause the drop to deform slightly before it reaches the surface.

In a later paper Savic (2) made some allowance for the effect of surface tension forces near the surface. The solution was not however adequate for low Weber Numbers where the influence of surface tension is very important. When drops do not wet the surface, the expansion of the surface under the drop requires a significant expenditure of energy, having a very significant effect on the dynamics. This influence of surface tension cannot be neglected.

In a more recent study, Wachters (6) photographed the impact of 2 millimeter diameter droplets dropped from a capillary tube onto a heated metal surface. The dynamics of the collision were studied using photography with a stroboscopic flash and with a single flash synchronized with the fall of the drop.

The deformation of the drop was found to be too complex for any form of mathematical description. The partial differential equations were formulated for potential flows of the drop during collision. Allowing the surface tension effect term to approach zero, it was predicted that on initial contact the velocity with which the liquid spreads on the surface would be very great. Since this was observed experimentally at high Weber Numbers, Wachters concluded that the model was reasonable and that therefore the effect of viscosity was of little

importance. It followed that the density, surface tension
and diameter were alone sufficient to characterize the
collision. This is expected to be an even better approxi-
mation at lower velocities because the ratio of the Weber
to the Reynolds Number, indicating the relative magnitude
of the viscous forces and surface forces, decreased with
decreasing velocity.

Wachters found that the residence time of the
drop on the surface was approximated by the period of
the basic mode of a vibrating drop as given by Rayleigh
(7) for small deformations. This was not a valid approach
as it assumed that the time of impact and rebound were
functions of the diameter, density and surface tension
of the drop alone, independent of the impact velocity.
In fact, Wachters found that for a given size of drop the
residence time on the surface decreased with increasing
impact velocity.

Wachters found that the column of fluid formed
when the drop leaves the surface breaks into a number of
smaller drops when the Weber Number exceeded 40. He
found that when the Weber Number exceeded 80, a droplet
would break up on impact. In this case the small droplets
formed continued to travel away from the center of impact.
It is probable that these breakup phenomena are not solely
characterized by the Weber Number. The Weber Number will,
on the basis of the principle of dynamic similarity,
determine the ratio of any dimension to the diameter of

12

the drop, but the time scale of breakup processes will be
a function of absolute dimensions. For instance, if one
considers the breakup of a laminar jet, the time scale
will be proportional to the diameter of the jet to the
2/3 power (21). Consequently breakup phenomena will not
be characterized by the Weber Number alone but should
be a function of the initial drop diameter as well.

B.   Heat Transfer from the Surface to the Drop

The first recorded scientific observations of a
drop resting on a surface in film boiling were made by
Leidenfrost (5). He noted that the drop did not wet the
surface and that the vapourization time was comparatively
long. This is now known as the Leidenfrost Phenomenon.

Wachters (6) measured the heat transfer to drops
at their saturation temperature using a calibrated
heat-flux meter. The change in size and the increase in
drop temperature on impact were measured for drops at
temperatures below their boiling point, but no measurements
of heat transfer were possible because of the relatively
large effect of convective evaporation on the size and
temperature of the drop as it travelled away from the
surface.

Experimentally, Wachters found that the amount
of heat transferred was sufficient to evaporate only
about 1/10 of one percent of the mass of the drop when
the surface temperature was above 500 degrees Fahrenheit.
With lower temperatures the amount of evaporation was
larger, apparently due to heat transfer by direct contact
between the drop and the surface.

A steady-state model for heat conduction and
vapourization underneath the drop was presented, assuming
the existence of a vapour film beneath the drop. It was
assumed that vapour inertia was negligible, that the under-

side of the drop was flat and that there was no interaction between heat conduction and vapour flow. This model could be solved if the force across the film and the area of the underside of the drop were known. This area was measured from experimental photographs and the force across the film was calculated from experimental measurements of the change of position of the center of gravity of the fluid body with time.

The surface underneath the drop was assumed to be at a constant temperature. An analysis wherein heat is conducted across a film of average calculated thickness for a time equal to the period of vibration of the drop indicated that the temperature drop in the surface was negligible in comparison to the total temperature differences, independent of the drop size. The calculated film thickness was found to be very small early and late in the collision process. This was caused by the fact that during the initial impact and the final pushing off from the surface the area of contact underneath the drop was small and the rate of change of momentum of the drop was large. The results of this analysis indicated an amount of evaporation less than that measured experimentally but approaching it at high surface temperatures. This deviation was explained as being caused by partial wetting of the surface by the drop.

This study was extended to spray cooling of a surface. An examination of the model indicated that the relative volume change of a drop due to evaporation on impact was proportional to the inverse of the drop radius to the 1/4

power, at the same temperature and Weber Number. The thickness

of the vapour film was calculated for a 60 micron drop to be

very small such that surface roughness could be quite signifi-

cant in its effect. The amount of heat transfer to the spray

drops was found to be much larger than predicted by the

model, particularly for oxide coated surfaces. This was

explained as being caused by wetting and by the inaccuracy

of the results.

The vapourization of a drop sitting on a hot surface

has been thoroughly investigated (3,4). Of particular

interest is the analysis of the problem of heat conduction

and vapour flow underneath the drop. Gottfried (3), like

Wachters, assumed that viscous forces alone were important in

determining the vapour flow. Gottfried's solution was nearly

the same as that of Wachters. It is, in this model, difficult

to reconcile the fact that a uniform film thickness gives

rise to a parabolic pressure distribution underneath the

drop whereas the hydrodynamic pressure at the bottom of

the drop is uniform. This assumption may, however, be made

more accurate by the influence of circulation inside the drop.

Baumeister, Hamill, Schwartz and Schoessow (4)

obtained a more exact solution in that they were able to

solve the problem without neglecting inertial effects on the

interaction between heat conduction and vapour flow. The

partial differential equations for heat transfer and flow

were transformed, using a similarity variable analysis, into a

set of ordinary nonlinear differential equations. These

were solved using an analog computor. A correlation between

two of the transformed variables allowed the combination of
the solutions of the separate equations for vapour flow and
for heat conduction, allowing the formulation of a single
equation giving the heat transfer coefficient as a function
of the radius of the underside of the drop and the force
across the vapour film. A uniform film thickness was
assumed. In this case, an analytical solution was not
possible unless heat transfer by radiation was neglected.
This was justifiable in that with a surface temperature of
600 degrees Fahrenheit the amount of heat transfer by
radiation was calculated to be less than 5 percent of the
total.

In a later study, Baumeister and Hamill (27) indicated
that the inertia of the vapour flowing underneath the drop
was negligible in its effect.

Sàvic (2) examined the problem of nucleate boiling
within cold drops during impact. The drops were in the
order of 1/10 inches in diameter.

Both Savic and Wachters assume that bubbles breaking
through the top of a cold drop are responsible for the
atomization which they observed to occur. Subcooled
nucleate boiling may produce intense ultrasonic vibrations
with the implosion of vapour bubbles. This could be responsible
for this phenomenon.

Of particular interest in the problem of heat
transfer to the drop is the possibility of contact between
the drop liquid and the surface. The work of Bankoff and

Mehra (8) and of Bradfield (9) indicates that liquid-solid contact may occur even when the surface temperature is well above the normal boiling point of the liquid. Bankoff and Mehra proposed that such contact was the principal means whereby heat was transferred from the surface to the liquid in the transition boiling regime. Bradfield photographed, from the side, drops sitting on a surface, and found that such contact occurs with water drops resting on a roughened surface as hot as 600 degrees Fahrenheit. A calculation of the interface temperature indicates that the liquid will be heated to nearly this temperature. It is generally recognized that a liquid may be heated to well above its normal boiling point in the absence of a nucleation site. The work of Hooper (10) indicates that a delay time of several milliseconds may be required for homogeneous (liquid phase) nucleation to occur. This may also be a factor in stabilizing such contact.

Bradfield indicated that this wetting was enhanced and stabilized by the addition of particles to the liquid or by roughening the surface, but no adequate explanation was provided.

The work of Burge (11) and Navick (12) on heat transfer from impinging liquid metal sprays indicates an amount of heat transfer so large such that it could only occur by direct contact between the sprayed liquid and the surface. No attempt was made to examine the phenomena of impact. With no boiling occurring, the phenomenon is quite differen

Mathematical Model of the Drop

Collision and Heat Transfer Process

An approximate model of the drop impact and heat

transfer process was formulated to determine the general

effect of various factors on the heat transfer process.

The model of the deformation and flow of liquid

at the surface was proposed on the basis of photographic

records of the actual phenomena at medium to high impact

velocities in cases where the drop does not appear to wet

the surface.

The equations arising from the model were analysed

on a digital computer, yielding an estimate of the variation

with time of the size of the bottom of the drop in contact

with the surface and the variation with time of the force

across the vapour film underneath the drop (Appendix L).

Using this information, assuming that the underside of the

drop was flat, it was possible to compute the approximate

amount of heat transfer during the impact process (Table III,

VI).

The model proposes that when the approaching drop

strikes the surface, the displaced liquid moves radially

away from the center of impact. The displaced liquid was

assumed to form a circular tablet of uniform thickness with

an edge of circular cross section. The colliding drop was

assumed to remain spherical above the top of the tablet

18

(Fig. 1, 2). Approximate energy and volume balances yielded
equations which described the shape of the tablet as a function
of time. A calculation of the rate of change of momentum
with time in the direction normal to the surface yielded an
estimate of the force across the vapour film.

FIG. Ia   MODEL OF DROP IMPACT

FIG.1b   MODEL OF DROP IMPACT

DROP BEFORE
IMPACT

ADVANCING

TIME

TABULAR BODY OF
LIQUID

D

HOT SURFACE

A

R

δ

FLOWING
VAPOUR FILM
OF UNIFORM
THICKNESS

HOT SURFACE OF UNIFORM TEMPERATURE
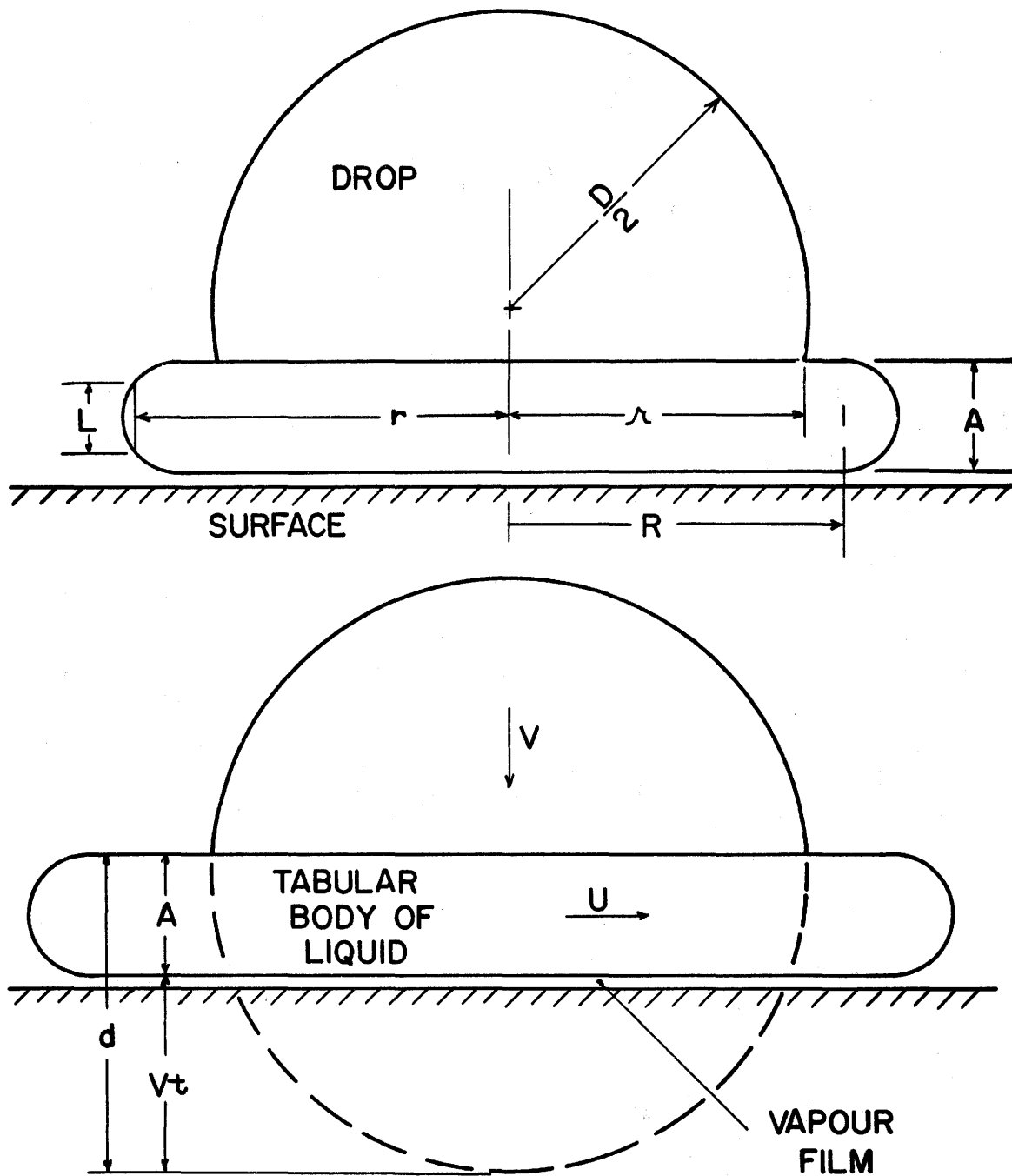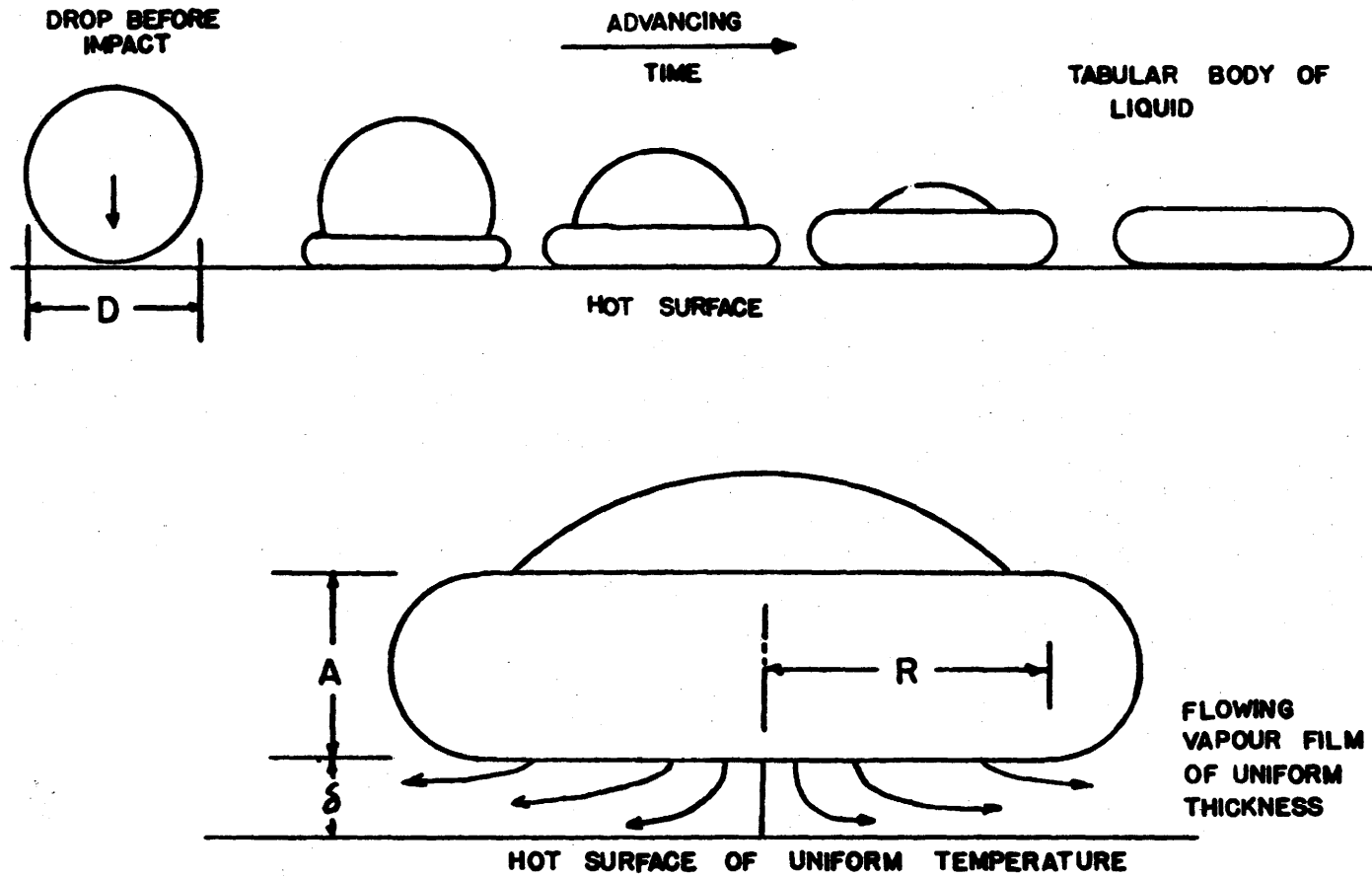
Figure 2

This photograph, taken with a high
speed camera, illustrates the impact and
rebound of a water droplet from a very
hot surface.

21

0.22 ms/frame
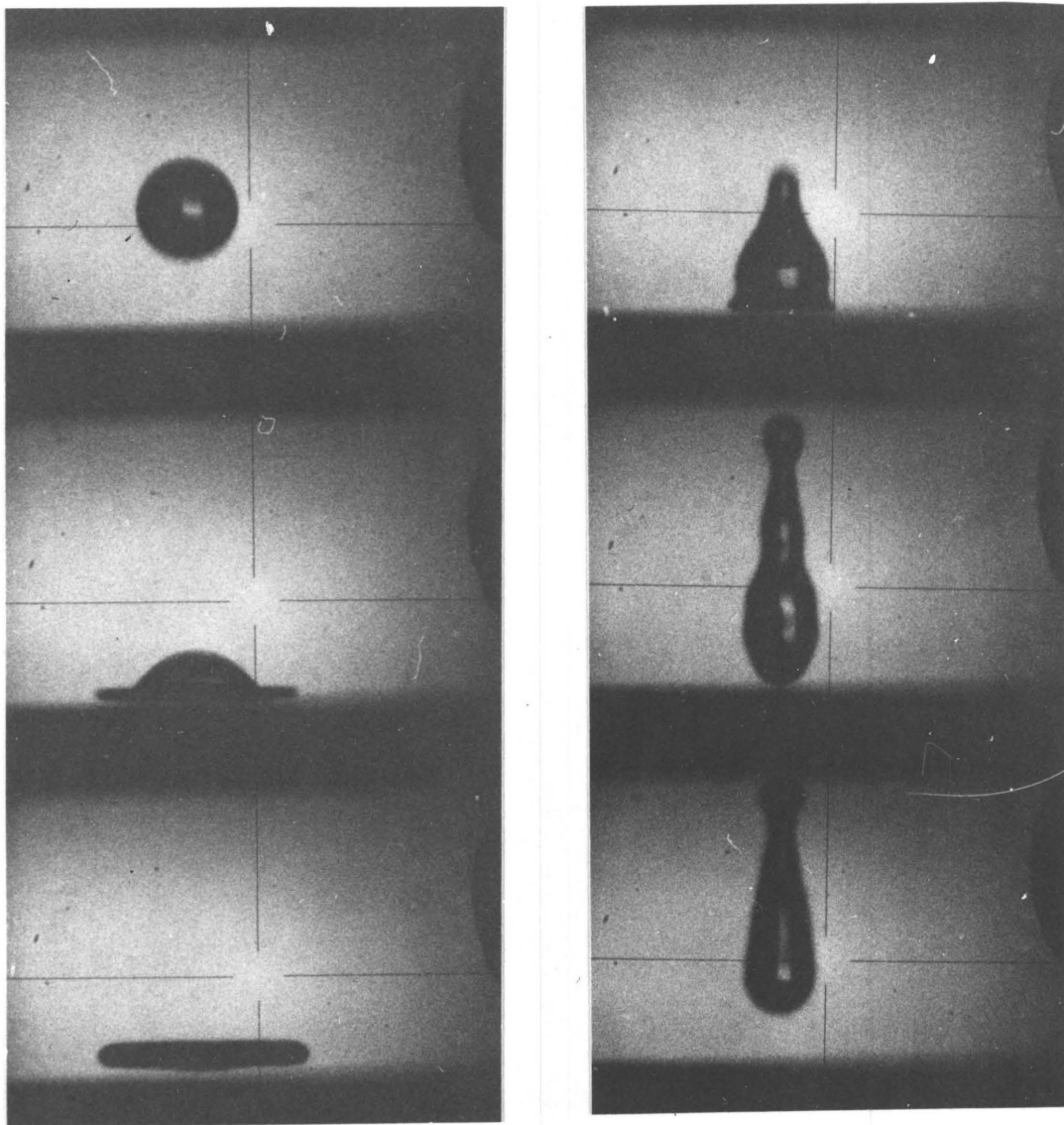
FIG.2   DIAMETER 400 MICRONS

VELOCITY 6 FEET PER SECOND

SURFACE TEMPERATURE 900 oF

Derivation of a Model Describing the Deformation and Flow of a Drop in Collision with a Nonwetted Surface

Major Assumptions

(1) Energy and volume are conserved with no viscous dissipation.

(2) Liquid properties are constant and equal to the values at the normal boiling point of the liquid.

(3) The drop remains spherical with uniform velocity above the top surface of the tabular body.

(4) The drop liquid becomes a uniform part of the tabular body immediately upon reaching the top surface of the tabular body.

Balance 1

The volume of the spherical segment of the drop having been absorbed in the tabular body is equal to the volume of the tabular body (Fig. 1)

Volume of Tabular Body

$$= \pi R^2 A + \int_{R}^{R + A/2} 2\pi r L \, dr$$

$$\left(\frac{A}{2}\right)^2 = \left(\frac{L}{2}\right)^2 + (r-R)^2$$

$$L = 2\left(\left(\frac{A}{2}\right)^2 - (r-R)^2\right)^{1/2}$$

$$4\pi \int_{R}^{R + A/2} r\left(\left(\frac{A}{2}\right)^2 - (r-R)^2\right)^{1/2} dr = \left(\frac{\pi A}{2}\right)^2 \left(R + \frac{2A}{3\pi}\right)$$

$$\text{Volume of Tabular Body} = \pi R^2 A + \left(\frac{\pi A}{2}\right)^2 \left(R + \frac{2A}{\pi 3}\right)$$

Volume of a Spherical Segment $= \frac{\pi}{3} d^2 \left(\frac{3D}{2} - d\right)$ where

d is the height of the spherical segment below the top surface

of the tabular body.

Let the drop velocity be V and let the drop contact the surface at time equal to zero.

$$d = Vt + A \qquad \text{(Fig. 1)}$$

Therefore

$$\frac{\pi}{3} (Vt + A)^2 \left(\frac{3D}{2} - Vt - A\right) = \pi R^2 A + \left(\frac{\pi A}{2}\right)^2 \left[R + \frac{2A}{3\pi}\right]$$

Solving for R;

$$R = \frac{-\pi A}{8} + \left(A^2\left(\frac{\pi^2}{64} - \frac{1}{6}\right) + \frac{1}{3A} (Vt + A)^2 \left(\frac{3D}{2} - Vt - A\right)\right)^{1/2}$$

$$\ldots \text{ equation 1}$$

Balance 2

The surface and kinetic energy of the spherical segment absorbed into the tabular body is equal to the surface and kinetic energy of the tabular body.

The Surface Energy of the Spherical Segment is equal to

$$\pi D d = \pi D (Vt + A) \gamma$$

The Kinetic Energy of the Spherical Segment is equal to

$$\left(\frac{\rho V^2}{2g_c}\right) \left(\frac{\pi}{3}\right) \times (Vt + A)^2 \left(\frac{3D}{2} - Vt - A\right)$$

The Area of the Base of the Spherical Segment is

$$\pi d (D-d) = \pi (Vt + A) (D - Vt - A)$$

The Surface Energy of the Tabular Body is

$$(2\pi R^2 + \pi^2 A R + \pi A^2 - \pi (Vt + A) (D - Vt - A)) \gamma$$

In calculating the kinetic energy of the tabular body, assume that the radial fluid velocity, U at any point in the tabular body does not vary in the axial direction. Assume also that the axial velocity of the fluid in the drop up to the top of the tabular form has a constant value V.

These assumptions are expedient in allowing an estimation of the magnitude of this kinetic energy. They may only be considered a rough approximation, allowing the calculation of the radial velocity profile in the tabular body. Knowing the radial velocity it is then possible to calculate the kinetic energy of the tabular body. Some of the initial energy of the drop is assumed to exist as radial kinetic energy during the collision process, finally appearing as surface energy in the tabular body. This acts to slow the spreading of the tabular body on the surface.

Consider a radial section of the tabular body, situated under the drop, of constant radius r ($r < \mathcal{R}$) during a time interval Δt (Fig. 1).

Volume in at the top of the section equals

$$\pi r^2 \left(V + \frac{dA}{dt} \right) \Delta t$$

Volume out at the side of the section equals

$$2\pi r \left(A + \frac{dA}{dt} \frac{\Delta t}{2} \right) \left(U + \frac{dU}{dt} \frac{\Delta t}{2} \right) \Delta t$$

where $\left(A + \frac{dA}{dt} \frac{\Delta t}{2} \right)$ and $\left(U + \frac{dU}{dt} \frac{\Delta t}{2} \right)$ are average values

of A and U during the time interval Δt.

The increase in volume of the section equals

$$\pi r^2 dA = \pi r^2 \frac{dA}{dt} \Delta t$$

The volume in at the top of the section equals the volume out at the side of the section plus the increase in volume during the interval.

Therefore

$$\pi r^2 \left(V + \frac{dA}{dt} \right) \Delta t = 2\pi r \left(A + \frac{dA}{dt} \frac{\Delta t}{2} \right) \left(U + \frac{dU}{dt} \frac{\Delta t}{2} \right) \Delta t$$

$$+ \pi r^2 \frac{dA}{dt} \Delta t$$

Dividing by $\pi r \Delta t$:

$$r\left(V + \frac{dA}{dt}\right) = 2\left(A + \frac{dA}{dt}\,\frac{\Delta t}{2}\right)\left(U + \frac{dU}{dt}\,\frac{\Delta t}{2}\right) + r\,\frac{dA}{dt}$$

$$\lim_{\Delta t \to 0} U = \frac{rV}{2A} \qquad (r \leq \lambda)$$

Consider a Toroidal Section outside the area of contact between the drop and the tabular body $(r > \lambda)$.

Volume in at the inside
of the section at $r = \lambda$
equals: $2\pi\lambda\left(A + \frac{dA}{dt}\,\frac{\Delta t}{2}\right) U_\lambda \Delta t$

Volume out at the outside
of the section at $r = R$
equals: $2\pi_R\left(A + \frac{dA}{dt}\,\frac{\Delta t}{2}\right) U_R \Delta t$

Increase in volume of the section equals:

$$\pi r^2 \frac{dA}{dt} \Delta t - \pi \lambda^2 \frac{dA}{dt} \Delta t$$

The volume in at the inside of the section equals the volume out at the outside of the section plus the increase in the volume of the section during the time interval Δt.

Therefore:

$$2\pi\lambda\left(A + \frac{dA}{dt}\,\frac{\Delta t}{2}\right) U_\lambda \Delta t = 2\pi r\left(A + \frac{dA}{dt}\,\frac{\Delta t}{2}\right) U_R \Delta t$$

$$+ \pi(r^2 - \lambda^2)\frac{dA}{dt}\Delta t$$

Dividing by $\pi \Delta t$ and taking the limit as $\Delta t \to 0$, one obtains:

$$2\pi A U_\lambda = 2rA U_R + (r^2 - \lambda^2)\frac{dA}{dt}$$

$$U_R = \frac{\lambda U_\lambda}{r} - \left(\frac{r^2 - \lambda^2}{2Ar}\right)\frac{dA}{dt}$$

$$U' = \frac{V\lambda}{2A}$$

Therefore:

$$U_R = \frac{\lambda^2 V}{2Ar} - \left[\frac{r^2 - \lambda^2}{2Ar}\right] \frac{dA}{dt}$$

$$= \frac{\lambda^2}{2Ar}\left[V + \frac{dA}{dt}\right] - \frac{r}{2A} \frac{dA}{dt} \qquad (r \geqslant \lambda)$$

let $\quad Q = \frac{dA}{dt} \qquad\qquad P = \lambda^2 (V + Q)$

Integrating to obtain kinetic energy

$0 \leqslant r \leqslant \lambda$

$$\int_0^\lambda \frac{dmV^2}{2} = \int_0^\lambda \pi \, rAdr\rho \frac{V^2 r^2}{4A^2} = \frac{\pi\rho\lambda^4 V^2}{16A}$$

Assume as a simplifying approximation that the curvature of the edge of the tabular body may be accounted for in the integral of the kinetic energy to an outer limit of $r = R + A/3$.

$$\int_\lambda^{R + A/3} \pi\rho rAdr\left[\frac{1}{4A^2}\right]\left[\frac{P}{r} - Qr\right]^2$$

$$= \frac{\pi\rho}{4A} \int_\lambda^{R + A/3} \left[\frac{P^2}{r} - 2PQr + Q^2 r^3\right] dr$$

$$= \frac{\pi\rho}{4A}\left[P^2 \ln \frac{R + A/3}{\lambda} - PQ\left[(R + A/3)^2 - \lambda^2\right] + \frac{Q^2}{4}\left[(R + A/3)^4 - \lambda^4\right]\right]$$

Therefore, the total kinetic energy of the liquid in the tablet is then approximately equal to : -

$$\frac{\pi\rho}{4A}\left[\frac{\lambda^4 V^2}{4} + P^2 \ln\left[\frac{R + A/3}{\lambda}\right] - PQ\left[(R + A/3)^2 - \lambda^2\right]\right.$$

$$\left. + \frac{Q^2}{4}\left[(R + A/3)^4 - \lambda^4\right]\right]$$

Total Energy Balance

Surface Energy of Spherical Segment + Kinetic Energy of Spherical Segment = Surface Energy of Tabular Body + Kinetic Energy of Tabular Body.

Therefore:

$$\pi D(Vt + A)\sigma + \frac{\pi \rho V^2}{6g_c} (Vt + A)^2 (1.5D - Vt - A)$$

$$= \pi\sigma (2R^2 + \pi AR + A^2 - (Vt + A)(D - Vt - A))$$

$$+ \frac{\pi \rho}{4A} \left[\frac{\lambda^4 V^2}{4} + P^2 \ln \left[\frac{R + A/3}{\lambda} \right] - PQ ((R + A/3)^2 - \lambda^2) \right.$$

$$\left. + \frac{Q^2}{4} ((R + A/3)^4 - \lambda^4)) \right] \quad \ldots\ldots \text{eq. (2)}$$

Where: $Q = dA/dt$

$P = \lambda^2(V + Q)$

$\lambda^2 = (Vt + A)(D - Vt - A)$

Calculation of the Force Across the Interface

The force across the film is equal to the rate of change of momentum of the drop. Assume that the liquid in the drop loses all of its vertical component of momentum as it reaches the top of the tabular form. The liquid in the tabular body of fluid is assumed to have no vertical component of momentum.

$$\text{Force} = \frac{dmv}{dt} = V\rho \frac{d(\text{Volume})}{dt}$$

$$F = \pi V\rho (Vt + A)(D - Vt - A) \left[V + \frac{dA}{dt} \right]$$

Calculation Procedure

The objective was to obtain values for the radius of the tabular body in contact with the surface and the force of impact as a function of time during the impact.

It was assumed that the spherical drop approached and moved against the surface at a constant velocity. The volume of the tabular body equaled the volume of the sphere assimilated by it (eq. 1). The surface and kinetic energy of the tabular body equaled the initial surface and kinetic energy of the assimilated portion of the drop (eq. 2). A simultaneous solution of the two equations was obtained at sequential intervals of time in order to obtain an estimate of the rate of change of the thickness of the tabular body (dA/dt). This was necessary for the solution of equation 2.

The force of impact was assumed equal to the rate of loss of momentum of the drop as it was assimilated into the tabular body.'

The calculation procedure was to solve equation (1) (p. 23) for R and to substitute for R in equation (2) (p. 27). A root finding routine was used to solve for A, and R was then calculated. Starting with time equal to a small time increment, a solution was obtained, time was increased by one increment, and the solution was repeated. The calculation was complete at the end of the impact period (disappearance

of the drop into the tabular body), at which point the total surface energy of the tabular body was equal to the initial total surface and kinetic energy of the drop.

Values of (dA/dt) were calculated as a linear approximation using the value of A calculated for the previous time increment. Difficulties with indeterminate terms were overcome by tests inserted to detect and alter such terms. A marching search routine was included to ensure that only the first positive root value of A was obtained.

The linear distances in the mathematical solution were divided by the drop diameter and the time was divided by (D - AMAX)/V, where AMAX was the final value of A. This made the solution solely a function of the Weber Number and generalized time.

The time increment was chosen such that a decrease by a factor of two produced no change in the fourth significant digit of any of the calculated variables.

The computor program for this calculation may be found in Appendix L. The completed solutions are presented for comparison with similarly dimensionalized experimental values in Fig. 3 to 8. Typical results calculated using this model may be found in Table III, p. 264.

Figures 3 to 8

These figures illustrate the
variation with time of the radius and
thickness of the tabular body of fluid
in contact with the surface. All variables
are expressed in dimensionless form.
Experimentally measured point values may
be compared directly with the curves
derived from the impact dynamics model.

FIG. 3

WEBER NUMBER 3.1

WEBER NUMBER 0.8

X— EXPERIMENTAL VALUES OF R/D

⊖— EXPERIMENTAL VALUES OF A/D

—— MODEL VALUES OF R/D, A/D

DIMENSIONLESS DISTANCE (S/D)

DIMENSIONLESS TIME (TV/(D−AEND))

30

FIG. 4   DIMENSIONLESS   TIME   (T/((D-AEND)/V))

31

FIG. 5   DIMENSIONLESS TIME   (TV/(D−AEND))

FIG. 6

WEBER NUMBER 16.0-17.2
MODEL WEBER NO. 16.6

DIMENSIONLESS DISTANCE (S/D)

DIMENSIONLESS TIME (TV/(D-AEND))

X — EXPERIMENTAL VALUES OF R/D

⊙— EXPERIMENTAL VALUES OF A/D

— MODEL VALUES OF R/D, A/D

FIG. 7   DIMENSIONLESS TIME   (TV/(D-AEND)

WEBER   NUMBER   19.3-20.4
MODEL WEBER   NO. 20.1

X – EXPERIMENTAL   VALUES   OF   R/D

⊙ – EXPERIMENTAL   VALUES   OF   A/D

— MODEL VALUES   OF   R/D, A/D

34

FIG. 8   DIMENSIONLESS   TIME   (TV/(D−AEND))

WEBER   NUMBER   24.5−38.1
MODEL   WEBER   NO. 25.9

X − EXPERIMENTAL   VALUES   OF   R/D

⊙ − EXPERIMENTAL   VALUES   OF   A/D

— − MODEL VALUES OF R/D, A/D

Heat Transfer to the Impacting Drop Assuming
a Vapor Film Under the Drop

Assuming that a vapor film of uniform thickness exists
under the drop, it is possible to calculate, using the
solution of Baumeister, Hamill, Schwartz and Schoessow (4),
the heat transferred from the surface to the drop.

The integral of the pressure in the vapor film with respect
to the area underneath the drop equals the force across the
vapor film. This force is calculated from a momentum balance
in the previous model.

$$P = \frac{\alpha^2}{2g_c} \rho_g (R^2 - r^2) \qquad (4)$$

$$\text{Therefore Force} = \int_0^R P 2\pi r \, dr = \pi \frac{\alpha^2}{g_c} \rho_g \, r \left[R^2 - r^2 \right] dr$$

$$= \frac{\pi \alpha^2 \rho_g R^4}{4 g_c}$$

Solving for α :

$$\alpha = \frac{2}{R^2 g_c} \left(\frac{F}{\pi \rho_g} \right)^{1/2}$$

Neglecting radiant heat transfer and assuming that

$$\phi = 0.0815 \, \zeta^3 \qquad \text{(Appendix F)}$$

It may be shown that the heat transfer coefficient for
heat transfer from the hot surface across the vapor film
to the bottom of the drop is given by (4):

$$h = \left(\frac{(0.163)(2)}{\pi} \right)^{1/4} \left(\frac{1}{R} \right) \left(\frac{\lambda (K \Lambda)^3 \rho_g \, F}{\Delta T \mu_g} \right)^{1/4} \quad \ldots \text{eq. (3)}$$

For heat transfer from the surface

$$\lambda (K \Lambda)^3 = K^3 (\lambda + 0.5 Cp \Delta T)$$

For heat transfer to the drop

$$\lambda (K \Lambda)^3 = K^3 (\lambda - Cp \Delta T)$$

The total amount of heat transferred to the drop is then

$$Q' = \int_0^t 2\pi R h \Delta T \, dt$$

The equivalent volume of liquid evaporated is then given by : -

$$\text{Volume} = \frac{Q}{\lambda \rho}$$

The equivalent percentage change in diameter for small amounts of evaporation can be calculated from

$$\% \, \Delta D/D \;=\; 100.0 \times \text{Volume}/\pi \, D^3.$$

The calculated values of $\% \, \Delta D/D$ may be found in Table VI.

Estimation of the Influence of Surface Drag on the Spreading of the Drop on the Surface

Assuming that a film of vapor separates the drop from the surface, the possibility of an effect of the vapor flow on the spreading of the drop may be considered as follows : -

Assume that the undersurface of the drop expands in a manner such that the surface moves outwards at a rate which is proportional to the distance from the center. Consider a small area $2\pi r\,dr$ a distance r from the center. This area has a force on it equal to $\tau_r\,2\pi r\,dr$ where τ_r is the surface shear stress due to vapor flow in the fluid. Assume that in time dt this small area will move away from the center a distance of $\frac{r}{R}\frac{dR}{dt}\,dt$, where $\frac{dR}{dt}$ is the rate of increase of R with time. The total work done by this shear stress during a time $\triangle t$ will be

$$\int_0^{\triangle t}\int_0^R \tau_r\,2\pi r\,dr\left(\frac{r}{R}\frac{dR}{dt}\right)\,dt$$

$$=\int_R^{R+\triangle R}\int_0^R \frac{2\pi r^2\tau_r}{R}\,dr\,dR$$

$$\tau_r = \mu\frac{du}{dy}\Big/_{s,r} = \frac{\mu r}{g_c}\left(\frac{\alpha^3}{\nu}\right)^{1/2}\phi''(\zeta)_{z=\delta}$$

$$\int_0^R \tau_r\,\frac{2\pi r^2\,dr}{R} = \frac{\pi\mu}{2g_c}\left(\frac{\alpha^3}{\nu}\right)^{1/2}R^3\phi''(\zeta)_{z=\delta}$$

$$\phi'' = 0.4871\,\zeta \qquad \text{(Appendix F)}$$

$$\zeta = \left(\frac{\alpha}{\nu}\right)^{1/2}\delta = \left(\frac{\alpha}{\nu}\right)^{1/2}\frac{K\Lambda}{h}$$

where h is as derived previously.

The energy contribution provided to the drop by this influence in time $\triangle t$ is then equal to

$$\triangle E = \frac{0.2435\pi\mu}{2}\left(\frac{\alpha^2}{\nu}\right)R^3\frac{K\Lambda}{h}\triangle R$$

$$\text{where } \alpha = \frac{2}{R^2}\left(\frac{g_c F}{\pi\rho}\right)^{1/2}$$

$$h = \left(\frac{(0.163)(2.0)g_c}{\pi}\right)^{1/4}\left(\frac{1}{R}\right)\left(\frac{\lambda(K\Lambda)^3\rho_s F}{\triangle T\mu_s}\right)^{1/4}$$

$$\Lambda = (1 - c_p \Delta T / \lambda)^{1/3}$$

This was included in the energy balance with negligible change in the results. It may be concluded therefore, that this force has no significant affect on the dynamics of drop impact and recession.

D.   <u>Calculation of Vapor Film Thickness</u>

Film thickness is given by

$$\delta = \frac{k \Lambda o}{h} \quad \ldots\ldots\text{(eq. 4)(4)}$$

where $\Lambda o = 1/(1 + Cp\Delta T/3\lambda)$

and h is the heat transfer coefficient for heat transfer from the surface.

Calculation of Maximum Pressure in the Vapour Film

The pressure in the vapour film is given by

$$P' = \frac{\alpha^2}{2} \frac{\rho}{g_c} \left[R^2 - r^2 \right]$$

where $\alpha = \dfrac{4\, g_c F}{R^4 \pi \rho}$

$$P' = \frac{2F}{\pi R^4} \left[R^2 - r^2 \right] \quad \ldots\text{(eq. 5)}$$

The maximum pressure occurs at $r = o$ when

$$P' = \frac{2F}{\pi R^2}$$

The model solutions indicate that for the 3-700 micron drops used the maximum pressure under the drop rarely exceeds two atmospheres. This may, however, not be the case during the initial impact period, when the model of the dynamic process is not valid.

Calculations with very small drops, in the order of 10 microns, indicate that the pressure under small drops may be very high. Results are presented in Table VII.

F.   Calculation of Heat Transfer with Direct
                    Liquid - Surface Contact

If the drop liquid comes into direct contact with the
surface, heat will be conducted directly from the metal into
the liquid. If the liquid is assumed to be motionless then
a calculation of the amount of heat transfer is possible
assuming that both the surface and the liquid are semi-infinite
media in contact.

On contact the interface assumes a temperature which is
time - independent (8).

$$T_s = (Tm - Tl)/(1.0 + (KL/KS)(\alpha_s/\alpha_L)^{1/2})$$

$$+ Tl$$

The total amount of heat transferred per unit area as a
function of time is then given by

$$Q = 2.0 \, KL(Ts - Tl)(t/\pi \alpha_L)^{1/2}$$

The percentage change in volume of the drop that may be
caused by this amount of heat transfer is given by : -

$$100 \, \Delta VOL/VOL = 600Q \, (area)/\pi \lambda_\rho D^3$$

The fractional change in diameter is given by : -

$$\frac{\Delta D}{D} = 1 - (1 - \frac{\Delta VOL}{VOL})^{1/3}$$

where area is the assumed area of contact.

The percentage change in diameter was calculated as a
function of time for an assumed radius of area in contact
equal to the diameter of the drop on approach (Appendix L).
The calculated results for a 300 micron drop are presented
in Figure (9). An approximate range of contact time was
0.0006 to 0.0010 seconds.

PERCENT CHANGE IN DIAMETER EQUIVALENT TO HEAT TRANSFERRED

FIG. 9 TIME OF CONTACT (SECONDS)

Ts= BULK SURFACE
TEMPERATURE
Ti - INTERFACE TEMPERATURE

Ts=338°F
Ti =322°F

Ts=428°F
Ti = 401°F

Ts=572°F
Ti =526°F

43
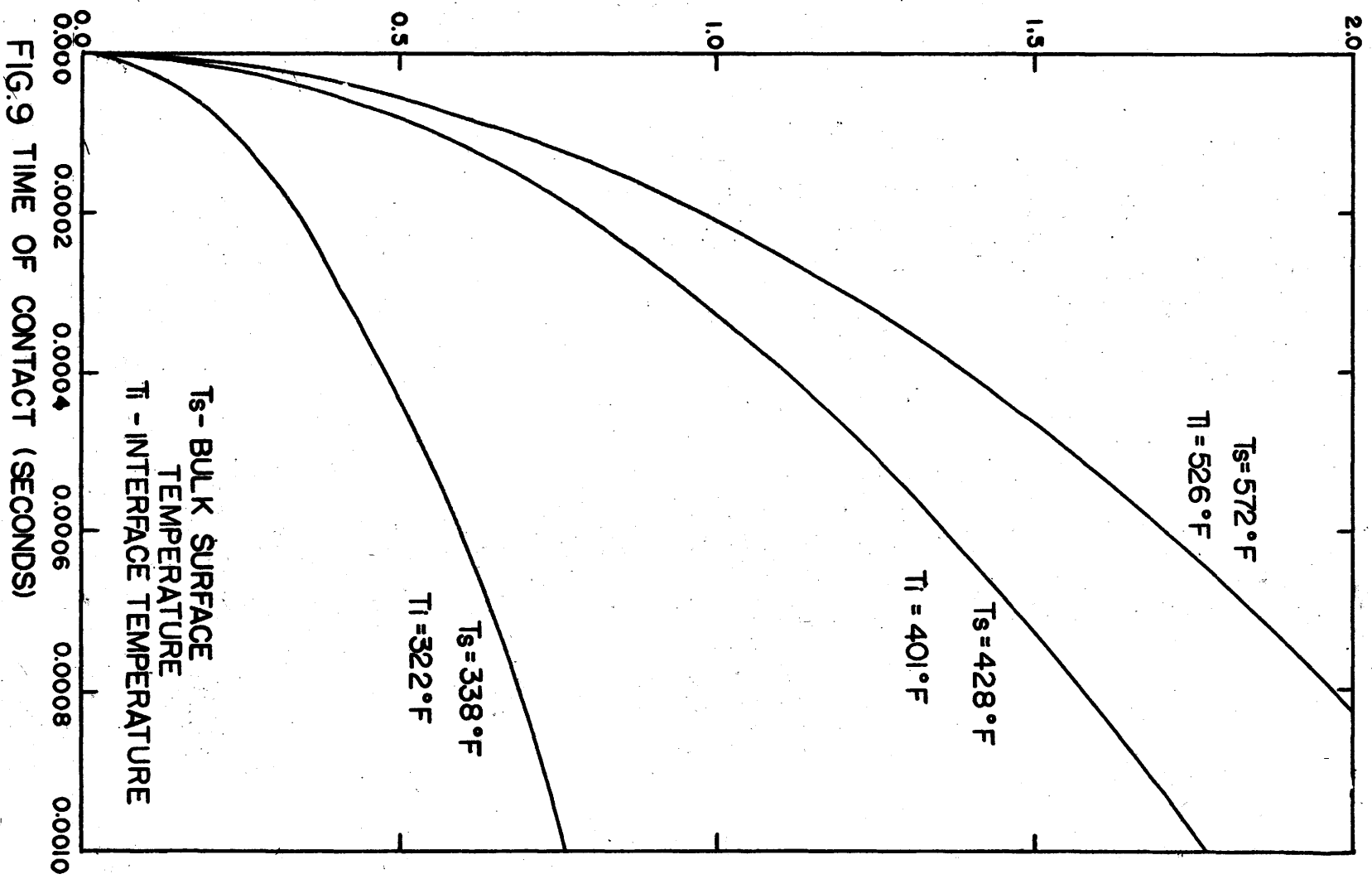
EXPERIMENTAL EQUIPMENT

The function of the experimental equipment was to produce the phenomena of the impact of a small drop with a hot surface, to yield a photographic record of this impact and to yield information which would allow the calculation of the amount of evaporation of the drop due to momentary contact with the surface.

The equipment was made up of five functional units: the drop projector, the target surface, the enclosure and supporting structure, the drop catcher and drop size measurement unit, and the drop impact photography unit. In addition, there were a number of supporting facilities such as electrical power supplies, controlled-temperature fluid-circulation units, and apparatus superstructure. The following section contains the information necessary to give the reader a basic understanding of the design and function of the experimental equipment. Further details may be found in Appendix B.

A great deal of experimental development was necessary before the final experimental equipment design was achieved. Details of this development are outlined in Appendix A.

THE DROP PROJECTOR

The drop projector was an assembly which formed a
drop, held it in film boiling in a spherical depression and
then projected the drop upwards to strike a fixed surface at
a predetermined location (Fig. 10, 11).

The bottom of the device consisted of stainless
steel piston which could move a short vertical distance in
its containing brass cylinder. A rod with a conical head
was fastened to the top of this piston. A spherical depression
was cut into the center of the flat upward-facing base of the
conical head. The entire head was heated to a high temperature
such that a small drop placed in the depression did not wet
the surface, but floated on a cushion of its own vapour.
The head was heated by an electric heater which contacted
the conical surface of the head when the piston was in the
lower position.

The drop was formed by condensation from the steam
atmosphere inside the apparatus onto a loop of glass capillary
tubing, cooled by cold water circulated through it. It was
dropped from the loop into the depression and was observed
sitting in the depression through a telescope with a scale
graticule. When it evaporated to the desired size, compressed
air was admitted through a solenoid valve into the cylinder.
The piston then moved quickly upward to the top of the
cylinder, sending the drop toward the target surface.

46

Pt-10%Rh INSERT

HEATER
WINDINGS

CERAMIC
INSULATION

TEFLON
COVER

SPRING
SUPPORTS

AIR ESCAPE HOLES

PISTON

ONE
INCH

AIR FROM
RESERVOIR
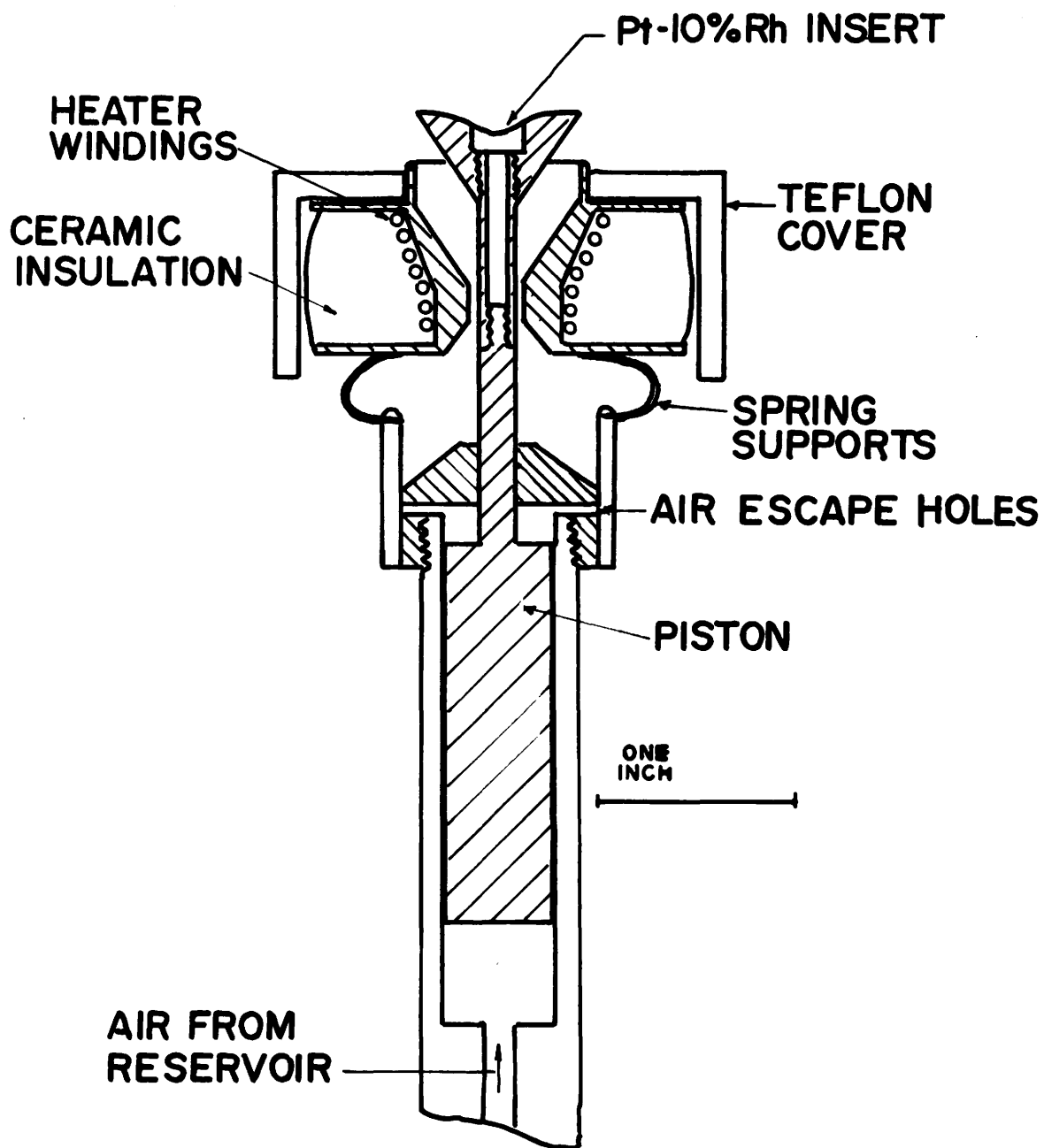
FIG. 10   DROP PROJECTOR
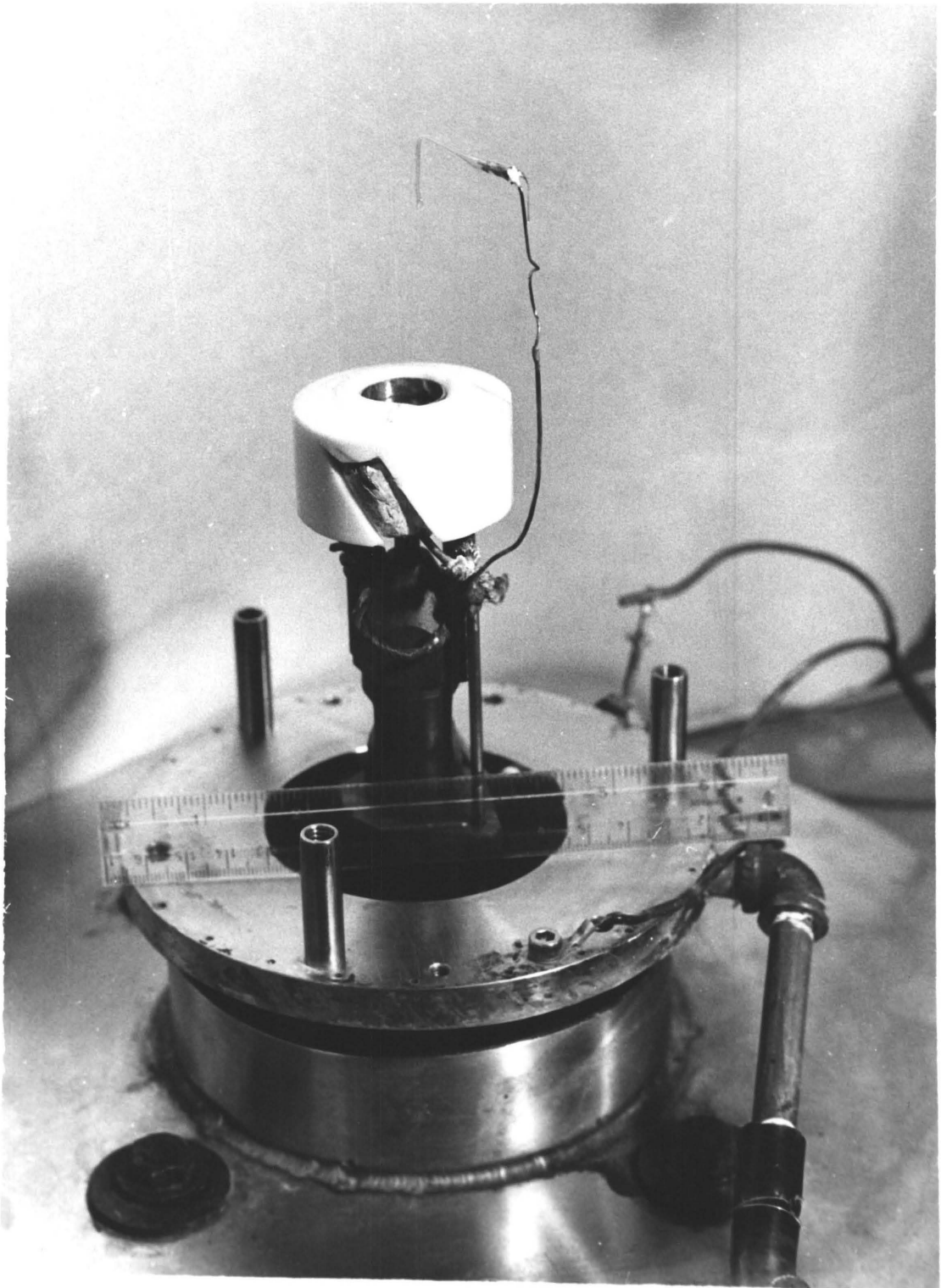
FIG.11   DROP   PROJECTOR

THE TARGET SURFACE ASSEMBLY

The surface with which the drop collided was situated at the end of a small vertical platinum-rhodium pellet (Fig.12, 13). The end of the pellet was cut at an angle of 8 1/2 degrees to the horizontal, to make the drop rebound back into the drop catching pan. It was polished to a mirror finish (0.3 micron abrasive) for some tests and roughened (No. 600 grit silicon carbide) for others. It was suspended from four vertical Nichrome wires welded to the top end, and was heated by means of an electric current flowing through these wires. The power supply used was a 12-volt 100-ampere variable unit. The surface temperature was measured by a platinum-rhodium thermocouple welded into the center of the pellet. The heater unit was enclosed in a Vycor tube which was held in place by a fitting in the roof of the apparatus.
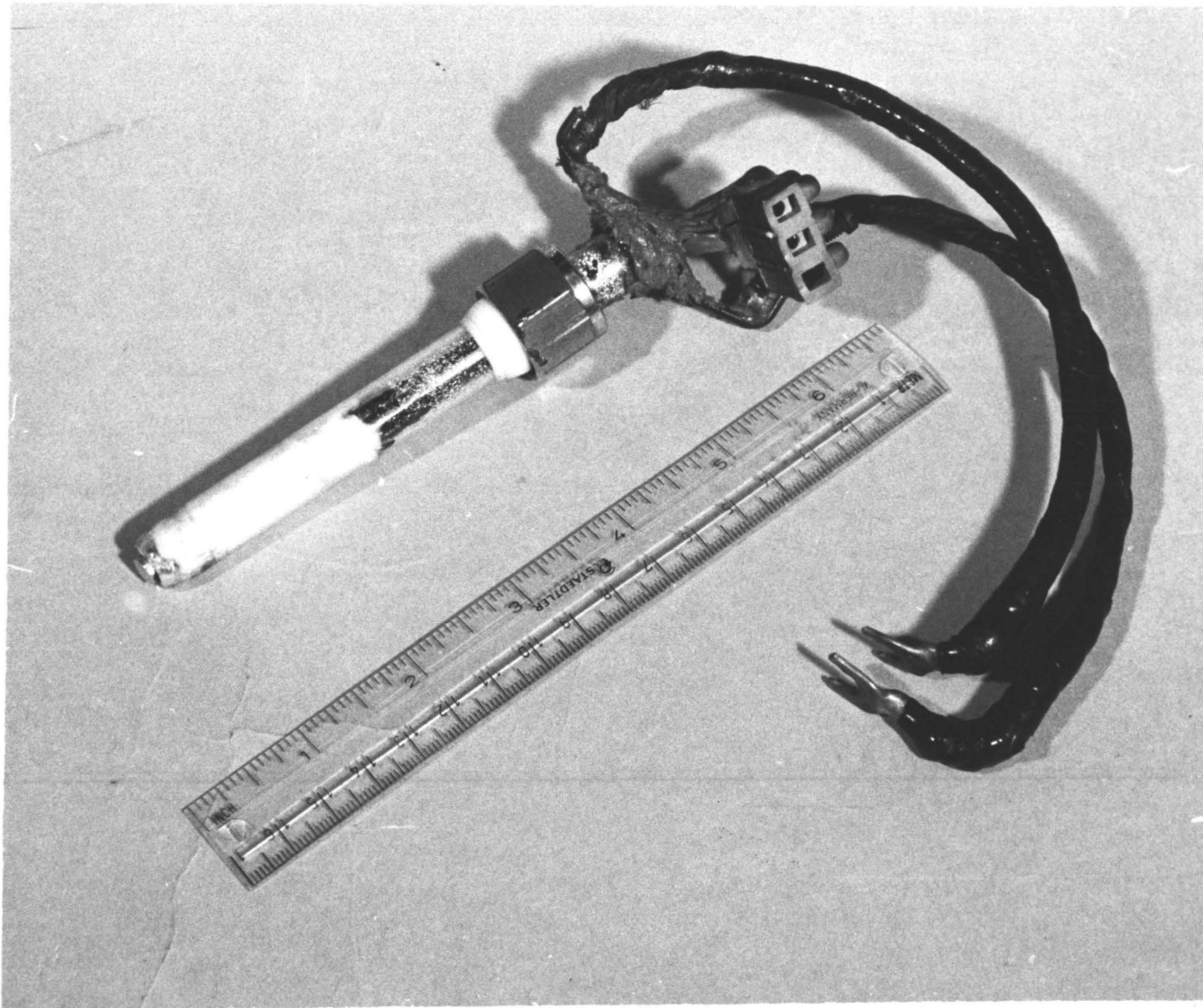
FIG.13   TARGET SURFACE ASSEMBLY

THE DROP CATCHER

The drop was caught on rebounding from the surface in a silicone-oil filled glass-bottomed pan (Fig.14,15). The glass was coated with a layer of silicone rubber to prevent the drop from wetting its surface. The pan was heated to 115 degrees centigrade before insertion into the apparatus in order to prevent water condensation in the oil from the steam atmosphere inside. After the drop was caught, the catcher was removed from the apparatus and a glass plate placed over the drop in the oil to prevent diffusional evaporation of the drop. The drop was then photographed with a magnification of 30X using a substage microscope.

TEFLON GASKET

OIL-FILLED GLASS-BOTTOM PAN

HEATER

GLASS SLIDING COVER

GLASS COVER FOR DROP IN OIL

HOLE FOR PASSAGE OF DROP

DOUBLE GLASS BOTTOM

1/2 SCALE
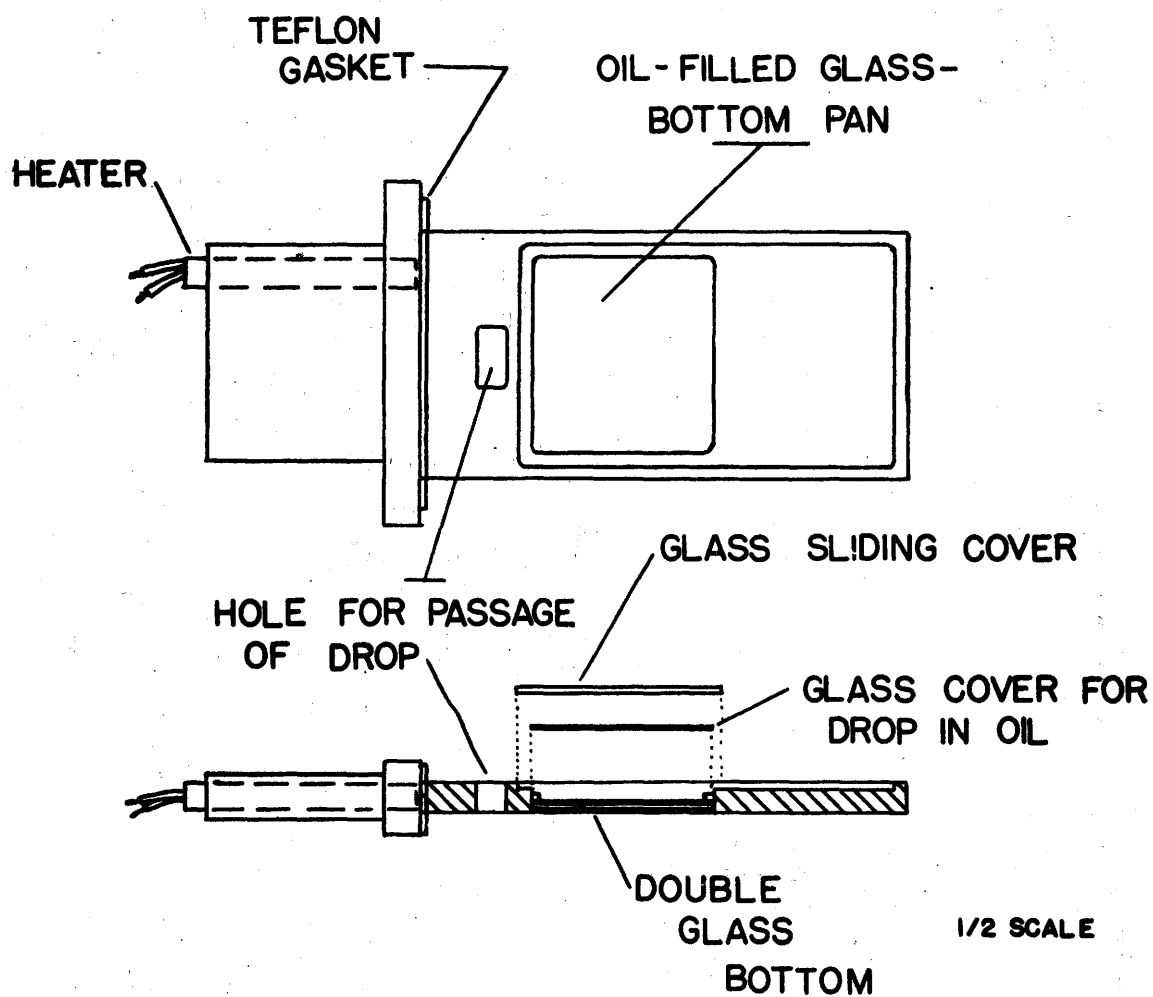
FIG. 14   DROP CATCHER ASSEMBLY
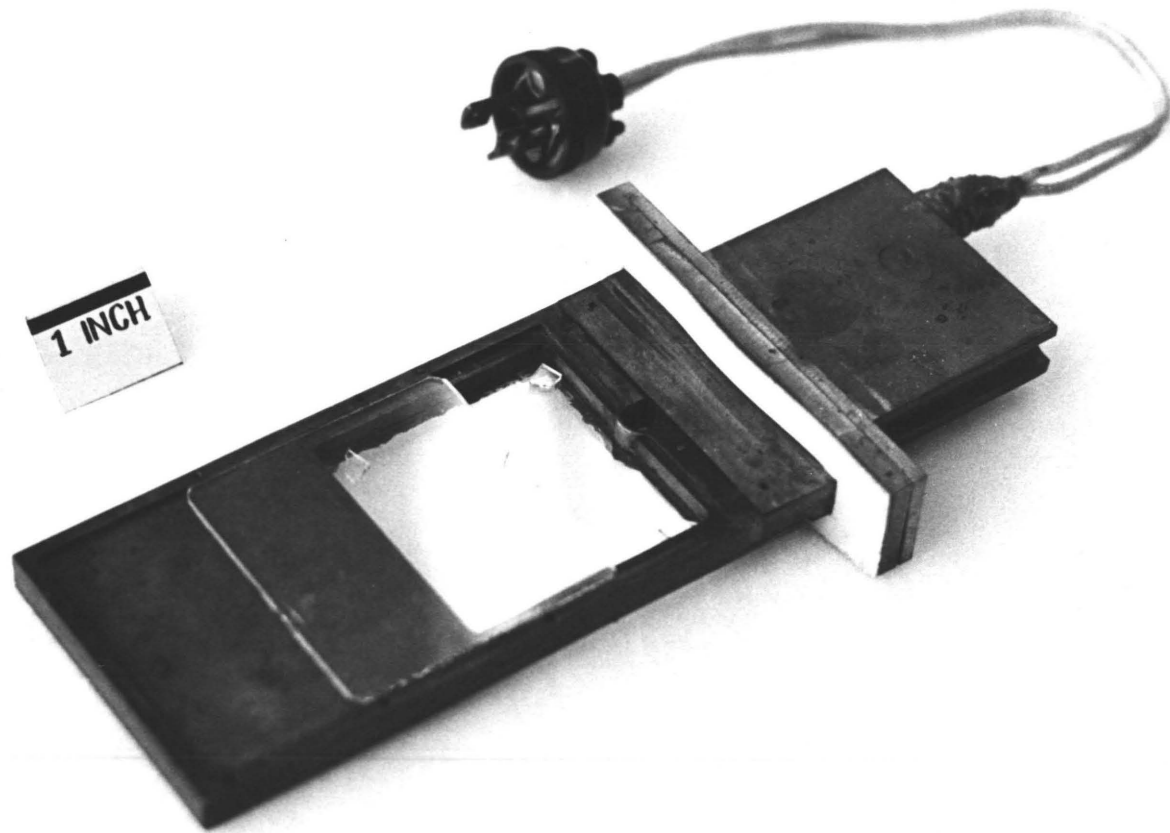
FIG. 15   DROP CATCHING PAN

1 INCH

THE ENCLOSURE

The enclosure was made up of three parts; a base, a box enclosing the target surface and a glass pipe connecting the two (Fig. 16, 17).

The base consisted of short length of 3 inch diameter flanged pipe closed off at the bottom with a flat plate. The drop projector was mounted in the center of the base plate. A heating element in the base plate served to boil water in the bottom to generate a steam atmosphere inside the apparatus.

The glass pipe sitting on the top flange of the steel pipe was heated with heating tape to prevent condensation and thus allow necessary observation of the drop projector inside.

The top of the apparatus consisted of a stainless steel box designed to support the target surface and allow insertion of the drop catcher. The impact of the drop on the target surface was photographed through a double front window. The window was heated by glycol circulated through the window in order to prevent condensation on the inside. The light for photography came through a tube in the back of the box. The drop catcher was inserted through a slot in the front.

A 0.0005 inch platinum-rhodium thermocouple, inserted through the side of the box, was used to measure the vapour temperature in the interior.

The entire apparatus was mounted on a heavy concrete table designed to minimize vibrations.

TARGET SURFACE
ASSEMBLY

VIEWING PORT

TOP
STEAM VENT

PREFOCUS ROD
ASSEMBLY

WINDOW

SLOT FOR INSERTION
OF DROP CATCHER

VAPOUR TEMPERATURE
PROBE

DROP
PROJECTOR

GLASS PIPE

DROP FORMER

BOTTOM
STEAM VENT

SOLENOID VALVE

BASE HEATER

SCALE 1/4
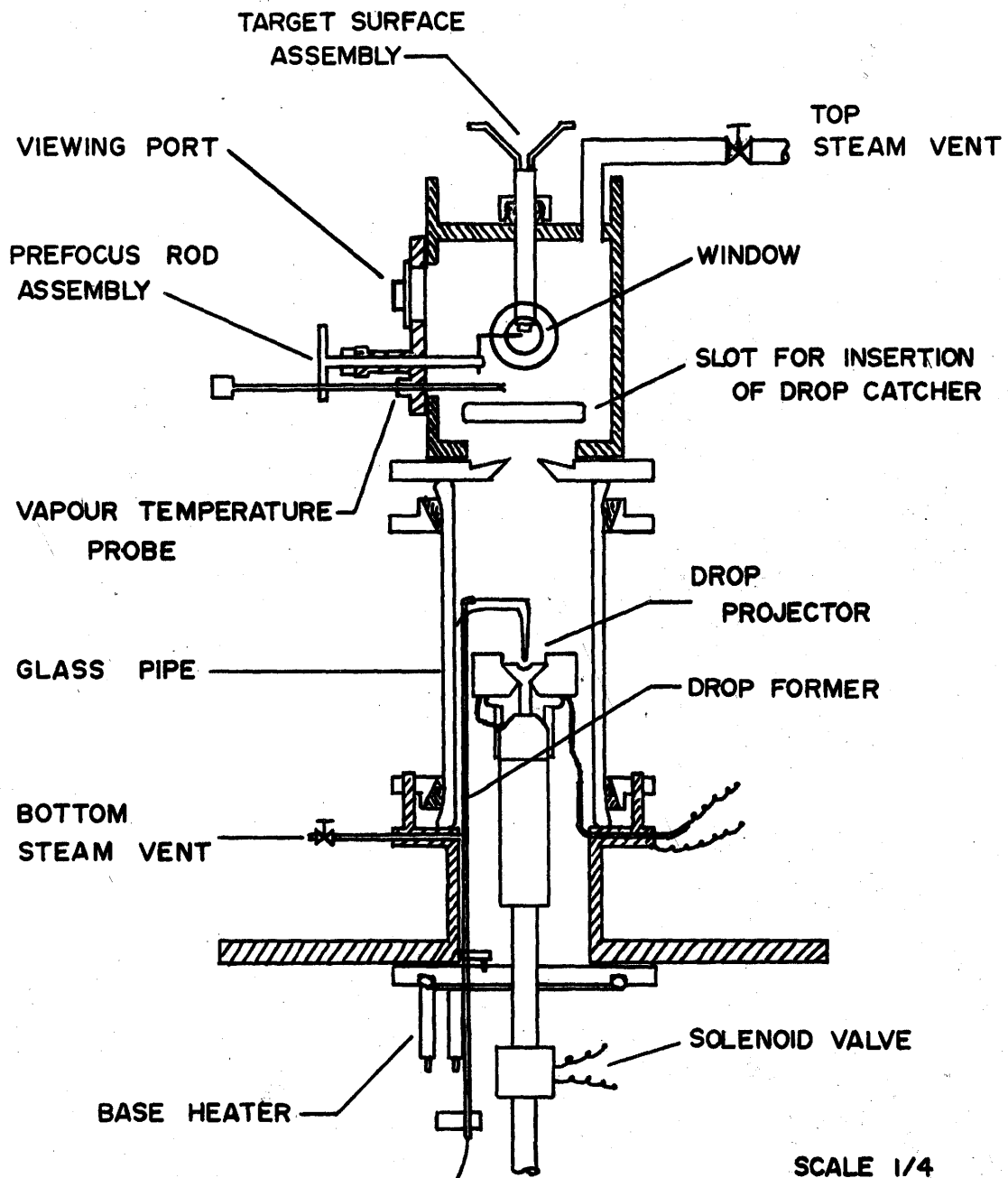
FIG. 16   APPARATUS USED IN THE INVESTIGATION OF
DROP IMPACT ON A HOT SURFACE
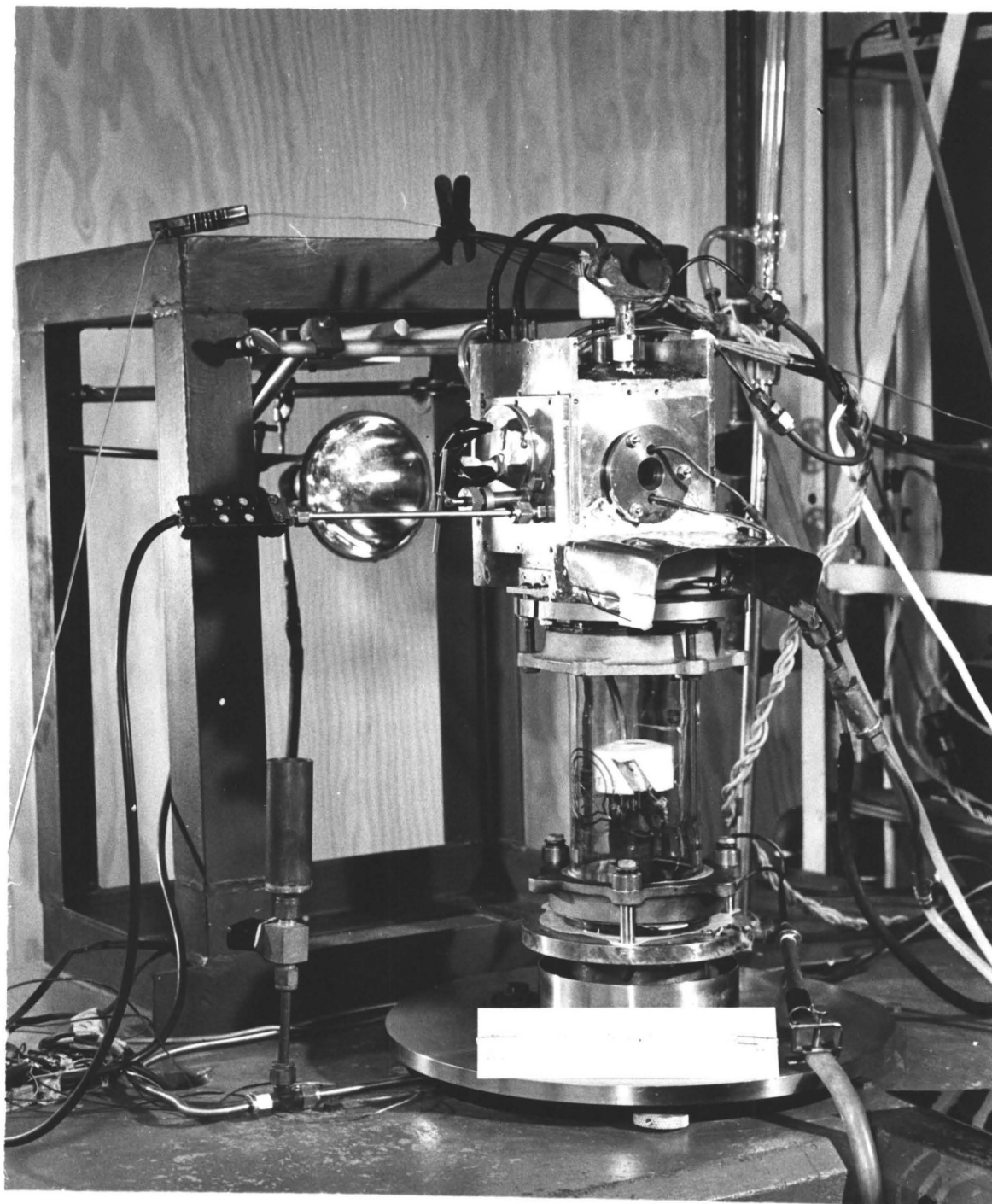
FIG. 17   APPARATUS WITHOUT INSULATION

PHOTOGRAPHY OF DROP IMPACT

The impact of the drop on the surface was photographed using a "Fastax" high-speed 16 mm. motion-picture camera operating at 4600 frames per second. Light for photography was provided by a stroboscopic flash lamp synchronized with the camera, and yielding an exposure time of approximately 3 microseconds. Details of the stroboscope can be found in Appendix D.

Before operation, the camera was focused on a horizontal "calibration" rod near the target surface. This rod was positioned slightly off to one side of the point of impact as determined from previous tests. Consequently, focusing with the rod projecting into one side of the field of view was equivalent to focusing on the point of impact of the drop.

PROCEDURE

The basic procedure was to project a drop at a hot surface, to photograph the impact and to catch and photograph the drop after it had rebounded from the surface. The following section is intended to allow the reader to understand how this was done. A detailed account of the entire experimental procedure may be found in Appendix C.

Prior to an experimental test, the target surface and the drop projector surface were inspected and cleaned. The base of the apparatus was filled with distilled water and all the various heaters were turned on. After several hours, the apparatus filled with steam and the flow of steam out the top of the apparatus cleared the interior of air. The drop catcher was cleaned with solvent and placed in an oven at 115 degrees Centigrade. The camera and stroboscope control circuits were prepared for operation and a potentiometer was connected to measure the target-surface temperature.

Ten minutes prior to an experimental run, silicone oil saturated with water at 100 degrees centigrade was poured in the drop catcher in the oven and a roll of film was loaded into the Fastax camera. After loading the drop catcher into the apparatus, a period of 15 minutes was allowed to clear out any air. During this period the drop projector was cleansed of superficial dirt. To do this, a drop was placed in the depression and then removed again using the drop former. The Fastax camera was focused on the calibration rod and the stroboscope light was positioned in place.

A drop was formed on the loop of glass tubing, placed on the drop projector and observed until it evaporated to the desired size. The camera was started and, after a delay of 1.25 seconds to allow the camera to accelerate, the solenoid valve was activated and the stroboscope light started. The drop was fired upwards and rebounded off the target surface

into the drop catcher.

The drop catcher was removed from the apparatus. The glass cover was immediately placed over the drop in the oil and the drop or drops were photographed using the substage microscope with 30X magnification.

Approximately 5 times magnification was obtained on the Fastax film. A measurement of the two image sizes allowed the calculation of the change in size of the drop due to heat transfer from the surface.

A considerable number of experimental runs were made with the target surface polished to a 0.3 micron mirror finish (Fig. 18). Later, a number of runs were made with the surface roughened with No. 600 grit silicon carbide abrasive (Fig. 19). This was intended to provide a superficial indication of the effect of gross surface roughness.

The apparatus was later purged of silicone oil by refluxing organic solvents in the interior. Runs were then performed without any attempt to catch drops in an attempt to observe any influence of the silicone oil in the system.
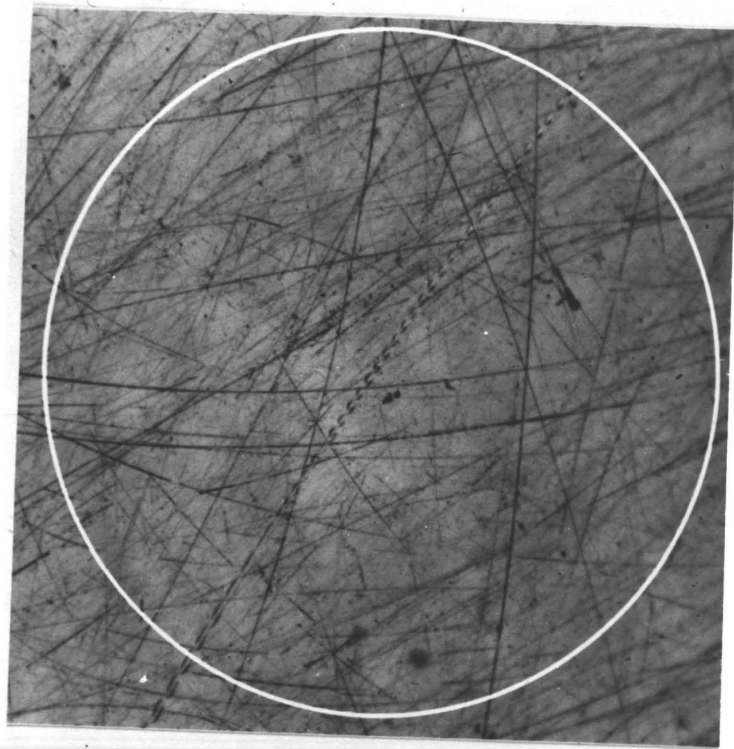
FIG.18   REFLECTION

MICROGRAPH   OF

POLISHED   SURFACE
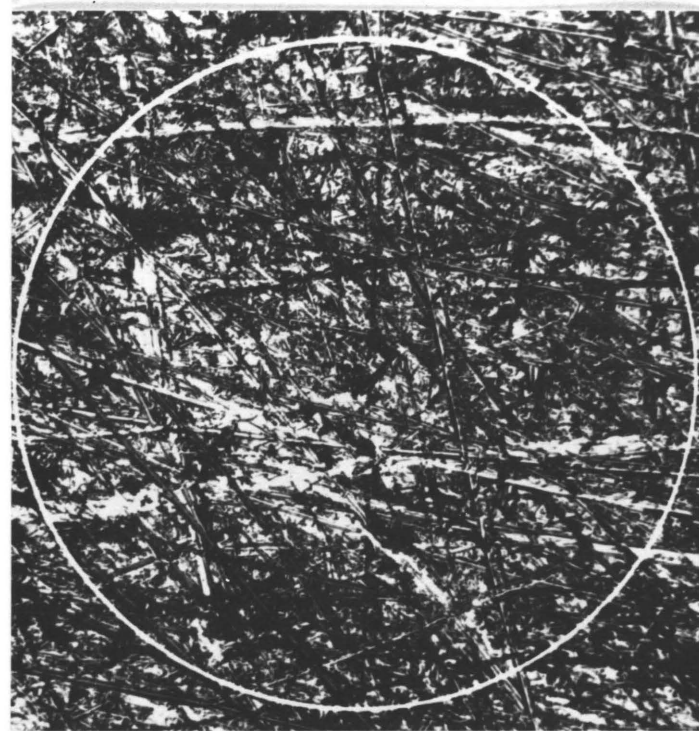
FIG.19   REFLECTION

MICROGRAPH OF

ROUGHENED SURFACE

CIRCLE   DIAMETER   I.0   MM. -I000 MICRONS-

ANALYSIS AND DISCUSSION OF RESULTS

Part 1   COLLISION DYNAMICS

(a) Description of Impact and Rebound of the Drop

When a drop hits a very hot surface the vapour
generated underneath the drop prevents it from wetting the
surface. If the impact velocity is not too high, surface
tension forces hold the drop together and it flattens out
into a circular tablet-shaped body (Fig. 20). After flattening
out, the surface tension forces cause the tablet to contract,
with the liquid at the perimeter flowing toward the center.
The liquid in the center lifts away from the surface as a
column (Fig. 20) or, at high Weber Numbers, as a cone
shaped body (Fig. 2)(p.21).

The drop leaves the surface as an elongated body,
vibrating as it recedes from the surface. This vibration
is essentially a flux between the surface energy and the
internal kinetic energy with oscillation about the drop's
center of mass.

Some of the initial impact energy is lost in viscous
or fluid-friction dissipation inside the drop during impact
and rebound from the surface. The remainder appears as
vibrational and translational kinetic energy in the receding
drop. The recession velocity of the drop is appreciably
lower than the approach velocity (Fig. 21). The ratio of the
recession to the approach velocity decreased with increasing
Weber number (Fig. 22). Normally well over half the initial
kinetic energy appears as vibrational energy in the receding

63
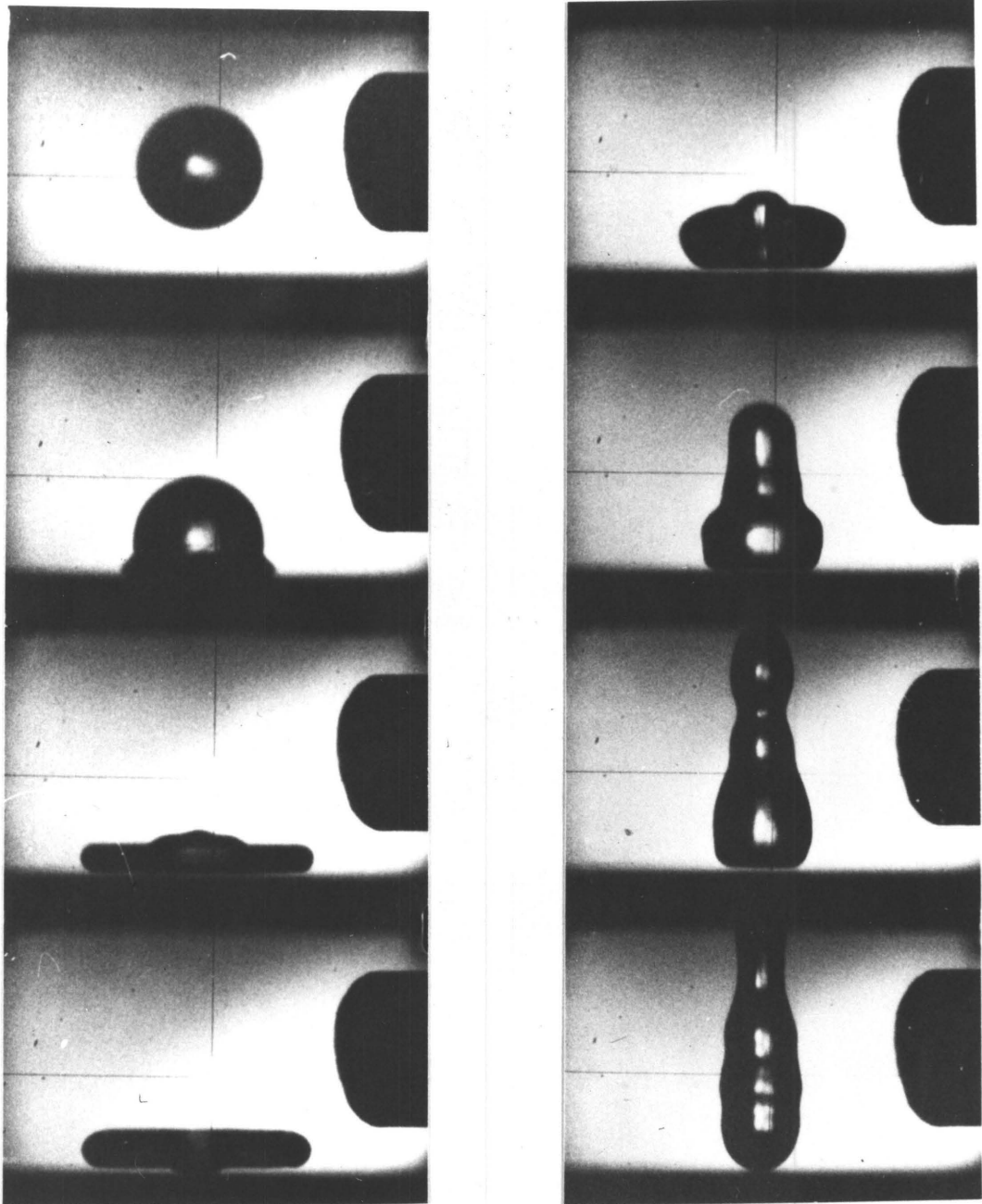
FIG. 20   DIAMETER 580 MICRONS

VELOCITY 4.9 FEET PER SECOND

SURFACE TEMPERATURE   710 °F.

FIG. 21   RELATION BETWEEN RECESSION AND APPROACH VELOCITY
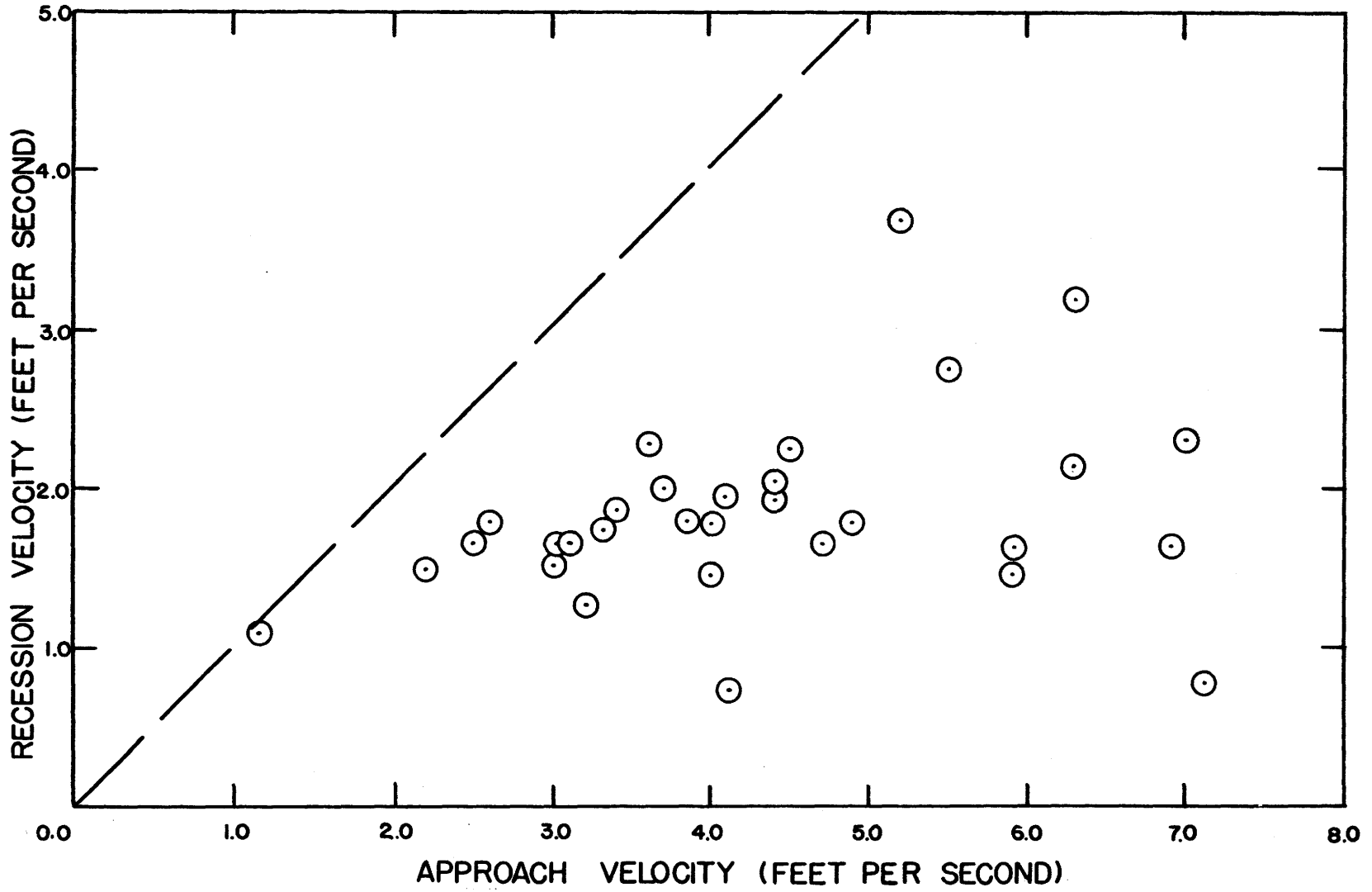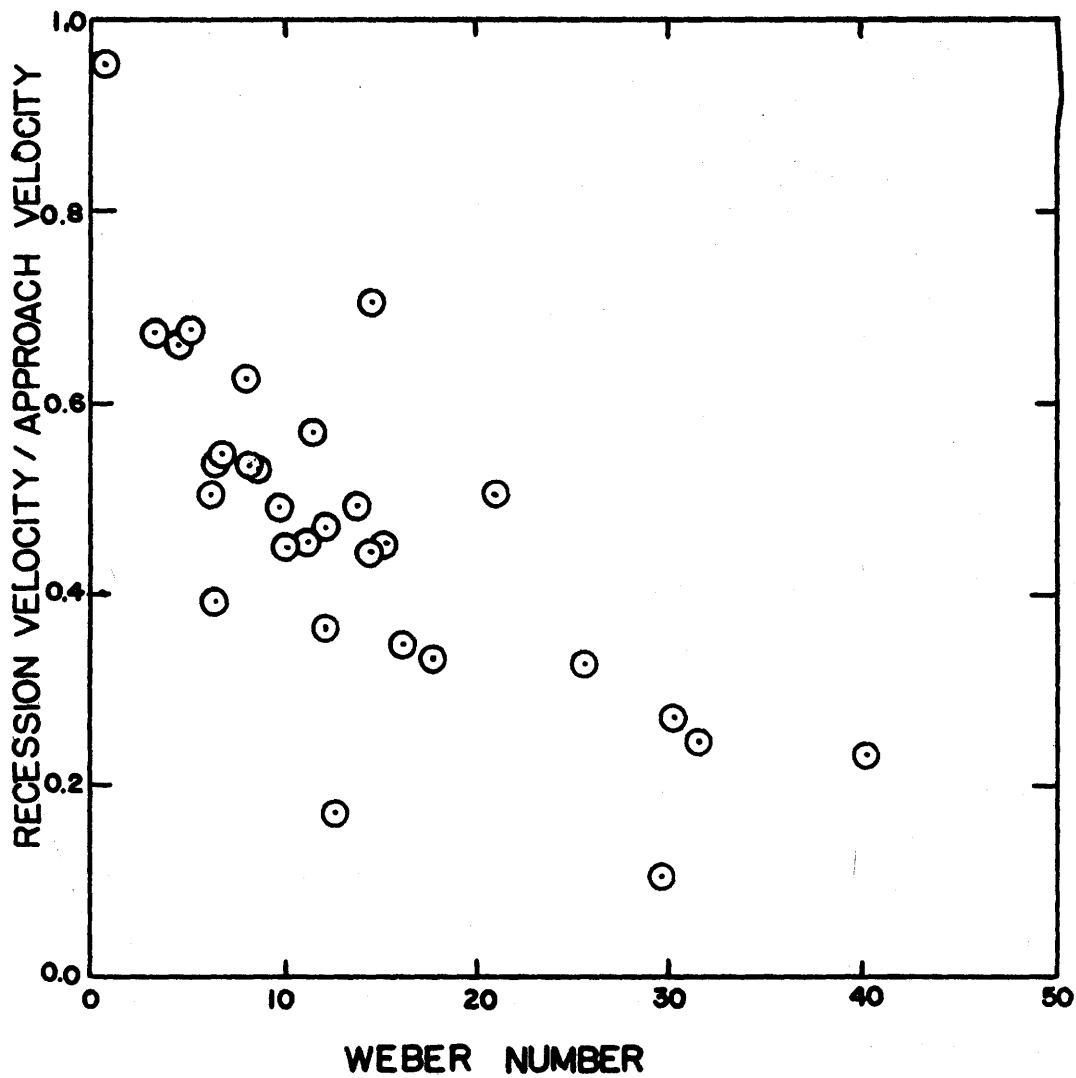
FIG. 22   RELATION BETWEEN THE RATIO OF
RECESSION TO APPROACH VELOCITY
AND WEBER NUMBER.

drop, the fraction increasing with Weber Number (Fig. 23).

Provided the drop did not wet the surface, it approached very close to the surface only during the initial impact and during the final "pushing off" from the surface. At these times the surface area in contact was small. Between the beginning and the end of the collision, the vapour generated underneath the drop held the drop away from the surface (Fig. 2).

(b)   BREAKUP PHENOMENON

When the Weber Number of the approaching drop exceeded a value of approximately 10, the drop separated on leaving the surface into two or three small drops (Fig. 2,20). This resulted in a decrease in vibrational energy in the receding drops because of the increased surface area and therefore surface energy. Breakup did not influence the net kinetic energy because there was no net force exerted on the mass of the drops in the process. Usually after breakup these drops receded from the surface at different velocities. They were observed on occasion to combine again a short distance from the surface.

Wachters did not observe this occurrence with his 2 millimeter drops below a Weber Number of 20 (6). In Wachters experiments the gravitational force was acting toward instead of away from the surface, but the gravitational acceleration was so much less than that experienced by the drop during impact as to be insignificant in its effect. This breakup phenomenon will depend on the stability of the elongating column of liquid formed when the drop

leaves the surface. The fact is that although the size of
this column relative to the size of the drop depended on
the Weber Number, the factors influencing the stability
depended on the actual size (21). Therefore, the breakup
phenomenon was not solely characterized by the Weber Number
of the approaching drop.

Similarly, drops were thrown off at the edges of
the flattened drop, continuing to travel away from the
center of impact, when the Weber Number exceeded 45 (Fig. 23).
Wachter's criteria was a Weber Number of 80. Part of this
difference may be explained by the fact that Wachters used
cold drops with a surface tension of 84 dynes per centimeter,
making no allowance in this for the effect of drop heating by
heat transferred from the hot surface. All the photographs
taken during this study were with water drops at their
saturation temperature with a surface tension of 58.9 dynes
per centimeter.

(c) Effect of Surface Phenomena on the Impact Dynamics

The recession velocity was not controlled entirely
by the dynamics of the drop impact and rebound when, at the
low surface temperatures, the drop stuck to or wetted the
surface. Wetting was not consistent in its effect and could
retard or prevent separation of the drop from the surface
or could, by blocking the flow of vapour underneath the drop,
cause the accumulation of vapour which then blows the drop
off the surface (Fig. 24).

RATIO OF THE KINETIC ENERGY BEFORE AND AFTER IMPACT AS A FUNCTION OF WEBER NUMBER.
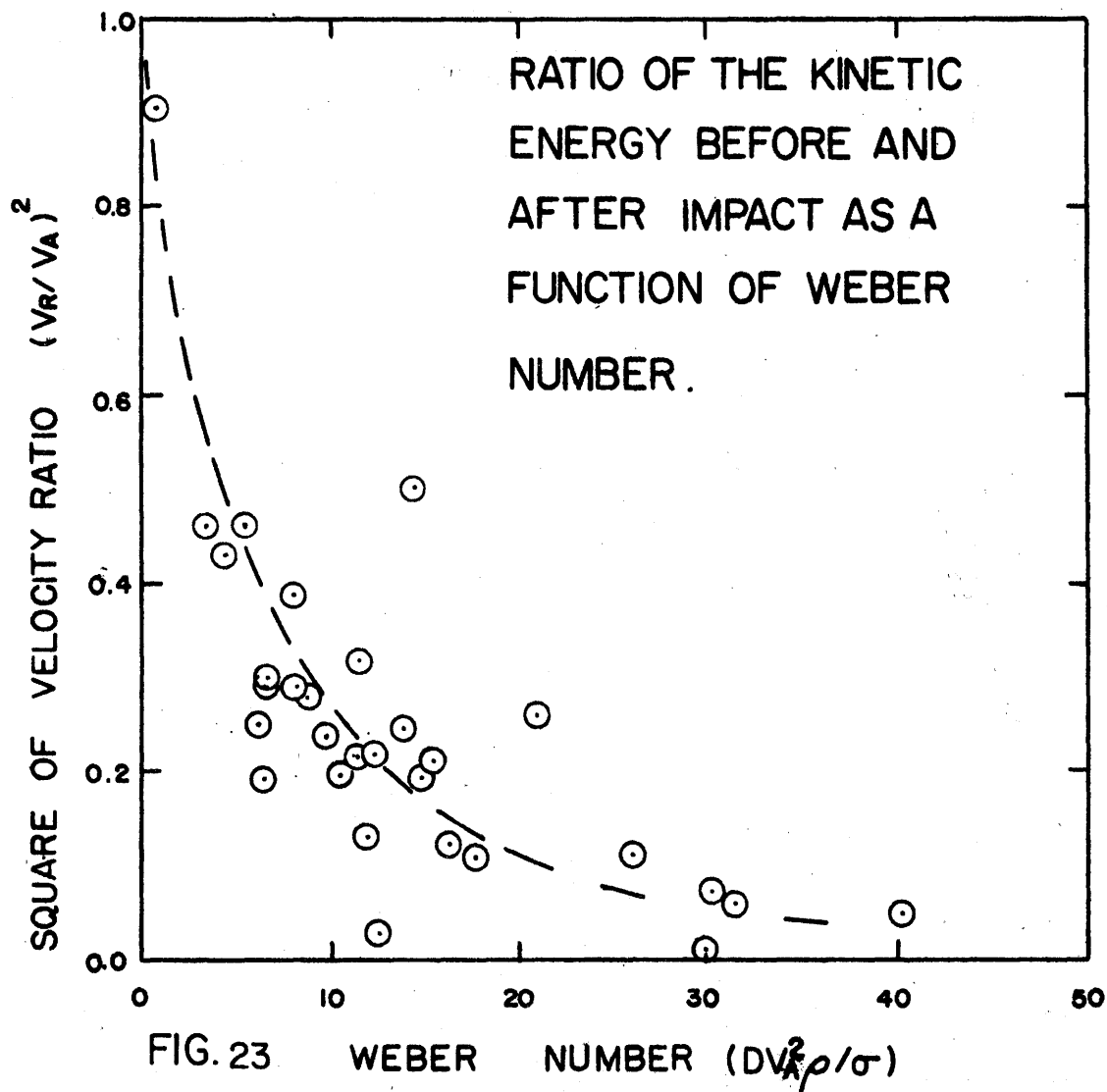
FIG. 23   WEBER   NUMBER $(DV_A^2\rho/\sigma)$

FIG.23   DIAMETER   530   MICRONS

VELOCITY 7.6 FEET PER SECOND

SURFACE TEMPERATURE 470 ºF

Figure 24

This photograph of a colliding
drop illustrates the way in which a drop
may be blown off the surface by vapour
generated beneath it.
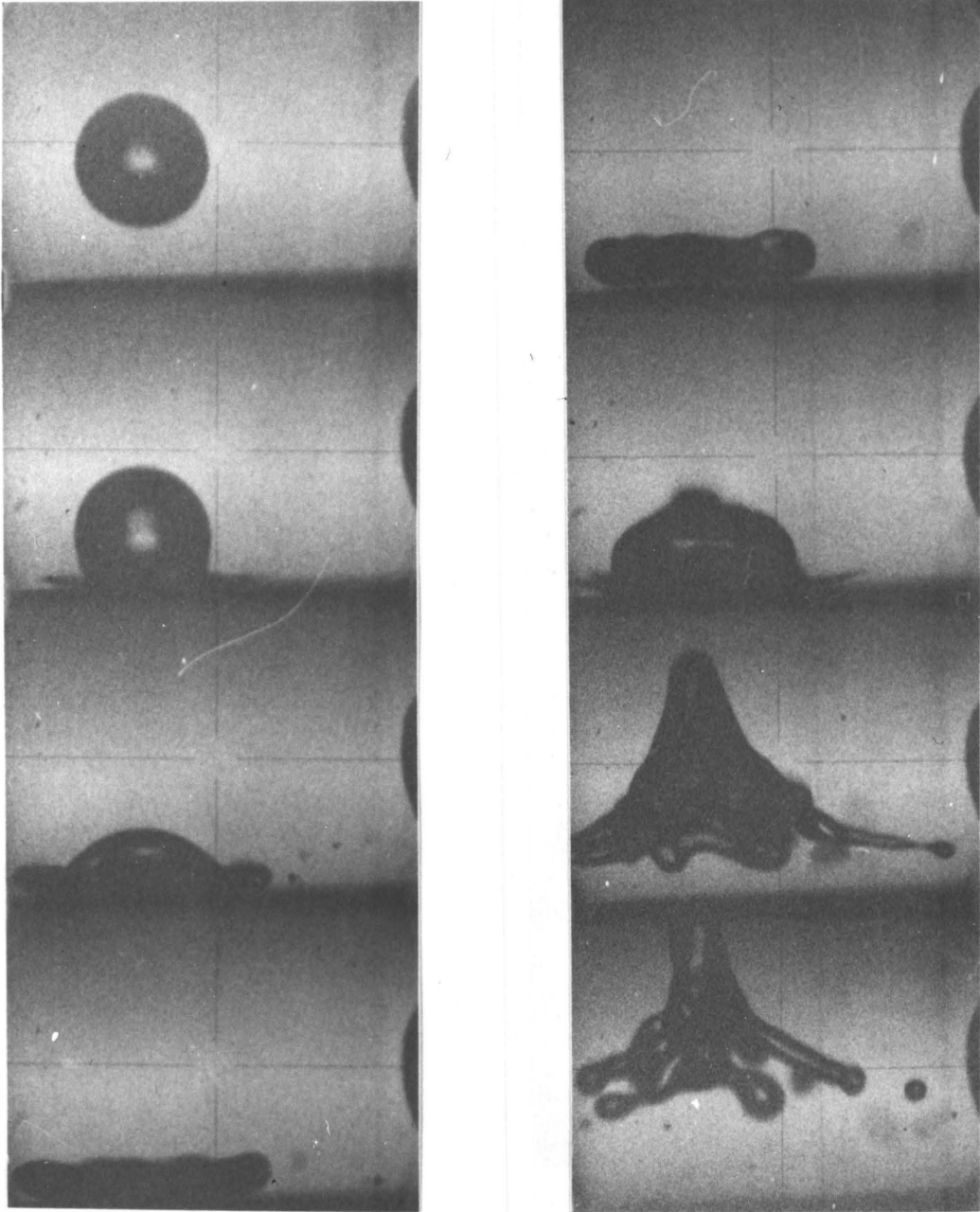
FIG. 24   DIAMETER 590 MICRONS
                 VELOCITY 4.3 FEET PER SECOND
                 SURFACE TEMPERATURE 375 oF.

An estimation was made of the influence of surface drag due to vapour flow under the drop, assuming that the drop was separated from the surface by a vapour film (Section 2). The results indicated no appreciable influence. The surface temperature did not appear to influence the drop impact dynamics except in its effect on wetting.

(d)   <u>Mathematical Model of the Drop Impact</u>

The model of the initial impact process, based on a kinetic and surface energy balance, was found to be sufficient as a first approximation of the dynamic behaviour of the drop during the impact period (Fig. 20). The derivation of the model is given in section on.Heat Transfer and Dynamics Models. The model results and the experimental measurements are presented in dimensionless form, with the tablet thickness, A, and the tablet radius, R, given as a fraction of the drop diameter, D and the time given as a fraction of the model total impact time, $((D-AEND)/v)$, where AEND is the final value of the tablet thickness, as calculated from the model energy balance, and v is the initial approach velocity of the drop. Presented in this form, the model results are a function of the Weber Number of the impacting drop only.

The model was found to be unrealistic at the initial instant of impact. Its weakness lay in the assumption that the drop did not "see" the surface until it reached the top of the tabular form. This assumption was evidently not valid during the first period of impact, as the model generally

predicted a radius in contact that increased more slowly
than was measured experimentally (Fig. 4, 5). This
assumption does however appear reasonable for the drop as a
whole, as measurements of the velocity of the top of the drop
indicated that it did not decelerate during impact (Fig. 25).
This is further supported by the analysis of Savic (2).

The model does not conform with the physical process
when the Weber Number of the drop is less than one. At
these low Weber Numbers the drop flattens slightly but
there is no formation of a tabular body separate from the
impacting drop.

(e)   Viscous Dissipation of Energy During Impact

During the process of impact, part of the initial
kinetic energy of the drop was evidently dissipated by
viscous forces inside the drop. This was indicated by
the fact that the maximum radius of the tabular form
measured experimentally was found to be less than the
model predicted (Fig. 7). The surface energy of the tabular
form was apparently less than the initial kinetic and surface
energy of the approaching drop. The ratio of the experimental
radius to the model radius was calculated for 31 of the
impacting drops. In order to determine whether or not
a significant correlation existed, this ratio was correlated
with the Drop Reynolds Number and the Drop Weber Number
using a very simple linear equation (Fig. 26). The
correlation coefficient for the Reynolds number was
0.7436, larger than the value of 0.6133 obtained

Figures 3 to 8

These figures illustrate the
variation with time of the radius and
thickness of the tabular body of fluid
in contact with the surface. All variables
are expressed in dimensionless form.
Experimentally measured point values may
be compared directly with the curves
derived from the impact dynamics model.

WEBER NUMBER 3.4-5.4
MODEL WEBER NO. 4.4

WEBER NUMBER 6.2-9.2
MODEL WEBER NO. 8.8

X - EXPERIMENTAL VALUES OF R/D
O - EXPERIMENTAL VALUES OF A/D
— MODEL VALUES OF R/D, A/D

DIMENSIONLESS DISTANCE (S/D)

DIMENSIONLESS TIME (T/((D-AEND)/V))

FIG. 4

73
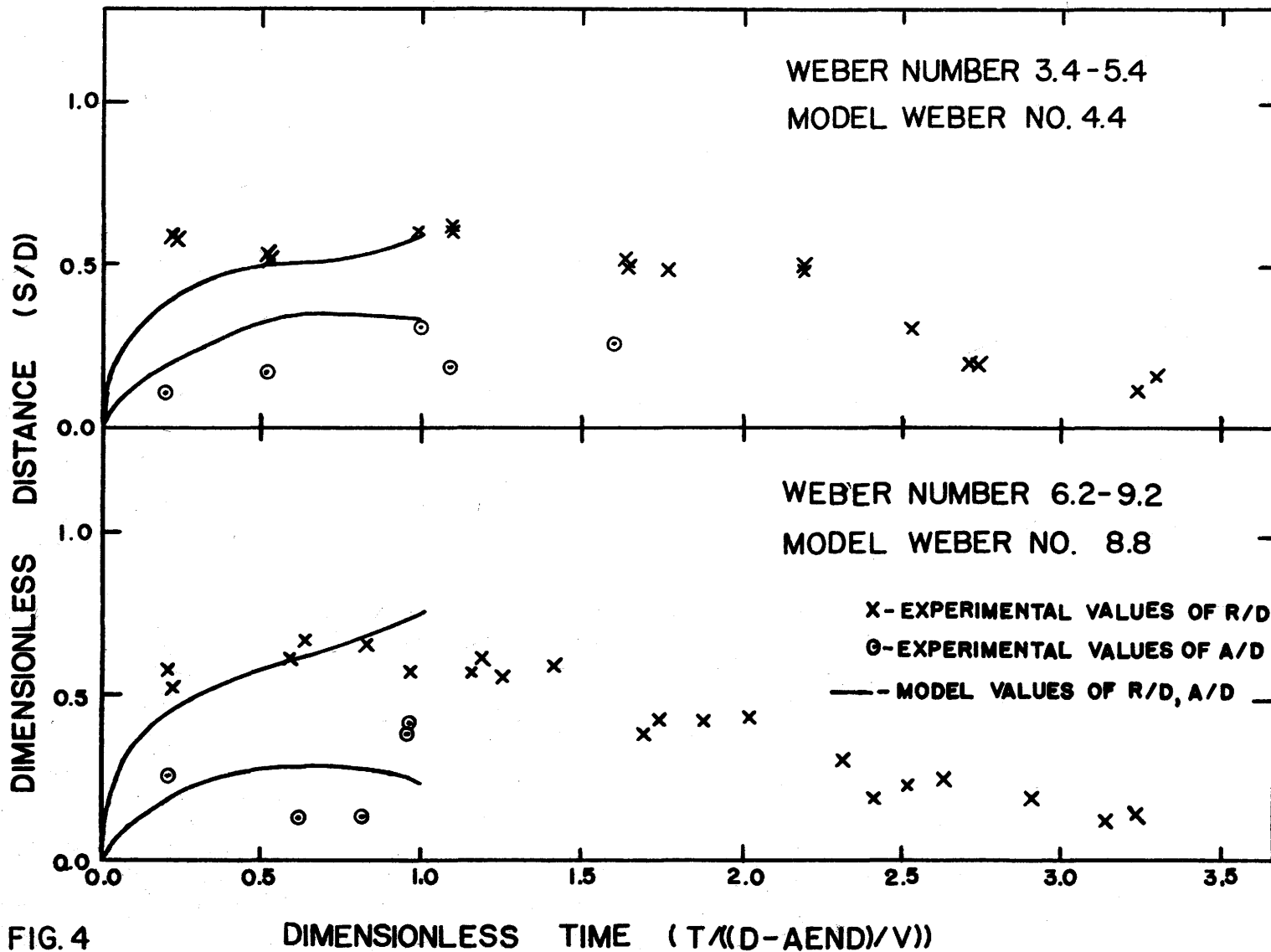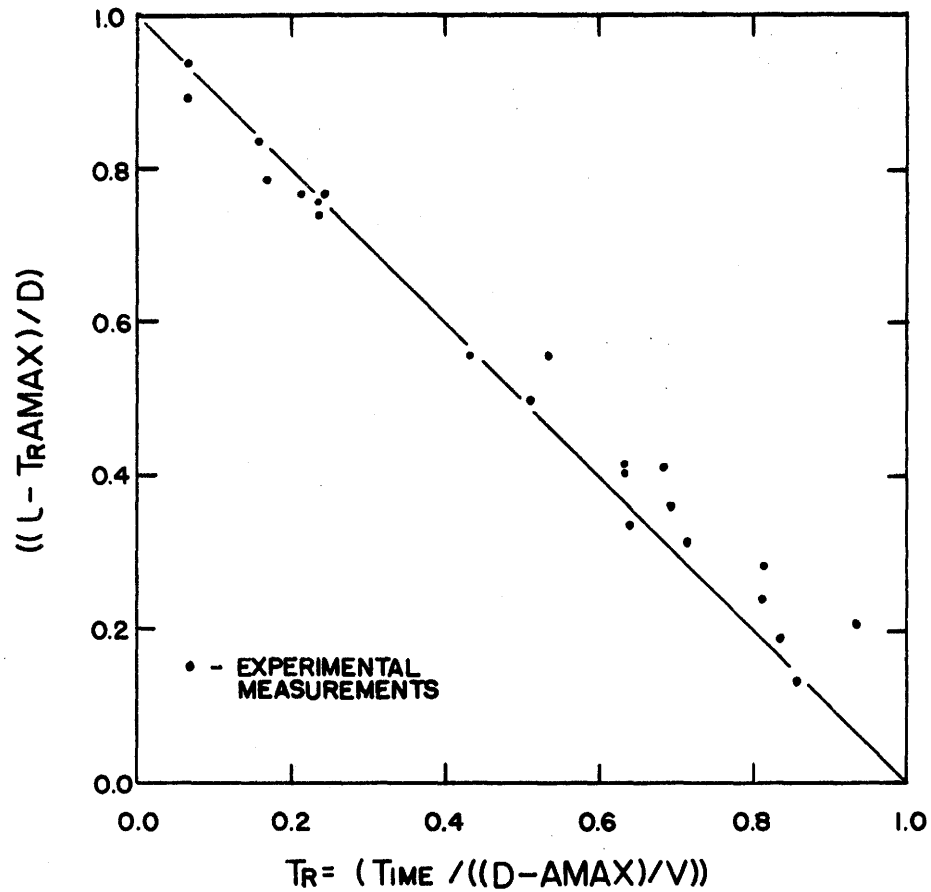
FIG. 25 THE OBSERVED RELATION BETWEEN THE
POSITION OF THE TOP OF THE DROP AND
TIME AFTER INITIAL IMPACT, EXPRESSED
IN GENERALIZED FORM.

FIG.7

WEBER NUMBER 19.3-20.4
MODEL WEBER NO. 20.1

X — EXPERIMENTAL VALUES OF R/D

⊙ — EXPERIMENTAL VALUES OF A/D

— MODEL VALUES OF R/D, A/D

DIMENSIONLESS DISTANCE (S/D)

DIMENSIONLESS TIME (TV/(D-AEND)
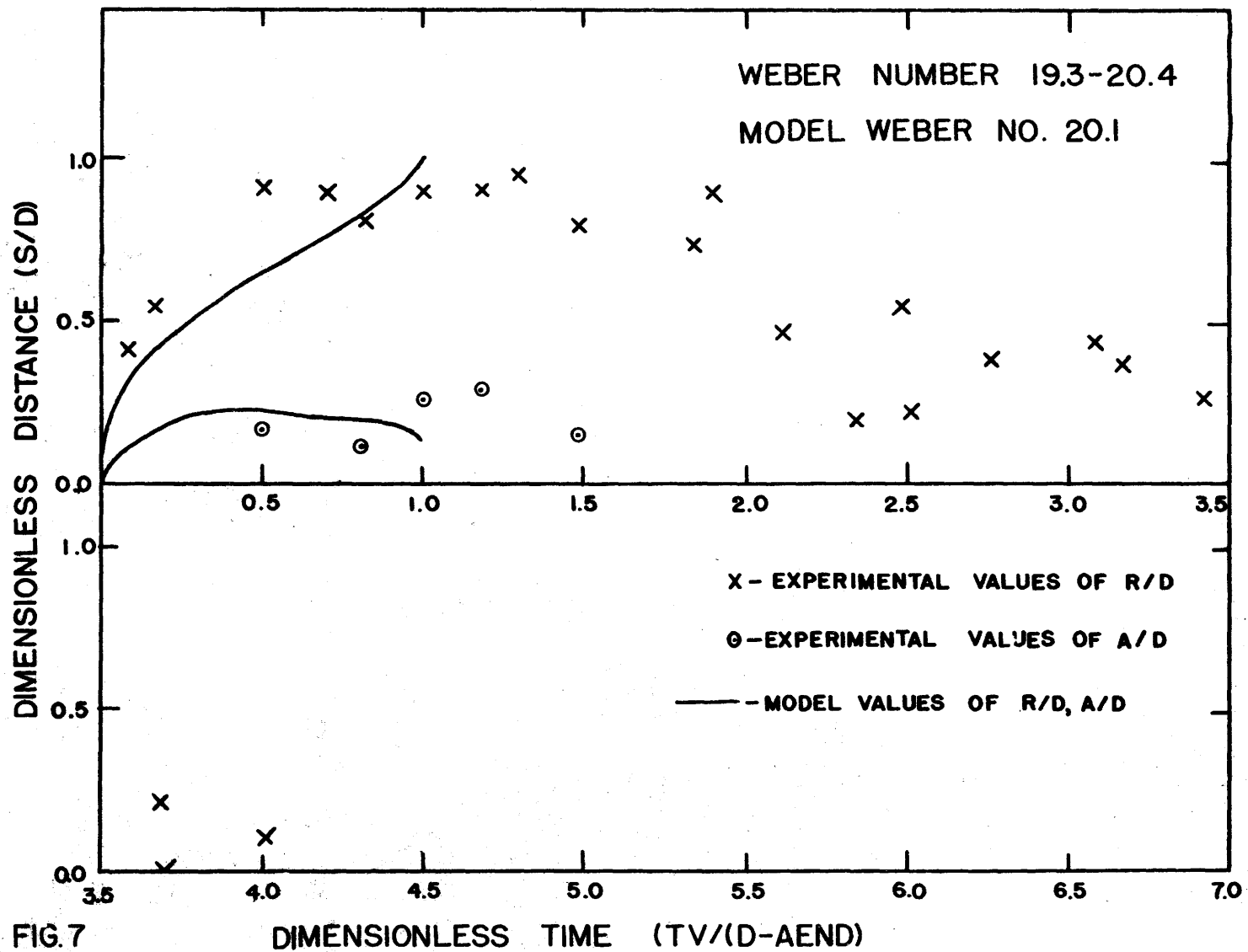
Figure 26

      This illustrates the correlation
between the Drop Reynolds Number and the
discrepancy between experimental results
and results calculated using the impact
dynamics model. This tends to support
the hypothesis that this discrepancy is
caused by viscous dissipation effects.

FIG. 26 DISCREPANCY BETWEEN

MODEL AND EXPERIMENTAL MAXIMUM RADIUS

IN CONTACT AS A FUNCTION OF REYNOLDS NUMBER
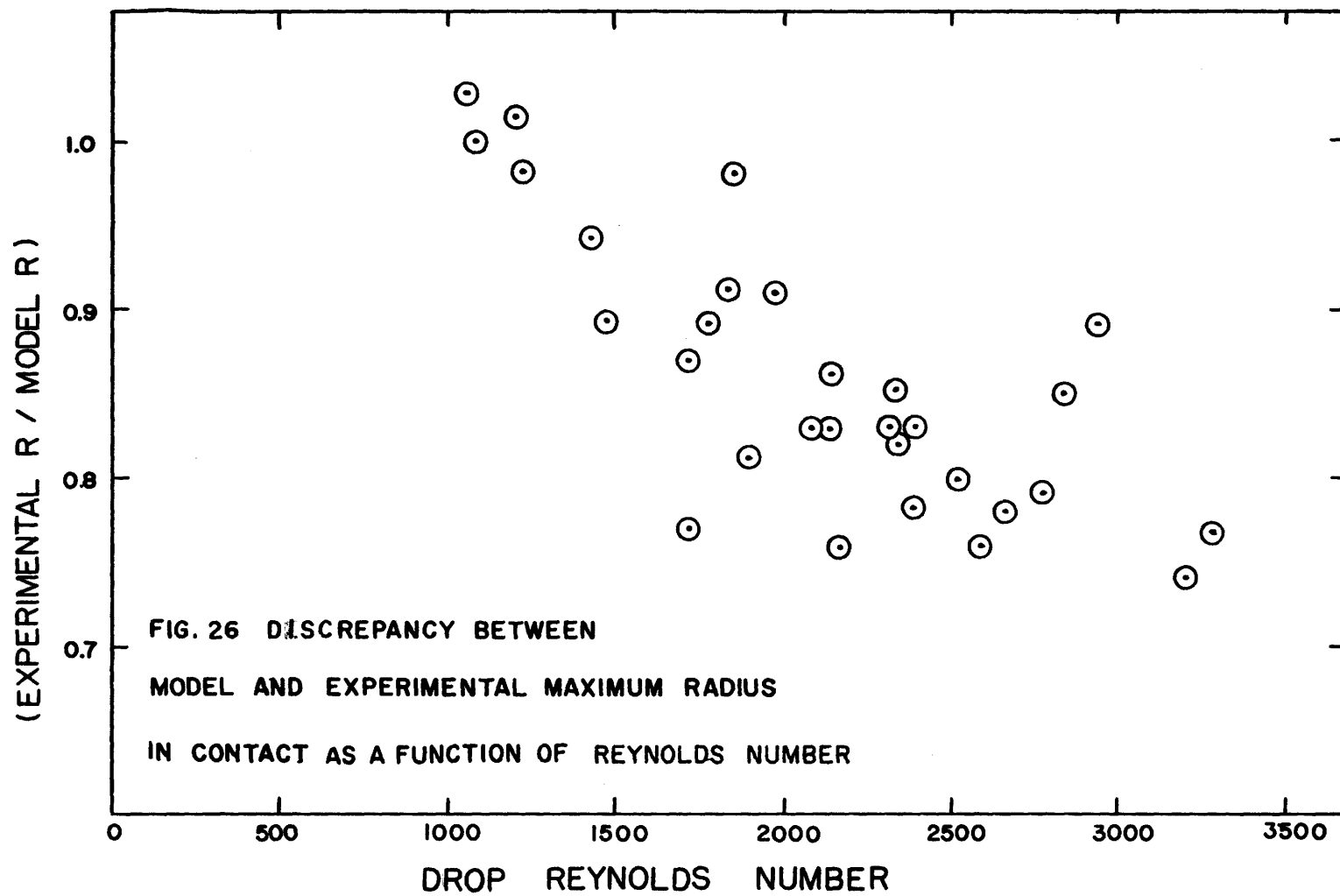
for the Weber Number correlation. Both correlations were significant at the 89.9 percent confidence level for 30 degrees of freedom (18). On the basis of the larger correlation coefficient for the Reynolds Number correlation, it might be concluded that this discrepancy between the model and the experimental results was due to viscous dissipation, but the possibility that it could have been partly a dynamic phenomenon cannot be ruled out. For example, it might have been due in part to an increase in the tablet surface area and therefore surface energy caused by a depression appearing in the top surface of the tabular body as the inertia of the top part of the drop carries it down past the top surface. This may be observed in the photographs of Wachters (6).

The ratio was greater than one for Reynolds Numbers at the lower limit, perhaps due to the influence of surface tension gradients beneath the drop. Surface tension gradients could be caused by differences in temperature at different areas on the drop surface.

The contraction of the tabular form generally required two to three times as long as the impact, the dimensionless time increasing with Weber Number (Fig.4,6). The actual residence time of the drop on the surface varied from 0.6 to 1.5 milliseconds.

Part 11   HEAT TRANSFER TO THE IMPACTING DROP

(a)   Experimental Measurements

The change in drop diameter on impact was determined for drops of diameters from 300 to 700 microns, impacting

FIG. 6   DIMENSIONLESS TIME (TV/(D-AEND))
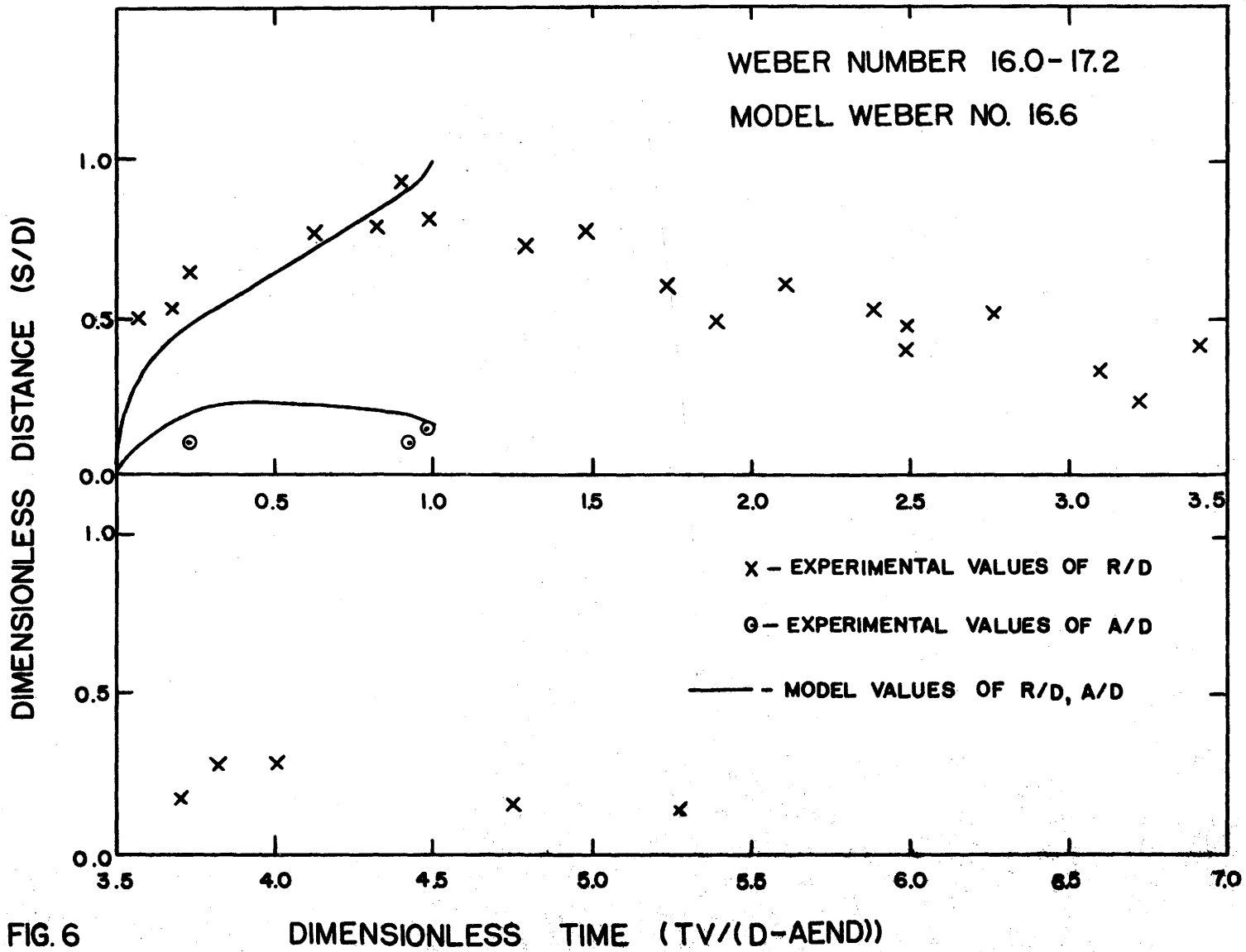
the surface at normal velocities of from 2 to 8 feet per second. Target surface temperatures ranged from 300 to 900 degrees Fahrenheit. These results, with calculated Weber Numbers, drop Reynolds Numbers and surface temperatures are tabulated in Table I (P. 256).

The percentage change in drop diameter was plotted as a function of Weber Number (Fig. 27). The percentage change in volume, indicative of the relative amount of heat transfer was plotted as a function of surface temperature (Fig. 28). Most of the data wose obtained using a surface with a mirror finish. A limited quantity of data were obtained for a roughened surface, as indicated (Fig. 28).

(b) The Effect of Surface Temperature and Mechanism of
     Heat Transfer

The amount of heat transfer was very dependent on the surface temperature, tending to increase with decreasing surface temperature. The amount of heat transfer varied widely with surface temperatures under 550 degrees Fahrenheit. Examination of the photographs of drops colliding with the surface in this lower temperature region showed that a large amount of heat transfer corresponded to an irregular rebound of the drop from the surface, often with small drops of spray being thrown off to one side (Fig. 29). Also, on occasion, wet spots were observed on the surface as the drop receded (Fig. 30). Conversely, a small amount of heat transfer corresponded to a regular rebound with no spray formation or evident wetting (Fig. 20). It appeared as if

Figure 27

This illustrates the fact that
there is no significant relation between
the amount of heat transfer to the drop
and the impact Weber Number.

FIG. 27 RELATION BETWEEN PERCENT CHANGE IN DROP DIAMETER AND WEBER NUMBER.

FIG. 28 PLOT OF EXPERIMENTAL PERCENT VOLUME CHANGE AS A FUNCTION OF SURFACE TEMPERATURE

• MIRROR FINISHED SURFACE

X ROUGHENED SURFACE
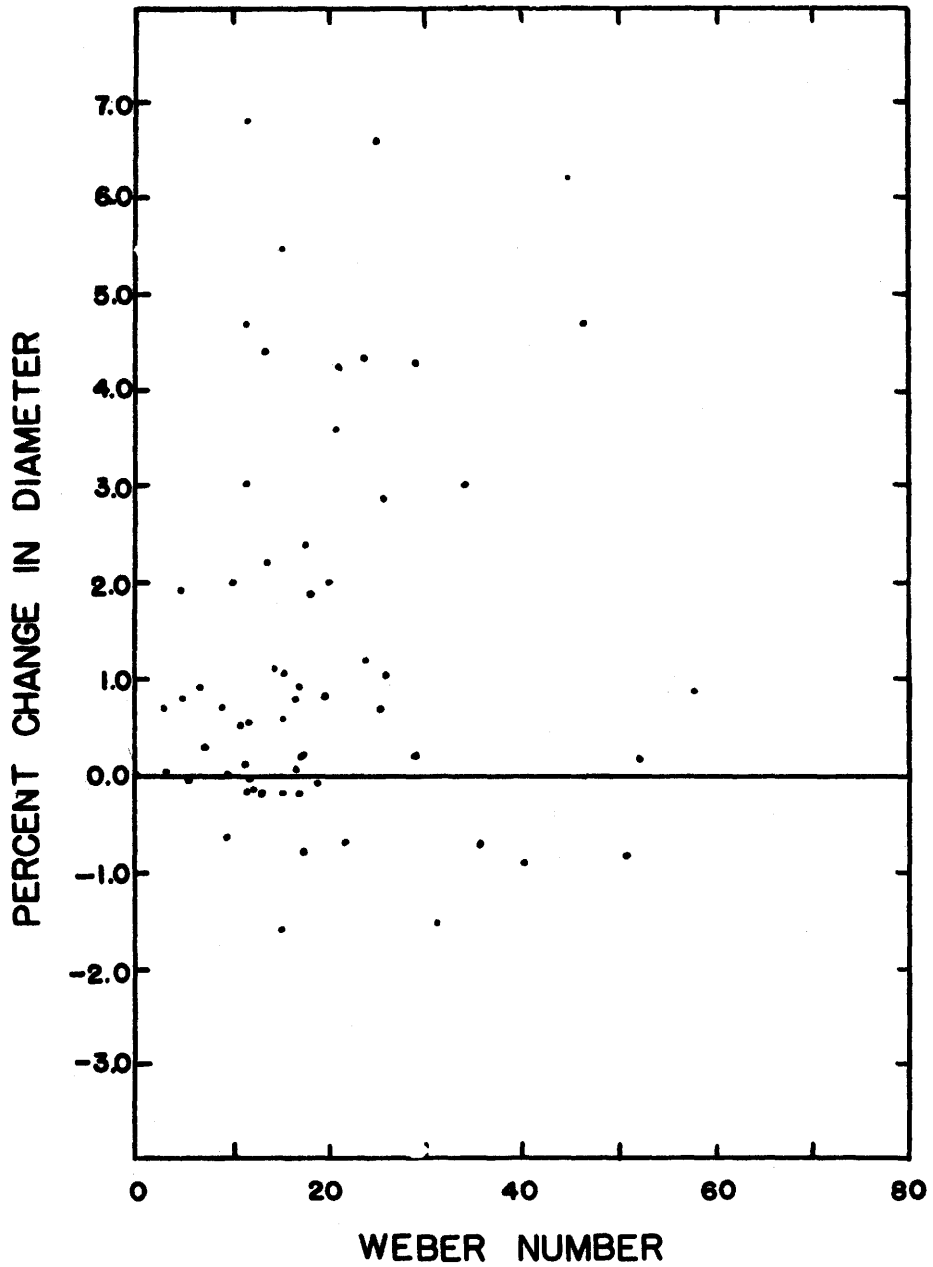
Figure 29

This photograph of a colliding
drop illustrates the way in which vapour
generated beneath a drop may blow a
hole through the middle of the flattened
drop.
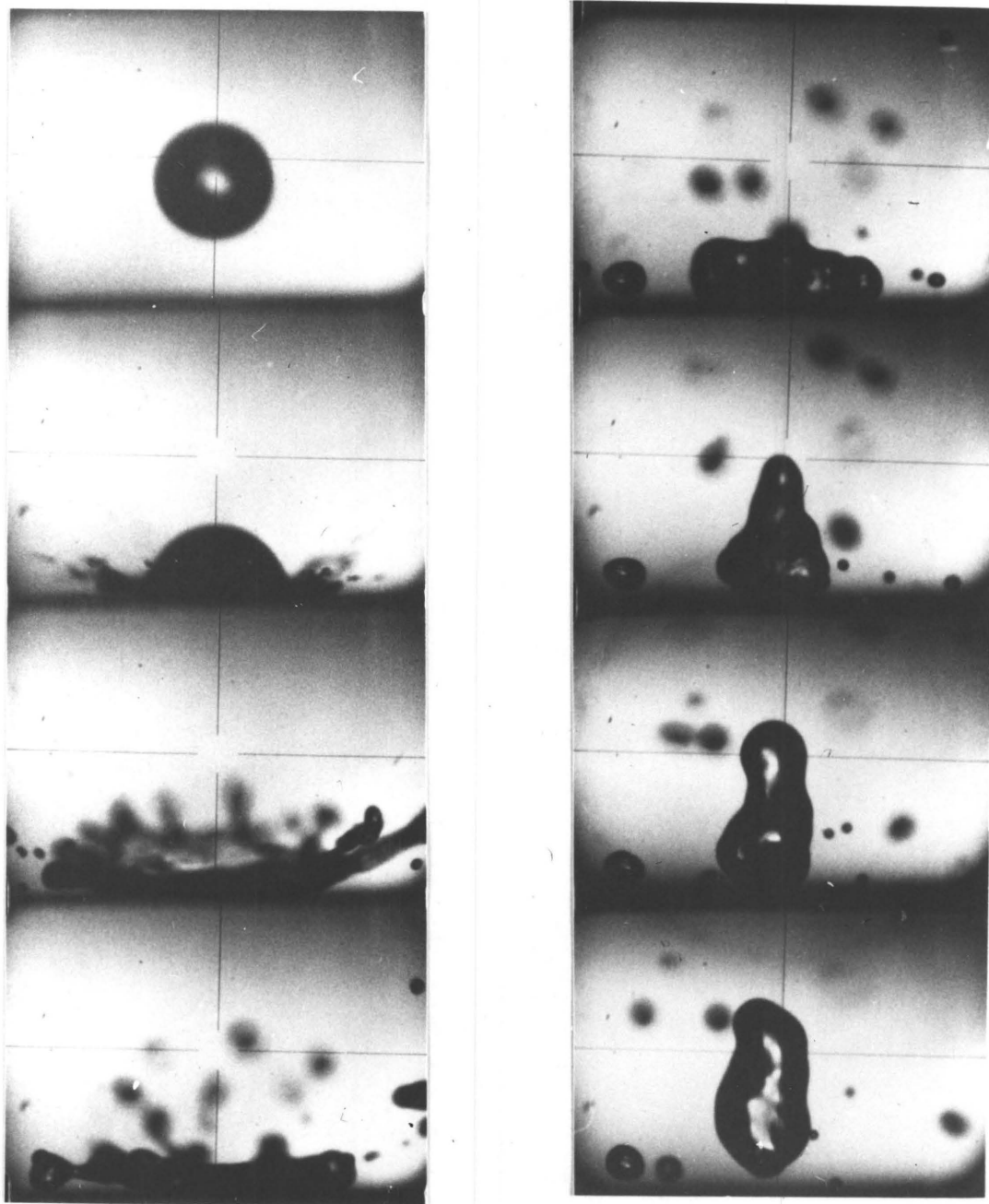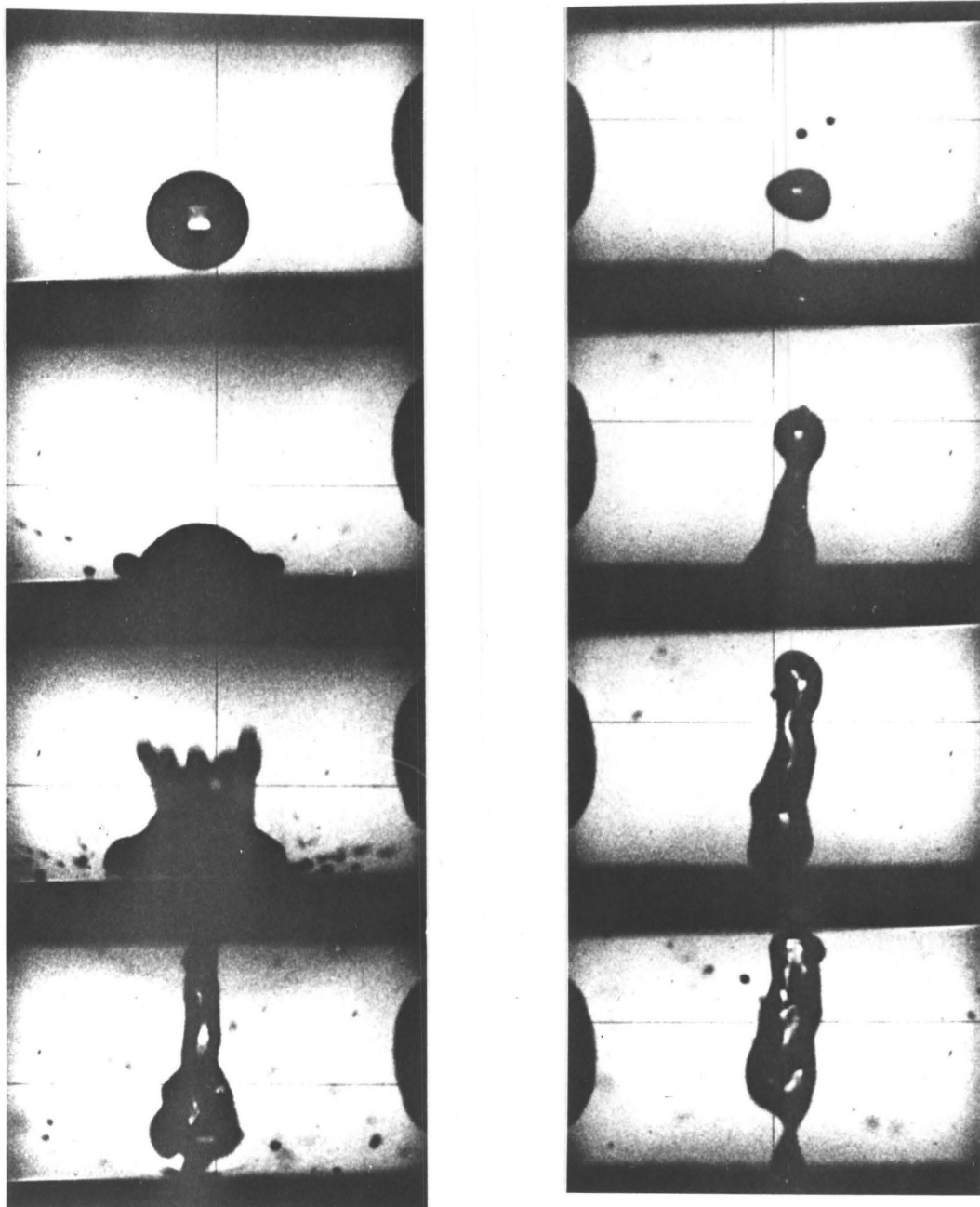
FIG. 29   DIAMETER 460 MICRONS

VELOCITY 4.1 FEET PER SECOND

SURFACE TEMPERATURE   406 oF.

Figure 30

This photograph of a colliding
drop illustrates wet spots left on the
surface by the drop on departure from
the surface. The distribution of the wet
spots shows no order or symmetry.
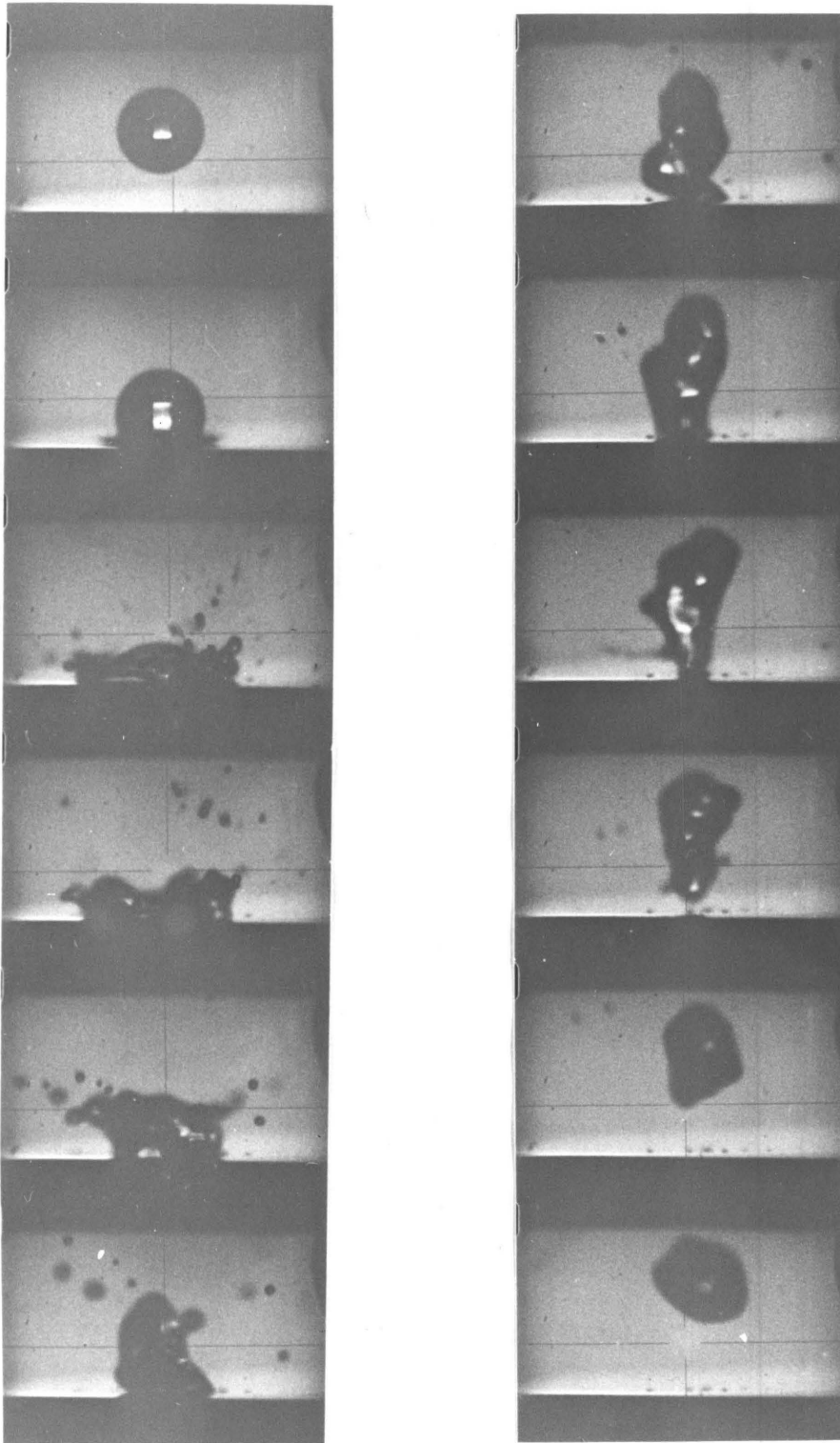
FIG.30   DIAMETER 500 MICRONS

VELOCITY 41 FEET PER SECOND

SURFACE TEMPERATURE   320 oF.

the amount of heat transfer depended on the amount of wetting and that extensive wetting occurred only when the surface temperature was below approximately 550 degrees Fahrenheit. The observations of Wachters confirm this hypothesis ((6), p. 86, Fig. 3.17, 3.18, 3.19).

(c)   The Vapour Film Model

For the case where no wetting occurs, Wachter's model of heat transfer through a vapour film and the similar model used in this study predict that the amount of heat transferred by this mechanism will be very small (Table II). The vapour film underneath acts to thermally insulate the drop from the surface.

(d)   The Direct Contact Model

The amount of heat transfer experimentally measured could only have occurred by direct contact between the liquid and the surface. Comparison of the percentage change in diameter that would be produced by direct conduction of heat from the surface into the drop, predicted using a semi-infinite heat-conduction model, with the experimentally measured values shows that the experimental values (Table I) were in fact occasionally several times greater than these calculated values (Fig. 9). This could be attributed to the effect of fluid flow across the surface during the impact on the temperature profile in the liquid, to nucleate boiling phenomena (17), or to liquid being left on the surface by the departing drop.

FIG.9 TIME OF CONTACT (SECONDS)
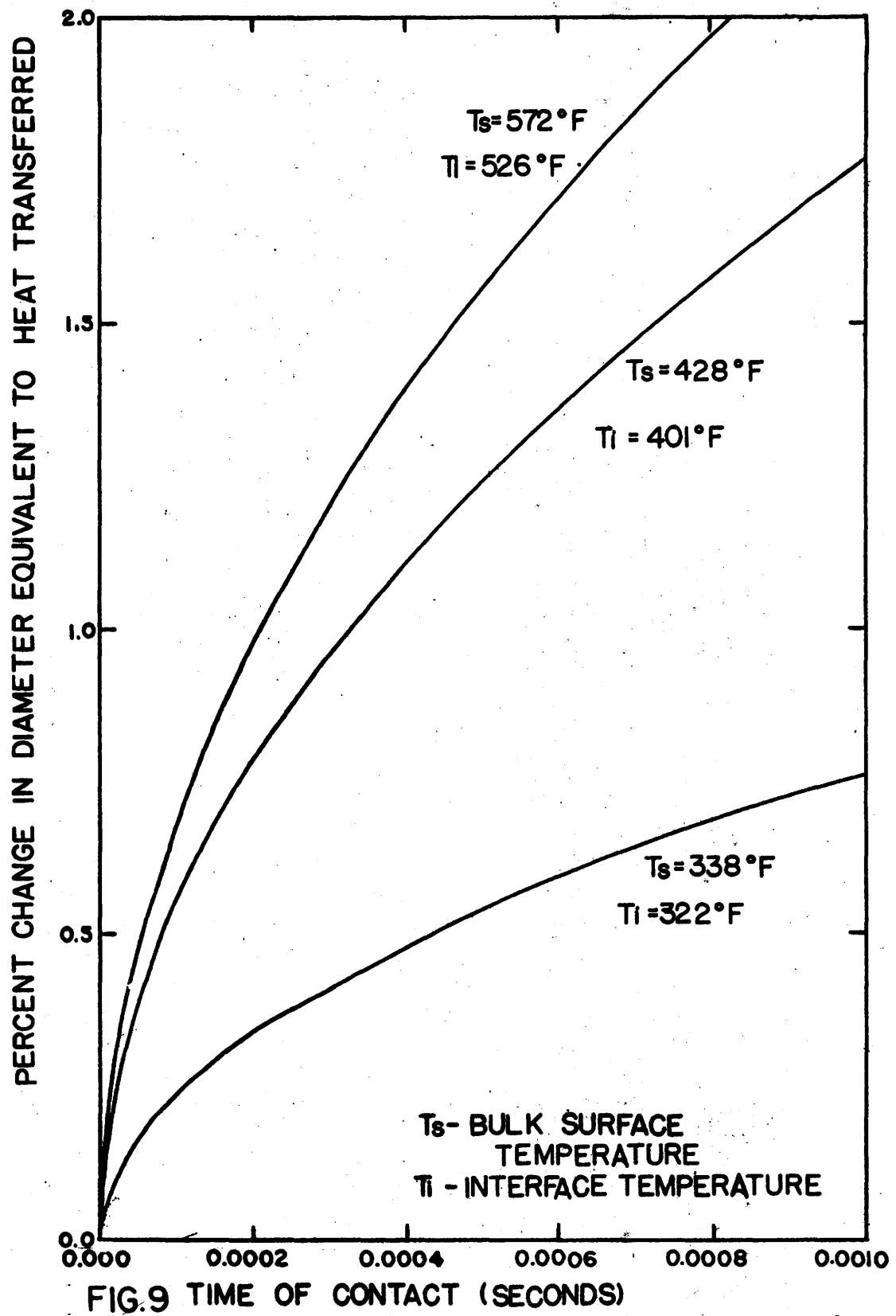
Bankoff and Mehra (8) indicate that direct contact between the liquid and the surface may be common in the transition boiling regime (surface temperatures of 280 to 320 degrees Fahrenheit for pool boiling on a polished surface (15)). Bradfield (9) has observed liquid-surface contact with a drop resting on polished surface at 600 degrees Fahrenheit.

Heat transferred by direct conduction into the drop may be partially dissipated by vaporization at the upper surface of the drop during contact. The remainder may be carried away from the surface as superheat. The amount of superheat in the drop leaving the surface necessary to cause later evaporation of five percent of its volume is approximately 30 degrees Centigrade.

This amount of superheat, distributed throughout the drop, is theoretically not sufficient to cause homogeneous nucleation inside the drop (16). In cases where bubbles were observed to form and grow, nucleation may have occurred on a particle of dust in the drop or in a local region of high temperature. The importance of a delay time in nucleation is unknown but possibly significant (10)(Fig. 31).

(e)   Factors Controlling Wetting

No consistent relation was discernible between the diameter and velocity of the drop and the amount of heat transfer that occured. It appeared therefore that the amount of wetting and therefore the amount of heat transfer was controlled largely by local surface conditions at the point
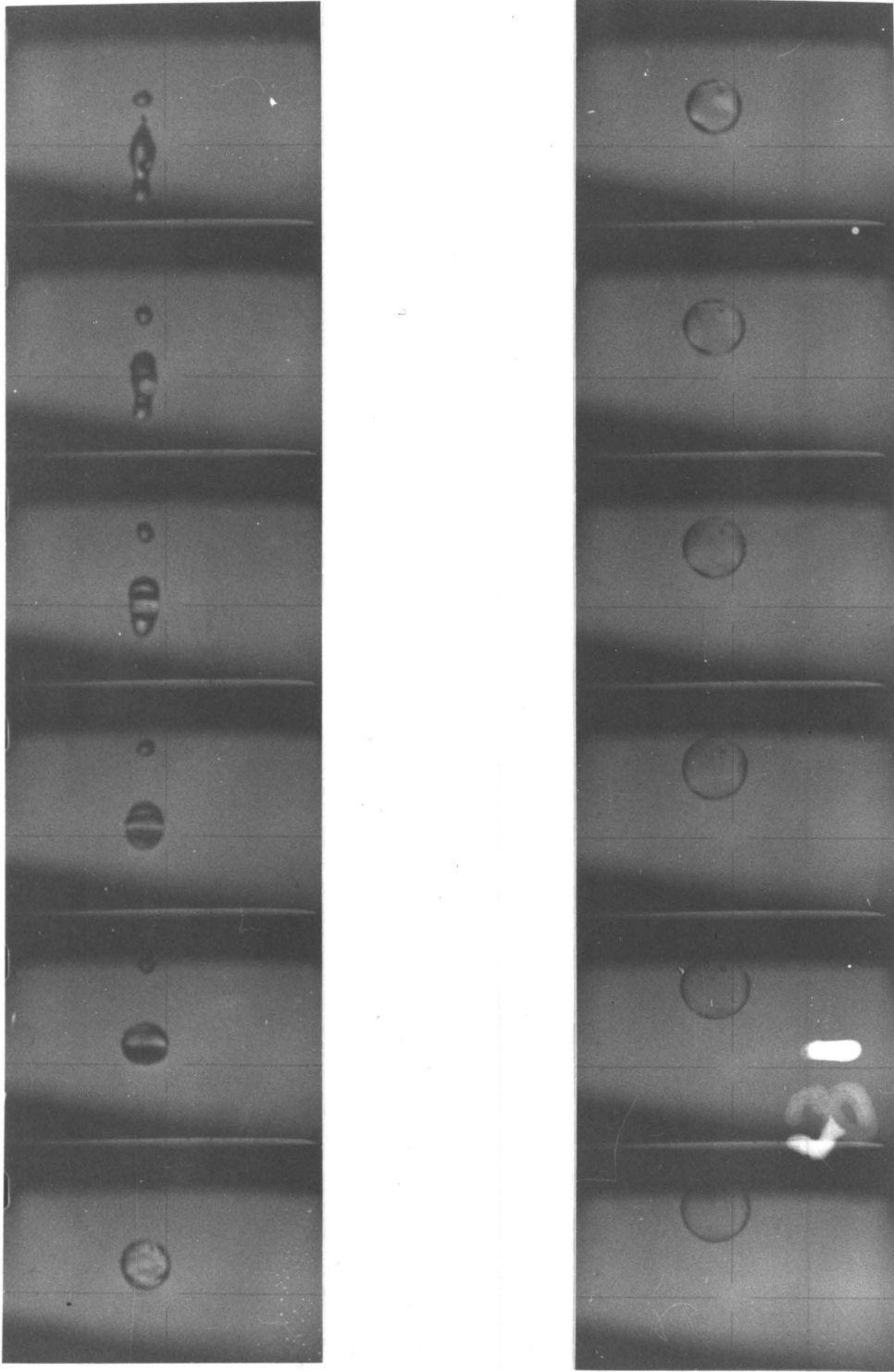
FIG.31   SURFACE TEMPERATURE 900 oF.
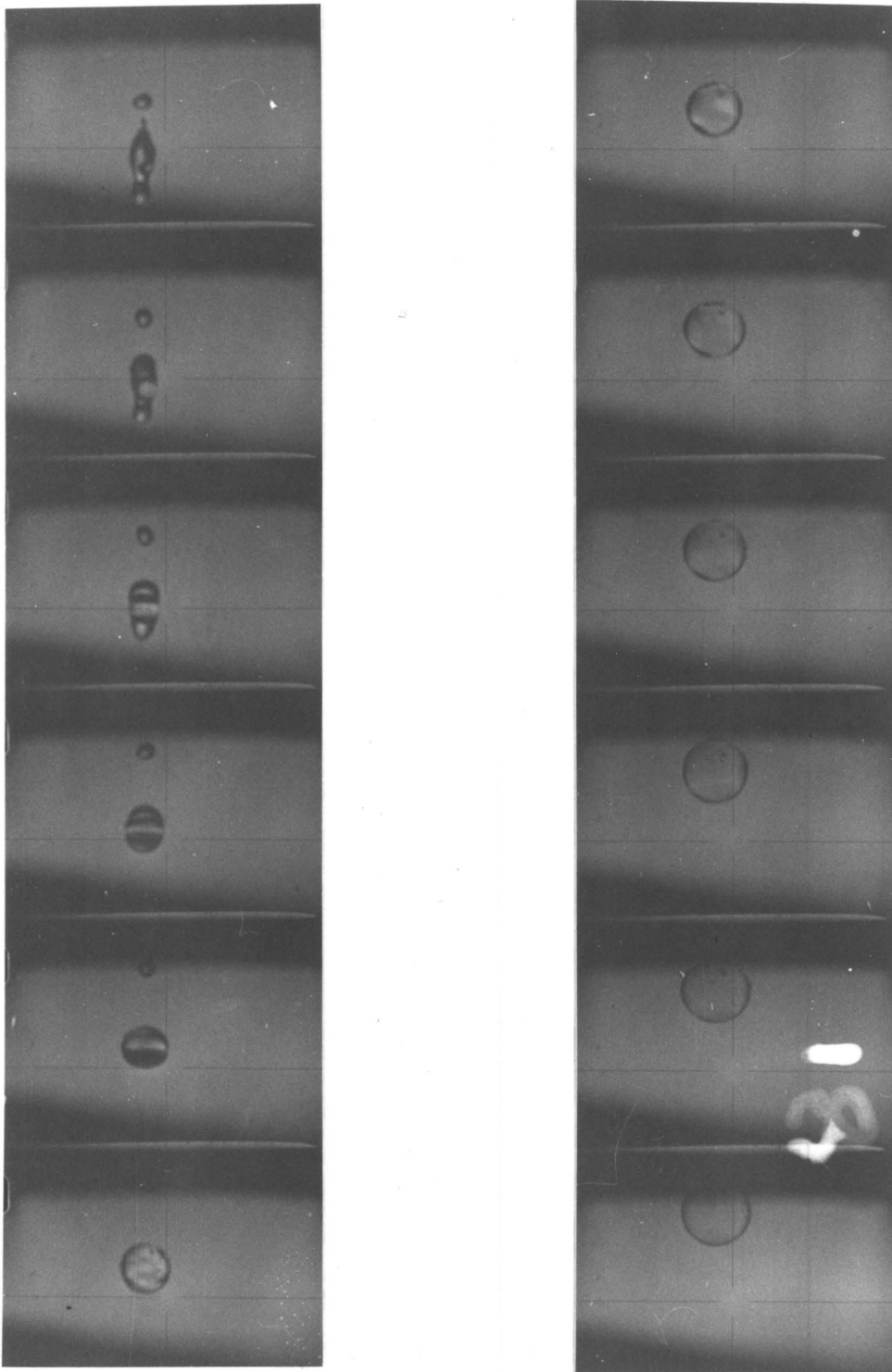
FIG.31   SURFACE TEMPERATURE 900 oF.

of impact of the drop. A plot of percentage change in diameter
against Weber Number however, indicated that a large amount
of heat transfer was unlikely with an impact Weber Number
under 10 (Fig. 27).

In order for wetting to occur the drop had to approach
at some point to within several molecular diameters of the
surface, close enough for intermolecular forces between the
surfaces to be strong enough to neutralize the intermolecular
surface tension force maintaining the liquid surface.

In theory the drop could never touch the surface
as long as vapour was being generated at its bottom surface.
The rise in pressure underneath the drop could cause the
surface liquid to become effectively subcooled, perhaps
allowing a closer approach. The pressure underneath the drop
was calculated using the impact model proposed in this study
(Table VII)[*]. The pressure underneath the 300 to 500 micron
drops   was calculated to be only very slightly above
atmospheric pressure, such that this was not likely an
important influence. However, the calculated pressure
underneath 10 micron drops impacting with a Weber Number
of 10 was in the order of several hundred pounds per square
inch. This may explain why higher heat transfer rates were
obtained by Wachters with a spray system (6).

The model proposed in this study was not however
realistic for the analysis of the initial instant of impact.
In the first place the model assumes that the drop undergoes
flow and deformation according to a rigidly defined pattern

[*] p. 268

which has no basis on any grounds other than it corresponds approximately to the gross physical appearance of the collision. Secondly, flow patterns and changes occur very rapidly during the time just after impact, so that the results of the model in this region of time depended upon the size of the time iterations. The analysis of Savic and Boult (1) may be considered more exact for this purpose. Their analysis yielded an infinite pressure under the drop at the initial instant of impact. This analysis however neglected the influence of the presence of vapour beneath the drop or the effect of vapour generation and as such was not adequate. Thus this influence remains a matter of conjecture.

If one assumes that the drop never quite reaches the plane of the surface, it follows that the drop can only wet the surface at points of roughness projecting from the surface. Since any roughness will not extend more than a fraction of a micron above the surface, the drop surface must approach to this distance. The collision dynamics -- heat transfer model indicates that as the drop spreads out on the surface, the vapour film becomes more than several microns thick (Table III).[*] Wetting can therefore only be initiated during the first contact of the drop with the surface. Surface conditions at the very point of impact may therefore be very important in determining whether or not wetting occurs.

[*] p. 264

In addition, the impact velocity had to be sufficient to bring the drop close enough to the surface for wetting to occur. This was probably the reason why wetting was less common with Weber Numbers under 10.

(f) Factors Controlling the Extent and Duration of Wetting

Once wetting does occur, surface tension forces will determine whether or not the wetted area will grow. If the surface tension between the liquid and the surface is small, as with cold drops colliding with a cold wettable surface, then the wetted area will grow very rapidly. With a high surface temperature, the water-vapour surface tension will be low in the superheated region next to the surface. The variation in surface tension along the liquid surface will cause movement of the surface from the area of low surface tension to the area of high surface tension. This is referred to as the Marangoni effect (28). This will cause the movement of surface liquid along the vapour-liquid interface away from the solid surface, tending to drain any film of liquid advancing along the surface. More important, with increasing surface temperature, the forces of molecular attraction between the liquid and the interface will be lessened. The wetting angle increases until at the liquid critical point (705 degrees Fahrenheit for water) there is no difference between the interfacial energy of the wetted and nonwetted portions and no force at all tending to cause the wetted surface to expand.

This effect was quite noticeable in the photograph by
Bradfield (9) where quite a large wetting angle was observed.
The rate of growth of the wetted area could also be limited
by inertial and viscous forces in the liquid and vapour
film.

The drop is spread out on the surface by the impact.
It is then pulled together by surface tension forces which
act to throw it off the surface again. In cases where the
drop wet the surface, the low surface tension of the liquid
at the solid interface and the generation of vapour under-
neath the drop usually caused the liquid drop to break away
from the surface again (Fig. 30). When the surface temperature
was low, under 300 degrees Fahrenheit, a drop on wetting the
surface occasionally remained on the surface, going into
violent nucleate boiling.

As the wetted area expands over the surface, small
bubbles of vapour may be retained in pockets of roughness
in the surface. These could provide nucleation sites for
bubble formation and growth. The vapour formed may act to
separate the liquid from the surface again. Drops were on
occasion evidently blown off the surface by this
vapourization phenomenon (Fig. 24). With the growth of
bubbles the potential heat transfer becomes much larger because
of the residual film of water left under the bubble (17). The
onset of nucleate boiling could quickly cool the surface to
the extent that wetting would be quite stable. This was
evidently what occurred in cases where the drop remained

without rebounding from the surface.

(g)   The Influence of Surface Roughness

At surface temperatures of 450 to 500 degrees
Fahrenheit, added roughness appeared to increase the
amount of heat transfer (Fig. 28). This could be caused by
the cooling of roughness projections to a temperature where
wetting was more stable. At lower surface temperatures the
effect of roughness did not appear as pronounced. Perhaps
with extensive roughness the liquid did not fill the
microdepressions in the surface, such that heat transfer
was limited by conduction through a reduced area of contact
and the presence of a greater number of vapour pockets
allowed vapourization to proceed easily to separate the drop
from the surface.

(h)   The Effect of Silicone Oil

Measurements of condensate surface tension in the
silicone oil contaminated atmosphere inside the apparatus
indicated that the silicone oil had no noticeable affect on
the water-water vapour interfacial tension (Appendix K).
The photographs of drop impact in a steam atmosphere without
silicone oil contamination indicated that the silicone oil
did not act to prevent wetting of the solid surface by the
drop, so that the drop collision dynamics were essentially
the same as previously observed.

CONCLUSIONS

(1) The amount of heat transfer between a surface and an impacting drop is negligible unless the drop extensively wets the surface.

(2) When wetting does occur the amount of evaporation of a 200-800 micron diameter drop varies from approximately one to ten percent by volume unless the drop sticks to the surface without rebounding.

(3) Provided the drop has a certain minimum impact velocity, the occurrence and extent of wetting is controlled largely by the temperature of the surface and the surface conditions at the point of impact.

(4) A drop in colliding and rebounding from a non-wetted surface generally loses most of its kinetic energy, the fraction increasing with the Weber Number. Most of this energy appears as vibrational energy in the receding drop.

DISCUSSION OF ERRORS

The basic object of the quantitative part of the experimental study was to measure the amount of heat transfer from the hot surface to the drop. If the drop was at its boiling point on hitting the surface and did not evaporate due to any other cause, then the change in diameter of the drop was equivalent to the amount of heat transfer from the surface to the drop. It was necessary therefore to measure the change in diameter of the drop as accurately as possible and to eliminate any extraneous causes of evaporation.

The change in diameter of a drop due to evaporation on contact with the surface was very small, perhaps on occasion less than 1/10 of one percent. Since the drops were only 0.03 to 0.07 centimeters in diameter, the change in diameter was only in the order of 0.0002 centimeters (for a 1/2 percent change in diameter). Consequently, extraordinary effort was applied in examining and minimizing all possible sources of error. A great deal of time was expended to this end, as outlined in the Development Section.

a) Temperature of the Drop as it Approached the Surface

To ensure that the drop arrived at the surface at its boiling point, the interior of the apparatus was closed and purged with steam generated in the base for at least 15 minutes prior to projecting the drop. A measurement of wet-bulb temperature inside the apparatus indicated that

less than five minutes was required to purge the interior of air after it had been opened. Care was also taken to avoid pulling air into the apparatus in condensing water on the drop former. An experimental test established a procedure whereby the rate of generation of vapour in the bottom was never less than the rate of condensation on the drop former. These precautions also ensured that evaporation of the drop on recession from the surface did not occur due to unsaturation of the interior atmosphere.

b) Evaporation of the Drop After Leaving the Surface

After striking the target surface the drop fell a distance of several inches into the oil filled pan. It was considered unlikely that any superheat was retained in the drop to be dissipated, without evaporation, in the oil. A calculation indicated that over 95 percent of this superheat would be dissipated in the 1/12 of a second necessary for the drop to travel from the surface to the pan (Appendix H). Any superheat in the vapour atmosphere through which the drop travels would however give rise to additional evaporation. This evaporation loss would be in the order of 1/10 of one percent by volume for a 300 micron drop for every 10 degrees Fahrenheit of superheat (Appendix E). Superheat was minimized by setting the power input to the wall and roof heaters at levels just sufficient to prevent condensation on the interior surfaces. A cooling coil around the target surface heater minimized superheat from that source. The flow of vapour from the base of the apparatus (which was superheated slightly

as it flowed past the very hot drop projector heater) was
stopped just prior to projecting the drop by shutting off
the top steam vent and allowing the steam to escape through
the bottom vent. A 0.001 inch diameter platinum-rhodium
thermocouple in the vapour indicated virtually no superheat
just prior to drop projection. There was unavoidably
some superheat close to the target surface but it was
probably not a major source of error.

c) Change of Drop Size After Being Caught

There was some question as to whether or not the
drop changed in size after landing in the oil. An approximate
measurement of the solubility of water in the oil indicated
a solubility of less than 0.01 percent by volume. In any
case the oil was saturated with water at 212 degrees Fahren-
heit prior to being poured into the drop catching pan. Any
water lost during the 10 minute period the pan stayed in the
oven was probably regained during the fifteen minute residence
in the saturated atmosphere inside the apparatus prior to
projection of the drop. The drop however was noticed to
change appreciably if left sitting in the hot oil exposed
to the outside atmosphere. This was caused by diffusional
loss of water through the oil to the atmosphere and by thermal
contraction due to cooling. This diffusional loss was
prevented by the glass cover plate. If the oil was allowed
to cool however, supersaturation of the oil with water caused
the drop to grow. Measurements indicated that the double
layers of glass on the top and bottom retarded cooling long

enough to allow several minutes for photography of the drop without appreciable error arising from this source.

d) Gain or Loss of Drops

A bubble of vapour was observed on occasion to form and grow inside the drop as it receded from the surface. This bubble on bursting could throw drops aside and result in a smaller drop being caught. This could occur after the drop left the field of view of the camera and could cause an error that would not be accounted for (Fig. 31).

The vibration caused by the drop projector was hypothetically the cause of the appearance of small drops of unknown origin in the oil (condensate from various sources). Sometimes as many as four or five drops appeared. It was usually possible to select the proper drops from their location in the pan but on occasion this may have been a source of error and was used as a basis for rejection of appreciably negative results (Fig. 28).

After an experiment, the bottom of the oil-filled pan was scanned completely in an effort to find all drops caught. Very small drops could be carried aside by convection currents in the vapour. Small drops were also lost when the drop spattered on impact or was broken apart at the surface by the vapourization phenomena. With the range of Weber Numbers used, this only occured when the drop wetted the surface at surface temperatures of 500 degrees Fahrenheit or less. The magnitude of this loss was estimated and accounted for by estimation of the size

and number of these drops. Generally error arising from the source was quite small. The loss of a 50 micron drop from a 300 micron drop will result in an error of only slightly less than 1/2 of one percent on the equivalent diameter.

e) Measurement of Drop Size in the Oil

The drop caught in the oil was occasionally found to be slightly eccentric. This was probably caused by dust on the drop surface, sometimes visible and sometimes not. If this eccentricity exceeded 1/2 percent, the experiment was discarded. The error was accounted for by tabulating the maximum and minimum dimensions and using these to calculate a probable range in the result. Error caused by flattening of the drop due to gravity force was negligible. (Appendix I).

Dimensions of the drop could be measured to better than 1/10 percent accuracy. The magnification of the substage microscope used to photograph the caught drops was calculated from the photograph of a 0.020 inch scale. Exact correspondence was found between the 0.020 inch scale and the micrometer-stage tool-makers microscope used for the size measurements of the film-image. This microscope could be used to measure dimensions within ± 0.0005 inches.

f) Measurement of the Diameter of the Approaching Drop

The major source of error arose in the measurement of the diameter of the drop as it approached the surface. The roughly 5 1/2 times magnification used in the photography was sufficient to yield an accuracy of better than 1/4 of one percent when the drop was in perfect focus. However,

the point of impact varied slightly so that the drop was usually slightly out of focus. Also, the drop exhibited slight vibratory distortion with drop diameters over 400 microns. These two factors contributed to cause a considerable degree of uncertainty in the actual diameter of the drop. The degree of uncertainly is indicated in the calculated confidence limits on the measurements (Table IX[*]). The confidence limits were calculated using a student's t test probability distribution from a number of measurements of diameter in two directions. The number of measurements was increased with decreasing clarity of the drop up to a maximum of 25. The test was not entirely valid as the clarity of the image was usually worse in the direction of travel because of blurring due to drop motion. The statistical test was however judged to be better than a purely subjective judgement of a confidence limit.

There was probably some degree of systematic error, caused by bias in judging the middle of the blurred edge of the photographic image and by nonlinearity in the relation between photographic image density and exposure.

The degree of flattening of the approaching drop, caused by aerodynamic forces, was estimated to be less than 1/10 of one percent of its diameter (Appendix G).

An error arises in the measurement of the approaching drop size from the photographic image if a nonparallel light source is used for photography. This is caused by reflection of light off the surface of that portion of the drop on the

[*] p.269

side of the camera. The size of this error was measured by selecting a straight uniform cylindrical rod of diameter approximately equal to the size of the drop to be measured. The end of the rod was cut off at an angle to its axis. It was then positioned with its end face oriented toward the camera. The dimension of the shadow photograph of the face, measured perpendicular to the axis of the rod, yielded a measure of the true diameter of the rod. This was compared with the apparent diameter to yield an estimate of the error. This error was found to be less than 1/10 of one percent.

The wire from which the calibration rod was made was found to vary in diameter from one point to another. Its diameter at the point used for image calibration was measured from the normal direction of view using the micrometer stage microscope with an estimated maximum error of less than 0.15 percent.

Shrinkage of photographic film in processing was measured and found to be approximately 0.1 percent. This was automatically accounted for in that the calibration rod image was used to scale the photographs.

g) Measurement of Drop Velocity

Drop velocities were calculated from measurements of the distance the drop moved per frame. The image of the edge of the target surface was not clear. Therefore, the calibration rod was used as a point of reference. When the calibration rod was not visible, the cross hairs on the film

were used. The latter procedure gave rise to larger errors because of the tendency of the Fastax image to bounce up and down. The time period between frames was calculated to within 1/2 percent using the timing marks on the film. The maximum possible error in the velocity measurements varied from 5 to 10 percent depending on the sharpness of the image of the drop. The velocity measured was the velocity normal to the surface. The drop approaches the surface at an angle of 8 1/2 ± 1 degrees to the surface normal.

Wachters (6) found that the velocity component of a drop parallel to the surface remained unchanged during impact and had no effect on the dynamics of the collision. There was more uncertainty in the validity of such an assumption when the drop wets the surface. With an angle of approach of 8 1/2 degrees the tangential velocity component was approximately 15 percent of the normal component. A more important criteria of behaviour, the kinetic energy of the tangential velocity component, was only 2 percent of the normal component. Thus it may be concluded that its influence was not likely to be very important.

h) Target Surface Temperature

The target surface temperature was measured using a thermocouple welded into the center of the platinum-rhodium pellet within 1/8 of an inch of the surface. It indicated the true surface temperature within a few degrees (Appendix J). An error could have arisen in that sometimes the surface temperature changed rapidly due to quenching by condensate

accumulated inside the tube enclosing the heater section.
To overcome this possibility the surface temperature was
measured both before and after an operating run. If the
difference was more than a few degrees the observation was
discarded.

i) <u>Estimation of the Total Error in Diameter Change Measure-
    ment</u>

In the calculation procedure, the approach-diameter
measurement mean and confidence limit values were reduced
to actual dimensions and, with the similarly reduced measure-
ment of the caught-drop diameter, were used to calculate the
mean (most probable) and 90 percent confidence limit values
of the percentage change in diameter due to evaporation (Table1, IX).
The best available estimate of the overall experimental
accuracy is given by the variation in the experimental
results obtained for surface temperatures above 600 degrees
Fahrenheit (Fig. 28). The variation in these results could
not be statistically analyzed because the number of drop
size measurements and therefore the number of degrees of
freedom was different for different experimental observations.
The variation in the diameter change appears however to be in
the order of one percent of the diameter. The major error
arises in the measurement of the diameter of the approaching
drop.

CONTRIBUTION TO KNOWLEDGE

(1) The measurement of the amount of evaporation of a drop of 300 to 700 microns in diameter on striking a hot polished surface at a velocity of from 3 to 8 feet per second.

(2) Further elucidation of the mechanism of heat-transfer to, and of the impact and rebound dynamics of a small drop striking a very hot surface.

(3) Proposal and analysis of a model for the impact process yielding further information about the impact dynamics and the heat-transfer process.

(4) Development of an experimental technique for projecting a small drop upwards on a predetermined reproducible path.

(5) Development of a technique for catching a small drop in silicone oil in a glass bottomed pan in order to measure its size.

SUGGESTIONS FOR FUTURE STUDY

Of particular interest as an extension of this work would be an in-depth study of the influence of surface conditions on drop wetting and heat transfer. This might encompass such factors as surface roughness and the presence of oxide coatings on the surface. Also of interest might be the effect of adding materials to the liquid drop, although this would require the development of new techniques.

Bibliography

1. Savic, P. and Boult, G.T., The Fluid Flow Associated with the Impact of Liquid Drops with Solid Surfaces, Report No. MT-26, National Research Council of Canada, Ottawa, Ontario, Canada, 1955.

2. Savic, P., The Cooling of a Hot Surface by Drops Boiling in Contact with It, Report No. MT-37, National Research Council of Canada, Ottawa, Ontario, Canada, 1958.

3. Gottfried, Byron S., The Evaporation of Small Drops on a Flat Plate in the Film Boiling Regime, Ph.D. Thesis, Case Institute of Technology.

4. Baumeister, K.J., Hamill, T.D., Schwartz, F.L. and Schoessow, G.J., Chem. Eng. Prog. Symposium Series, 64, Vol. 62,52, 1966.

5. Leidenfrost, J.G., De aquae communis nonullis qualitatibus tractatus, Duisburg, 1756., "Treatise on Several Properties of Ordinary Water" Translated into English by Mrs. Carolyn Wares, University of Oklahoma, Norman, Oklahoma, 1964.

6. Wachters, L.H.J., De Warmteoverdracht Van Een Hete Hete Wand Naar Druppels in de Sferöidale Toestand. Ph.D. Thesis, Technische Hogeschool te Delft, Holland, 1965.

7. Lord Rayleigh, Proc. Roy. Soc., 29,71,1879.

8. Bankoff, S.G. and Mehra, V.S., A Quenching Theory of Transition Boiling, Ind. Eng. Chem. Fundamentals, 1,1,38-40,1962.

9. Bradfield, W.S., Liquid - Solid Contact in Stable Film Boiling, Ind. Eng. Chem. Fundamentals, 5,2,200-204, 1966.

10. Hooper, F.C. and Abdelmessih, A.H., The Flashing of Liquids at Higher Superheats, Proc. Third International Heat Transfer Conference, Chicago, Illinois, Vol. 4, p. 44, August 7, 1966.

11. Burge, H.L., High Heat Flux Removal by Liquid Metal Spray Cooling of Surfaces, AICLE. preprint No. 9, Seventh National Heat Transfer Conference, Cleveland, Ohio, August 1964.

12. Nurick, W.H., Transient Heat Transfer from a Liquid Metal Spray Impinging on a Vertical Surface, AICHE. preprint No. 34, Seventh National Heat Transfer Conference, Cleveland, Ohio, August 1964.

13. Perry, J.H., ed., Chemical Engineers Handbook, 3rd. ed., Fig. 1141A, p. 1021, McGraw-Hill Book Co., N.Y., U.S.A., 1953.

14. Hughes, R.R., and Gilliland, E.R., Chem. Eng. Progr., 48,10,497, 1952.

15. Ibele, W., Modern Developments in Heat Transfer, Academic Press, N.Y., U.S.A., p. 119, Fig. 29, 1963.

16. Ibid, p. 99.

17. Moore, F.D. and Mesler, R.B., "The Measurement of Rapid Surface Temperature Fluctuations During Nucleate Boiling of Water", AIChE. Jr. 7,4,620, 1961.

18. Volk, W., Applied Statistics for Engineers, McGraw-Hill Book Company, Inc., p. 231, 1958.

19. Fordham, S., On the Calculation of Surface Tension from Measurements of Pendant Drops, Proc. Royal Society (London), 1-16,194.A., July 28, 1948.

20. Andreas, J.M., et al., Boundary Tension by Pendant Drops, J. Phys. Chem., 42,1001, 1938.

21. Levich, V.G., Physicochemical Hydrodynamics, Prentice-Hall Inc., N.J., U.S.A., 1962.

22. Ranz, W.E., and Marshall, W.R. Jr., Chem. Eng. Prog., 48,141,173, 1952.

23. Jenkins, F.A., and White, H.E., Fundamentals of Optics, McGraw-Hill Book Co., Inc., N.Y., 1957.

24. Rupe, J.H., Third Symposium on Combustion, Flame and Explosion Phenomena, p. 680. The Williams and Wilkins Co., Baltimore, Md., 1949.

25. Gauvin, W.H., and Gravel, J.J.O., Proceedings of the Symposium on the Interaction between Fluid and Particles, London, 20-22, June 1962.

26. Zuber, Tribus and Westwater, International Developments in Heat Transfer, Aug. 28-Sept. 1, 1961, Paper 27, Part II, p. 230.

27. Baumeister, K.J. and Hamill, T.D., NASA Report TN D-3133, December, 1965.

28. Levich, V.G., Physicochemical Hydrodynamics, p. 384, Prentice-Hall, Inc., 1962.

29. Stanton, R.G., Numerical Methods for Science and Engineering, Prentice-Hall, Inc., 1962.

30. McAdams, W.H., Heat Transmission, McGraw-Hill, 1954.

31. Bennett, C.O., and Myers, J.E., Momentum, Heat and Mass Transfer, McGraw-Hill, 1962.

APPENDIX A

DEVELOPMENT OF THE EXPERIMENTAL EQUIPMENT

AND TECHNIQUE

A period of three years passed between the definition of the experimental objectives and their achievement. For clarity, chronological order is avoided and the discussion is loosely organized under the headings of various experimental functions or tasks.

The objective was to observe the impact of small drops on a hot surface and to determine the amount of heat transfer during this impact. If the drop was at its saturation temperature then the amount of heat transfer could be calculated from the change in diameter of the drop. The drop size region of greatest interest in the problem of heat transfer to two phase flows from hot walls is that produced by a conventional spray nozzle, drop diameters in the order of 10 to 100 microns. It was desirable therefore to observe the behaviour of drops as close to this in size as possible.

Measurement of the drop size and velocity before impact could be accomplished by taking a sequence of photographs of the drop at known time intervals just before impact. Since the change in diameter of the drop on impact was expected to be quite small, in the order of a few percent, the initial size of the drop had to be determined as accurately as possible. Consequently the drops had to be photographed with maximum feasible magnification.

This introduced difficulties since the depth of field of a photographic system decreases with increasing magnification. The drop had to strike the surface in the preset plane of focus of the camera lens system. Early tests indicated that the drop rebounds in a state of oscillation. Consequently, photography of the drop just after it leaves the surface did not provide a suitably accurate means of determining its size. Thus it was necessary to catch and hold the drop for size measurement. Elaborate precautions had to be taken to insure that the drop did not undergo further changes in size between impact and measurement.

It is assumed in the following dissertation that the reader is familiar with the apparatus as outlined in the experimental equipment section and in Appendix B.

PROJECTING THE DROP

The objective was to produce a clean drop of the
right size and velocity travelling on a path such as to
strike the surface at a predetermined location. The
initial idea was to take multiple-image photographs
of the drop side-lighted against a dark background using
a still camera and a pulsed or stroboscopic light. The
drop was to be obtained by a spray from a nozzle. Elimin-
ation of all drops but those on the right trajectory was
to be accomplished by a stack of plates with small axially
aligned holes. A photodetector would sense the approach
of a drop on the correct path and activate the stroboscope.
The construction of a stroboscope was begun and tests were
made with a 4 x 5 plate camera with a microscope mounted
in a lens board on the front. Neither this photographic
technique nor the drop-elimination technique were satis-
factory. Discussion with Dr. Westwater of the University
of Illinois indicated difficulties in using side-lighting
for drop photography. A test confirmed this difficulty.
A shift to motion picture photography was necessary when
changing from side to back-lighted or shadow photography.
An elaborate device was constructed to test the above
mentioned technique for extraneous drop elimination. It
proved unsatisfactory as the small drops appeared to be
deflected to one side in passing through the small holes.
Consequently, the drops leaving the last hole were not

necessarily on the correct path.

This failure led to the construction of a drop projector, a device to fire a drop upwards to hit the target surface at a predetermined location. The motive power for the drop comes from an air driven piston which can move a limited distance in a vertical cylinder. Several cylinder-piston assemblies were constructed during development. Each had an increasingly larger piston diameter and less piston-cylinder clearance in order to decrease vibration or whip at the upper end, and so improve the accuracy of the device. The piston was made of stainless steel and the cylinder of brass. At first, no oil was used as it increased friction between the piston and the cylinder. However, the accumulation of corrosion products from the brass caused the cylinder to stick. This problem was overcome by the use of a small amount of light silicone oil in the cylinder.

The top of the projector consisted initially of a vertical stainless steel rod extending from the piston, with an axial hole drilled in the top end, and with a teflon plug in the hole. The teflon plug projected beyond the end of the hole. The end of the plug was smoothed with fine emery paper and polished by rubbing on "Ditto" paper. A small drop was formed at the end of a stainless steel capilliary tube and placed in the centre of the teflon surface. The piston was then moved quickly upwards in the cylinder, by compressed air. When the piston came to

a sudden stop at the top of the cylinder, the drop on the top surface pulled out into an extended body with the top part breaking off and continuing on in the same direction of travel. The lower part remained in contact with the surface. A plexiglass target was set up about 18 inches away to test the accuracy of this device. The accuracy was not satisfactory, probably because of the effect of vibrations and because of slight irregularities in the teflon surface. The accuracy was improved by roughening the teflon surface but was still not satisfactory. Placement of a hole in the middle of the teflon surface and substitution of paraffin wax for teflon did not improve performance. A trial was made using a vertically oriented capillary tube to hold the liquid at the top of the piston extension but this also proved inaccurate. At this point evolved the idea of holding the liquid drop in film boiling. A conical depression was cut into the centre of a brass top constructed as described in the apparatus section. A spherical depression in the surface later proved superior to a conical one probably because of the relative immunity of the drop to the effect of lateral vibrations. The drop has a tendency to vibrate and bounce out of the spherical depression. This is overcome by adjustment of the surface temperature and by roughening the surface of the depression with No. 220 emery paper. The surface must be sanded with emery paper fairly frequently to obtain satisfactory operation. The reason for this is not clear.

This method of holding the drop yields very accurate results. The nearer the projector to the surface the more reproducible was the point of impact. The projector was positioned approximately 3 inches away from the surface. This appeared to be sufficient to allow any drop vibrations to be damped out naturally before the drop arrived at the surface.

This method did not prove successful with non-aqueous liquids as they invariably vibrate and bounce out of the depression.

It proved difficult to ensure an absolutely clean drop on the surface prior to firing upward because of the presence of dust and soluble impurities in the water. The drop, placed on the surface, was allowed to shrink by evaporation to a much smaller size before being fired upwards. This concentrated any impurities present. During operation the drop projector was contained inside the apparatus and although it could be observed through the pyrex pipe wall it could not be approached directly. The use of double distilled water fed in through a stainless steel capillary tube proved unsatisfactory. The unavoidable application of heat to the stainless steel tubing in fabrication evidently promoted the formation of corrosion products which contaminated the water. Following modification, the drop was formed by condensation from the steam atmosphere inside the apparatus onto the outside of a vertical loop of glass tubing. Cold water was forced through the glass tubing from the outside.

Difficulties arose also from the contamination of the water drop with oil. This oil came either from the steam atmosphere itself or arrived by surface flow along the support of the drop forming device. The oil came from seepage from the drop catching pan or from decomposition of the silicone rubber cement. It was only present in minute quantities but became a problem with the concentration of the drop by evapcration. The problem was successfully avoided by allowing the vapor generated continuously inside the apparatus to escape into the room, minimizing the accumulation of oil in the base. As an added measure, the charge of distilled water in the base was changed frequently.

The presence of dust in the drop was a problem which proved difficult to overcome. It came from a number of sources, including the ceramic covering on the drop projector heater and the insulation around the target surface heater wires. Attempts were made to eliminate the dust from all possible sources. Measures taken included covering the drop projector heater with a teflon cap, rebuilding the drop projector heater using stainless steel instead of brass, and substituting a teflon plug for the wooden plug used to block the drop catcher slot. These proved only partially successful. The problem was finally overcome by modifying the drop forming loop such that it could be manipulated close enough to the surface to pick the drop up again. Then, just prior to an experimental run, a drop resting on the surface and containing any dust thereon may be picked up and washed off the former

with further condensation. A new drop can then be placed on the cleansed surface.

A measure of the size of the drop in the depression was obtained using a telescope with a scale graticule and a large magnifying lens positioned near the outside of the glass pipe.

The clarity of the image varied considerably with the position of the telescope and magnifying glass. This distortion was caused by irregularities in the pipe wall. The difficulty was sufficiently overcome by successive trial adjustment of the lens and telescope positions. Considerable improvement was obtained in taping a flat disc with a hole in the centre over the end of the telescope objective lens, decreasing its aperture. The surface of the drop projector was lighted with a small lamp throwing a suitable beam of light. It was found that the size of the drop could be most easily distinguished when lighted from the direction of observation.

Superheat in the vapor in the upper box would have caused a decrease in the size of the rebounding drop during its travel from the surface to the drop catching pan. Since the drop projector heater was a major source of heat, efforts were made to reduce the heat losses from it. First it was enclosed in a cemented shell carved from light porous magnesia brick. The outside surface was covered with high temperature resistant R.T.V. silicone rubber. On use the rubber underwent decomposition, reacting with the steam and

producing a contaminating volatile oil. The heater was rebuilt with a laminated asbestos-fibrous alumina-ceramic cement structure. The heater wire was enclosed in woven glass spaghetti and wound on the spool shaped heater core. The insulation was then laid in layers on top. In a later effort to eliminate dust, the heater was rebuilt as before on a stainless steel core and with the exterior covered with a teflon cap.

THE TARGET SURFACE

The objective in designing a target surface was to present a perfectly smooth, clean, flat, metal surface at a known high temperature in the path of the drop. The surface had to be large enough in extent and formed on a body thick enough to be considered the boundary of a semi-infinite body.

The choice of a polished platinum strip 0.010 inches thick and 0.15 inches wide had an advantage in that it could be heated to a very high temperature by an electric current without corrosion.

The strip, approximately 3 inches long, was mounted in plexiglass and one side was polished to a 0.3 micron finish using a conventional abrasive polishing technique. It was then clamped at both ends to large copper bars projecting through the roof of the apparatus. These provided electrical leads and held the strip in position.

Initially the intention was to use high magnification, in the order of 60 times, in photography of the drop impact. The strip had an advantage in that it could be mounted very near to the glass observation window, necessary because of the short focal distance of a high power objective. This was a matter of some concern before the shift to 16 mm. motion photography, where the small film area places a maximum limit on the amount of magnification.

Initially the intention was to heat the strip very rapidly in order to avoid extensive superheating of the vapor inside. This was accomplished by effectively shorting the strip in series with a fuse across a low-voltage transformer. The fuse blows in a fraction of a second, by which time the strip has become very hot. The temperature achieved was roughly proportional to the square of the fuse rating. The temperature of the strip was measured using a large platinum-rhodium thermocouple made with 0.05 inch wire and spot welded to the strip near the center. The temperature of the strip was found to drop very rapidly after the initial heating. Calculations indicated that the heat loss was largely by conduction out the ends of the strip. The temperature change could be followed with a high-speed recorder, but the exact point on the trace corresponding to the time of impact of the drop was difficult to determine. A relay controlled circuit was then built to maintain the temperature constant after the firing of the fuse. It was initially designed to operate using alternating current, but the 60 cycle voltage variation upset the operation of both the high speed recorder and the conventional chopper-amplifier recorder later used in an attempt to measure the temperature. Provision was then made to use a battery power supply.

It was discovered that when the strip was heated it bowed out because of thermal expansion. In order to avoid this, the strip was placed under a calculated amount of tension. This resulted in a lengthening of the strip and rippling

of the polished surface. A change to a Platinum-10% Iridium alloy strip prevented this from occurring.

Since the drop did not strike the surface of the strip at the same location as the thermocouple, it was necessary to calculate the temperature distribution along the strip. This was difficult because the resistivity and thermal conductivity of Platinum-10% Iridium at high temperatures was not available, and because the large thermocouple constituted a heat sink of unknown properties. A platinum-10% rhodium strip was substituted and a number of 0.0005 inch platinum wires and one 0.0005 platinum-rhodium wire were spot welded to the strip at points spaced along the edge. This allowed the direct determination of a temperature profile along the strip. This gave rise to difficulties because it was necessary to clean and repolish the strip periodically, and it was difficult to do so without breaking the wires at the welds. Also, the more convenient continuous heating of the strip was contributing substantially to superheat in the steam atmosphere. A solution to these difficulties was found in redesigning the target in the cartridge form described in the apparatus section.

The surface must be repolished fairly frequently because the metal tended to vaporize preferentially at the grain boundaries, leaving a roughened surface. This was not difficult because the cartridge unit was easily removed. The "Ceramo" thermocouple used to measure target surface temperature was initially inserted into a hole in the top of

the pellet. This yielded a temperature indication which was uncertain due to heat conduction down the thermocouple from the much hotter region above the pellet. Also, the stainless steel sheath was completely destroyed by corrosion. To overcome this problem a V-shaped groove was filed into the side of the pellet down to the thermocouple hole. A new platinum-rhodium thermocouple with a platinum-rhodium sheath was fitted into the hole and the groove was filled with platinum-rhodium alloy using an electrical welding unit.

The alternating-current voltage used to heat the target surface upset the operation of a chopper-amplifier recorder but a slide wire potentiometer was found satisfactory in measuring the thermocouple e.m.f.

The cooling coil around the cartridge surface heater unit was initially encased in "R.V.T." silicone rubber. This decomposed in the steam atmosphere and had to be removed. Initially "aerochlor" chlorinated hydrocarbon oil was circulated through this coil by a large "Haake" circulating unit. The oil softened the "tygon" tubing used to contain it, causing it to burst. Flexible stainless steel tubing was substituted as rigid tubing tended to transmit vibrations from the pump to the apparatus. On testing, the temperature rise in the cooling coil was found to be excessive, the oil circulation rate being severely limited by the limited pressure output of the "Haake" pump. The decision was made to use tap water which was readily available at sufficient pressure. The "Haake" unit was used as a basic heating unit

along with an auxillary electric heater wound on the copper tubing. A counter current heat exchanger was found necessary to conserve heat. The "Haake" unit and electric heater were later replaced by an "American Standard" steam heat exchanger of 1.2 square feet heat-exchange area. This operated successfully with throttling on the input and output with a considerable amount of steam being vented to the drain. The amount of steam escaping into the room was cut down considerably by a jet of cold water played onto the copper venting tube. The cooling coil was occasionally plugged with fragments of scale but these were easily removed by reversing the input connection.

PHOTOGRAPHING THE DROP IMPACT

In order to photograph the drop impact at the surface,
it was necessary to build a window on the front of the appara-
tus and to maintain its temperature high enough to prevent
condensation on the inside surface. This was to be accomplished
by having two circular windows with hot fluid circulating in
between. As originally constructed the inside window was
cemented directly into the wall with epoxy resin. It was
separated from the outside window by an elaborately constructed
spacing ring. The outside window was held in place with a
retaining ring screwed into the front wall. The hot fluid
flowed through fittings into the wall itself and thence
through channels in the wall and spacing ring and through
between the windows. It was designed in this way to make
the window assembly as thin as possible. This was necessary
because, at the high magnification originally intended, the
focal distance was very short. A number of difficulties
arose. The fluid leaked out between the glass and the epoxy
seal, around the threads of the retaining ring and through
flaws in the welding covering the channels cut in the stain-
less steel wall. Also thermal stresses caused the glass to
crack. When lower magnification photography was decided
upon, the minimum thickness restriction could be relaxed.
The front wall and window assembly was rebuilt in the present
form, which proved entirely satisfactory. It was important
however, to avoid overtightening the nuts on the retaining

ring as this caused the windows to crack. Very thin neoprene gaskets were used, teflon being found too rigid to provide an adequate seal.

Ethylene glycol was circulated through the window as a heating fluid. It was heated and pumped with a size FE-1 "Haake" unit. The glycol became filled with corrosion products from the fittings in the pump and had to be replaced frequently. A screen and glass wool filter in the lead tubing helped reduce the amount of dirt. Plasticizer oil was leached from the tygon tubing by the hot glycol. This oil had a tendency to collect on the windows after a period of operation, making it necessary to clean them frequently. This problem was solved by polishing a dried film of detergent onto the glass surface before installation.

In measuring the size of a small drop by photography, a number of factors limited the precision of the measurement. There was the resolution of the lens system, the basic acutance or line definition of the film-developer combination and the quality of the image as determined by the light intensity, spectrum and incident direction, by the quality of the lens and by the distance of the object from the plane of focus. The allowable minimum depth of field was limited by the accuracy of the drop projector. The resolution of the lens system was inversely proportional to the Numerical Aperture, but so was the depth of field. Thus, decreasing the lens opening increased the depth of field but decreased the lens resolution and increased the amount of light

required. The absolute distance resolution on film was a product of the film image resolution and the degree of magnification. The depth of field was however also inversely proportional to the degree of magnification. Another problem arose in that the degree of magnification was limited by the drop velocity, because two images of the drop prior to impact were required in order to measure the drop velocity. The problem was approached by assembling a lens system to yield approximately the magnification desired followed by a reduction of the lens aperture until the minimum desired film exposure was obtained.

It is interesting to note that for a given magnification, the maximum depth of field obtainable was dependent only on the amount of light available and independent of the focal length of the lens. A longer focal length lens has the advantage of being farther from the object, thus reducing angular distortion.

The Fastax lenses with extension tubes were first used for photography of the drop impact. Magnification was approximately 2 times. The Fastax 7.5 K.W. arc light was used with a large parabolic reflector designed to concentrate the light. It did not provide sufficient illumination for any higher degree of magnification. In later work with the stroboscope the magnification was raised to about 5, using a 1.5 power microscope objective and a 7 power photographic (B & L Ultraplane) eyepiece. The aperture of the objective lens was reduced by a metal disc with a hole in the center

to the point where the amount of light admitted was just sufficient for the task. The lens system, mounted in a standard microscope tube fitted onto the Fastax extension tubes, had only 5 times magnification because the eyepiece-to-film distance was less than the standard 25 centimeters.

In choosing the film a number of letters were written to various companies requesting their assistance. Ansco was extremely cooperative, suggesting that a fine grain film with extended development yields results superior to those obtained using a faster film. Their Versapan was compared in tests with several other brands and was adopted as yielding superior results. It was interesting to note the lack of correspondence between film granularity and acutance or line definition. It was also noted that line definition can be improved if the film is the limiting factor by underdevelopment followed by treatment with an image intensifier solution.

The film was initially in a one quart quantity of "Acufine" developer for approximately 5 minutes at over 80 degrees Fahrenheit. Better results were obtained using a one gallon quantity of Ansco "Hyfinol" developer at 70 degrees Fahrenheit.

In running 100 foot lengths of film at its maximum rate through the Fastax W.F. 4S. camera, it was necessary to use a 400 foot balanced reel on the takeup spindle. Otherwise the initial tension on the film was too great, breaking the film. It was not possible to run a length of

film through the camera more than once as the film on running was cracked slightly near the perforations and broke on the second run. Also, the use of the 220 volt rather than the 115 volt input to the Goose Control usually caused the film to break.

The problem of aligning the optical axis of the camera with the surface was difficult because of the small depth of field. One technique used was to hold the point of a sharp needle on the surface with the needle held inclined to one side in the plane of focus of the camera. When the point of the needle was just visible but not its reflection, then the camera was correctly aligned. This method had the disadvantage of tending to mar the highly polished surface. Another technique, somewhat less precise, was to focus first on the front and then on the back edge of the target surface, noting the relative position of the two. The angle of the camera is then adjusted until both the front and back edge of the surface when in focus are at the same level in the field of view. The optical axis of the camera is then parallel to the surface. After measuring the angle of the camera using an adjustable protractor and level, it was simple to duplicate the alignment.

Before the impact of a drop could be photographed, it was necessary to focus the camera on the point at which the drop will hit. This was accomplished at first by focusing the camera on a needle point prepositioned at the point of impact. This was later replaced by a calibration rod of known

diameter positioned near to the surface and located such that it always projected at right angles slightly into the field of view. It was far enough to one side to avoid being hit by the drop and provided an ever present size reference on the film. This was desirable because film had a tendency to change size slightly in processing and according to ambient temperature and humidity. The magnification was changed slightly on occasion by accidental movement of the lens. This was later prevented by cementing the lens in place with rubber cement. This calibration rod also provided a fixed point of reference in the field of view. This was desirable because the front edge of the target surface was not in focus and was therefore not clear enough to provide a reference location for drop velocity measurement. The cross hairs on the film image were not suitable for this purpose because the film image tended to bounce or move up and down, an unavoidable phenomenon with a rotating prism camera.

It was difficult at first to adjust the position of the camera. This was overcome by the installation of a cross-feed from a lathe between the tripod and the base of the camera.

With shadow photography if the light source is not parallel, light will be reflected obliquely off the curved sides of a drop, yielding an image which is indistinct and undersize. To test the degree to which this was occurring the calibration rod was cut off obliquely with the end face

oriented away from the light. The dimension of the shadow image of this face perpendicular to the axis of the rod was then the true diameter of the rod. Initial tests showed this error to be considerable. Masking of a large part of the area of the ground-glass screen behind the surface reduced it to a tolerable value. The use of the light source was not very efficient and could probably be improved to allow greater depth of field and/or greater magnification.

The light for photography passes through a stainless steel tube passing through the back wall of the apparatus. It was intended to eliminate any heat radiation from the light source. It was filled originally with distilled water, but bubbles of gas formed on the walls and glass ends of the tube when the tube was heated. The water was therefore replaced by glycerol. The tube was at first completely sealed. On heating, the expanding liquid forced its way out through the seals at the ends and on cooling, air was drawn in. A small vertical tube was installed in the top of the tube, allowing for expansion of the liquid. The tube had to be checked for bubbles before operation. The glycerol in the tube turned yellow in use, perhaps due to the influence of the intense ultraviolet light from the flash tube. The glycerol had to be replaced every few days as this yellowing reduced the light intensity considerably.

The drop approaching the surface was found to be quite spherical except for fairly large drops of around 700 microns in size. A problem then arose in measuring the

equivalent spherical diameter of a vibrating drop. From a brief consideration of the physical deformation occurring the decision was made to measure the maximum and minimum dimensions of the image in all available frames. The equivalent diameter for each frame was calculated as follows:

$$D_{eq} = (D_{min.} \times D_{max.}^2)^{1/3}$$

The actual diameter chosen as correct was the maximum $D_{eq.}$ calculated. This assumes that the drop is a prolate elipsoid.

SIZE OF THE REBOUNDING DROP

Initial tests showed that the drop rebounding from the surface was not spherical but highly deformed. Initial attempts to measure the volume assuming radial symmetry indicated that the method was not sufficiently precise. Also it was evident that in many cases that the drop shape was not radially symmetric. The decision was then made to catch the drop, to remove it from the apparatus and to measure its size from a microphotograph.

An elaborate apparatus was constructed to catch the drop. It was designed such that it moved into place underneath the target surface after the drop had passed. The drop when rebounding would presumably fall into the catching pan. The oil in the 1/2 inch long by 1/4 inch wide pan was prevented from spilling when the pan was moved rapidly into place by a sliding glass cover. A pair of solenoids and a push button switch served to move the catcher assembly into place and to draw the glass cover back at the end of travel of the major assembly. After the drop was caght the glass cover could be replaced and the whole catcher removed from its stainless steel sleeve. The drop could then be photographed from below through the glass bottomed pan.

Tests of this device indicated that the drop often did not rebound directly back on the initial line of travel. This erratic rebound may have been caused by either turbulence

in the vapor in the top part of the apparatus or by some
phenomenon associated with the collision itself or more
probably, by both. The variation was such that the apparatus
had to be discarded and the small pan replaced by a much
larger stationary pan.

The present method of catching the drop was then
adopted. The apparatus was not designed initially with
this in mind, and the target was very near to a vertical
front wall. Consequently it was necessary to incline the
target surface forward so that the drop would rebound
backward into the catching pan. This inclination had an
unanticipated advantage in that in aligning the camera
with the surface, the drop arrives on an oblique path,
travelling through the plane of focus. The best image of
several may be selected and the coincidence of the path of
the drop with the plane of focus is not quite as critical a
requirement.

In constructing the drop catching pan some difficulties
were encountered with stress cracking of the glass bottom.
The substitution of "R.V.T." silicone rubber for epoxy
resin as a sealant proved most successful although care
had to be taken to clean the oil off the rubber after use as
the oil tended to soften the rubber. It was also found
advisable to allow the rubber to set in an oven at a tem-
perature of 120°C. This kept the glass in compression and
notably decreased its tendency to crack.

The drop catching pan was filled with Dow-Corning silicone fluid having 20 centistokes viscosity. At first the drop, after landing in the oil, settled down onto a glass surface treated with General Electric SC87 anti-wetting agent (dimethyl dichlorosilane). It was assumed on the basis of work by Rupe (24), that the angle of contact between the water-oil interface and the oil-glass interface was such that the drop could be assumed to be spherical. Considerable experimental work with a high surface temperature yielded erratic results. On reducing the surface temperature, the percent evaporation calculated from experimental measurements was almost invariably negative. A consideration of all possible sources of error led to the conclusion that the image of the drop after being caught was too large. Measurements of the size of the image indicated a variation in diameter around the circumference much as several percent. Photography from the side of drops resting on a treated glass surface in silicone oil indicated a contact angle in the order of 140 degrees. (defined as the angle between the water-glass and water-oil interface). Calculations based on measurements of the width of the base in contact and the diameter indicated an error of -1.4 ± 0.5 percent.

In a private communication, Dr. Stedman of the National Research Council, Ottawa, Ontario, indicated the likelihood that the drop might oscillate slightly in moving onto the surface and that since there is a difference in

the contact angle depending on the direction of the last motion of the line of contact, this would result in an eccentricity of drop shape.

Numerous oil-soluble emulsifiers were used to reduce the surface tension of the silicone oil but were not effective in preventing this wetting effect. This may have been because the oil-glass interfacial tension was simultaneously increased. The use of mineral oil yielded satisfactory results at low temperatures, but the results were again unsatisfactory at 100 degrees centigrade.

A solution to the problem was finally found in coating the surface of the glass with a thin film of General Electric "R.T.V." translucent silicone rubber. This was accomplished by dissolving the uncured rubber in roughly twice its volume of carbon tetrachloride. This was made up in a volume of approximately 5 cubic centimeters and spread on the glass surface using a glass rod. The carbon tetrachloride was allowed to evaporate and the rubber to cure at room temperature. Precautions were taken throughout this procedure to minimize dust contamination of the coating. When the silicone oil was added to the pan it penetrated the rubber surface, reducing the interfacial tension to a negligible value and yielding a water-surface contact angle of effectively 180 degrees. Qualitative tests indicated that the refractive index of the rubber and silicone oil were not significantly different, so that minor irregularities in the rubber surface did not distort the image of the drop

when photographed from below. It was not necessary to coat the glass cover with rubber. Treatment with SC87 was sufficient because the drop of water contacts it only momentarily if at all. The spacing between the glass cover and the rubber coated base plate was more than one millimeter, sufficient spacing for the largest drop.

The surface was found to age with use so that some wetting occurred This tendency was overcome by adding a few drops of oil to the rubber solution before spreading it on the surface, by wetting the surface with silicone oil from a dropping bottle after rinsing with carbon tetrachloride (procedure after every experimental run) and by the use of a mixture of Dow-Corning 50 cs. 200 and 20 cs. 555 silicone fluids. Both these have a density only very slightly less than that of water. Slight eccentricity was still occasionally encountered if particles of dust in the fluid came into contact with the drop.

Several measures were necessary to prevent condensate from entering the catching pan. Condensate falling from the roof was a problem especially when the surface temperature was low and the heat conducted from the surface heater into the roof was not sufficient to compensate for heat losses through the insulation. A thin stainless steel roof was installed to protect the back portion of the catcher. Two small cartridge heaters were cemented to the roof with "thermon" high thermal conductivity cement. The power input to these was controlled to reduce condensation to a minimum.

A heater was installed in the lower part of the front wall
to prevent condensation there. It was also discovered that
if the catcher was heated too hot, above roughly 115 degrees
centigrade before being inserted into the box, it caused
any condensate with which it came in contact to boil
vigorously, splattering small drops into the oil pan. A
cartridge heater was installed in the handle of the drop
catching assembly to prevent the catcher from cooling excess-
ively while sitting in the steam atmosphere, preventing
condensation on the metal at the front edge of the catching
pan.

In proposing this thesis, one must be certain
beyond all reasonable doubt that the size of the drop, as
calculated from a measurement of the diameter of the image
on the microphotograph, is the same as when the drop left
the target surface. The process of development included an
examination of all possible sources of error and an effort
to minimize and where possible to eliminate them. Since the
amount of evaporation at the surface is very small, any small
factor could result in a very large error.

The drop will evaporate to some extent during its
passage from the target surface to the surface of the oil.
This will be caused by superheat in the drop and superheat
in the steam; this latter condition is difficult to avoid
since heating surfaces are required to prevent condensation
and because large heat sources exist in the surface and
drop-projector heaters nearby. The temperature of the

atmosphere was measured using a 0.0005 inch diameter thermo-couple, fine enough to yield an accurate gas temperature. Initially the superheat was in the order of 20-30 degrees centigrade. This was reduced to less than ten degrees by surrounding the target heater with cooling coil, by thoroughly insulating the drop projector heater and by reducing the power input to all other heaters such that their heat output was just sufficient to prevent condensation . The evaporation of the drop due to superheat picked up at the surface or due to the thin film of very hot vapor directly adjacent to the target surface was considered as a legitimate part of the phenomena and was ignored. Evaporation could also be caused by air in the steam atmosphere. Air was introduced during the process of an experimental test with the opening of the side port and with the introduction of the drop catcher. A wet-bulb temperature measuring device was constructed in which a small thermocouple (0.0005 inch diameter) was placed in a drop of water. It was found that the wet bulb tempera-ture recovered to its equilibrium value within several minutes of opening the apparatus, indicating that a delay of 10 minutes after introduction of the drop catcher was more than sufficient to ensure a pure steam atmosphere (Fig. 32).

With the drop catching assembly in place, the vapor jetted up through the hole in the assembly. During a test this jet would blow the rebounding drop away and had to be eliminated. Initially this jet was eliminated by introducing a quantity of cold water into the boiling water in the base.

1 INCH
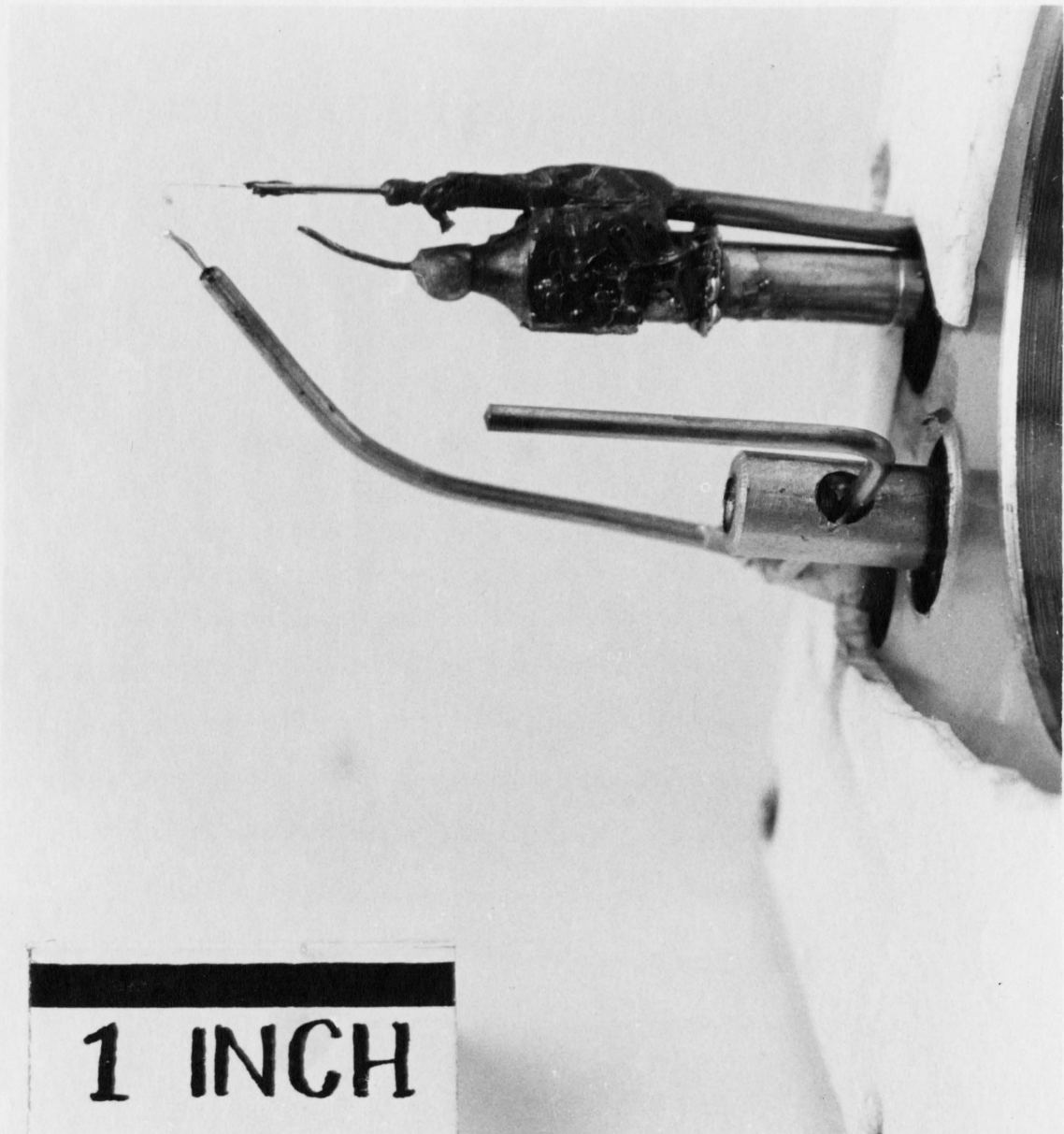
FIG.32   DEVICE FOR   SATURATION
TEMPERATURE   MEASUREMENT

The alternative procedure of venting off steam at the base was adopted to avoid the possibility of drawing in air by this procedure.

The next possibility to be considered was the change in size of the drop from the time it entered the oil until it was photographed. Before being placed in the catching pan, the oil was saturated with boiling water. It was then placed in the pan of the preheated catcher assembly in an air oven at 120 degrees centigrade. The surface of the pan was covered with its sliding glass cover to prevent the entry of dust and to retard the escape of water vapor. The catching assembly was then placed in the saturated steam atmosphere in the box for at least 15 minutes before a drop was caught. It was assumed that during this period the oil cooled to near 100 degrees centigrade, and that it reassumed its water saturated condition. On removal from the saturated atmosphere the oil will lose its saturation and the drop may change in size considerably in a relatively short time. In order to prevent this loss, the drop was covered with a glass cover enclosing it in a layer of oil between two glass surfaces. Another effect may occur at this point, since when the oil cools, the solubility of water is less and the drop may increase in size. In order to minimize this effect the glass cover was preheated to 120° C. and the bottom of the pan was insulated by a layer of air and an extra glass bottom. Every effort was made to photograph the drop as soon after removal from the saturated atmosphere as

possible. Initially a fairly high degree of magnification was used in the photography of the drops. This was reduced to a much lower value of approximately 20 in order that the drop be located and brought into view more quickly. It then required only about 1 1/2 minutes to photograph a single drop.

In taking these microphotographs, a problem of camera vibration during photography was solved with the adoption of a "Pentax S.1.a." 35 mm. camera body and flexible cord shutter release. The use of a green filter and a collimated lighting system resulted in improved results. Illford F.P.3 film used with Acufine developer yielded better line resolution than other combinations tested.

In the development of the apparatus considerable experience was obtained in the construction of electric heaters. This experience leads to the conclusion that where possible, package heater units should be used.

APPENDIX B

The foregoing is a very detailed description
of the experimental apparatus intended as a guide for its
assembly or for a critical analysis of its function. A
simplified outline may be found in the "Apparatus" section
in the main body of the thesis.

THE DROP PROJECTOR

The drop projector was an assembly which formed a drop, held it in film boiling in a spherical depression until it vapourized to the desired diameter and then projected it upwards to collide with the target surface (Fig.10).

The size of the drop was estimated by observation through a telescope with a linear scale graticule. The drop was lighted from the direction of observation using a 150 watt spot lamp.

The top of the projector was a solid 30 degree cone, 3/4 of an inch across the base, with its base facing upwards. It was constructed of brass with a 1/4 inch diameter platinum-10% rhodium center and a nickel plated top. A shallow spherical depression was machined into the center of the top surface. This surface was finished with No. 220 silicon carbide abrasive. The cone was fastened by a hollow 7/32 inch diameter stainless steel shaft to the top of the drop projector piston below.

The 1/2 inch diameter 2 1/4 inch long stainless steel piston was contained in a brass cylinder. The piston could move upward a distance of only 1 1/2 inches before it was stopped by a brass top screwed onto the top of the cylinder.

The piston was driven upward by compressed air, admitted into the bottom of the cylinder at the desired instant through a solenoid valve. The air pressure was
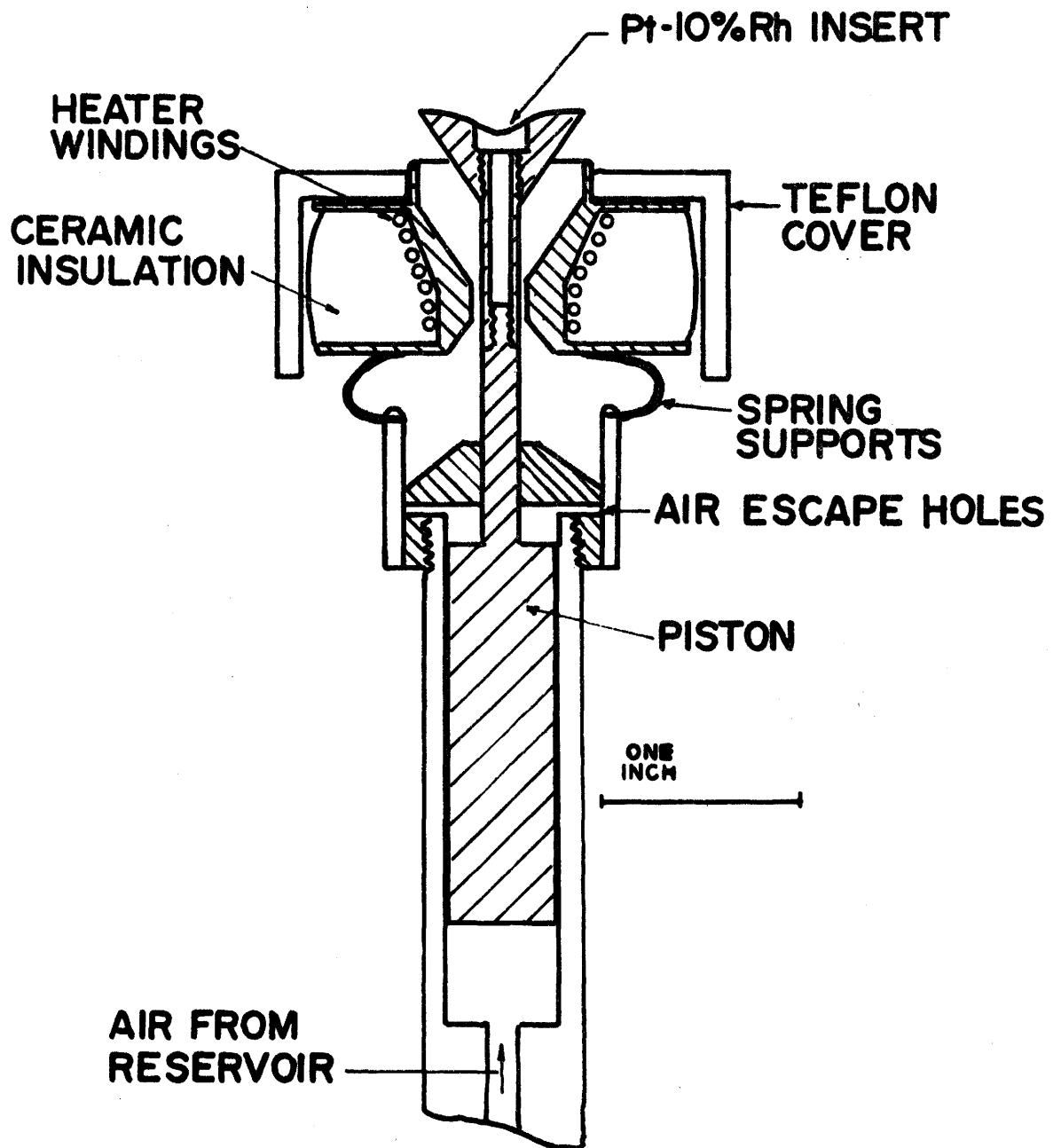
FIG. 10   DROP PROJECTOR

preset with an adjustable pressure-control valve. Provision was also made for evacuating the air system using a water jet ejector, for use in pulling the piston down.

At the lower end of the piston's travel, the conical surface of the top of the projector came in uniform contact with an electrical heater. This served to heat the top of the projector to a high temperature such that a drop of water would sit in the depression in film boiling. The heater consisted of a stainless steel spool, wound with Nichrome wire and encased in thermal insulation. It was mounted on two "U" shaped stainless steel springs fastened to vertical bars attached to the outside of the cylinder. The heater was enclosed in a teflon cap to reduce heat losses.

The cylindrical body of the drop projector was screwed into a brass shaft which passed vertically through a 3/4 inch stainless steel Swagelock fitting in the bottom of the apparatus.

The drop of water was formed by condensation on a loop of glass capillary tubing, (Fig. 11). When the drop was large enough it fell by gravity from the end of the loop into the depression in the top of the drop projector a short distance below. The glass tube was moved away before the drop was fired upwards.

One end of the glass tube was mounted with RTV silicone rubber on the end of a stainless steel capillary tube which was silver soldered at a lower level into a

larger vertical 1/8 inch stainless steel tube. The larger tube was fed through a 1/8 inch Swagelock fitting in the base of the apparatus, sliding in the teflon ferrules in the fitting. A handle attached to the 1/8 inch tube below the base, allowed manipulation of the drop former. A positioning device was locked with a set-screw onto the 1/8 inch tube near the base. It operated by means of a pin which dropped into a hole in the top of the base plate. A threaded rod projecting through the base plate allowed external adjustment of the distance the pin drops down into the hole. This enabled the reproduction of a preset position, allowing placement or removal of a drop from the spherical depression (Fig. 16).

Condensation on the glass loop was caused by forcing cold water from a one milliliter glass syringe through a dirt filter, a long extension capillary tube, through the glass loop and out into the bottom of the apparatus.
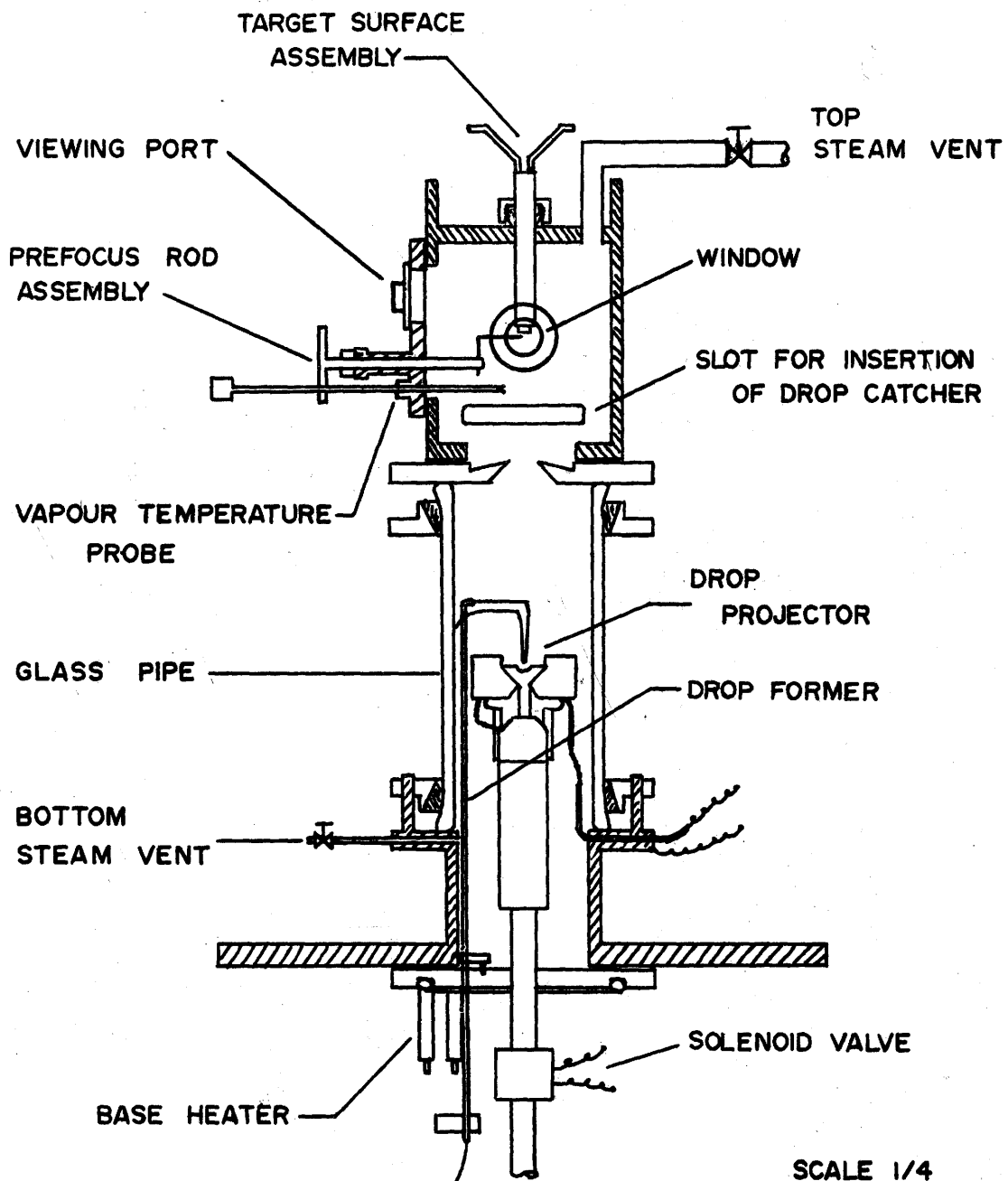
FIG. 16   APPARATUS USED IN THE INVESTIGATION OF
DROP IMPACT ON A HOT SURFACE

TARGET SURFACE ASSEMBLY

Directly above the drop projector was situated the target surface with which the drop collided. The surface was made at the end of a cylindrical platinum-10% rhodium pellet, 1/4 inch in diameter and 3/8 inches long (Fig.12). The end of the pellet was cut off at an angle of about 8 1/2 degrees from a right angle. The flat surface was polished to mirror finish. A standard abrasive paper polishing technique was used, the final abrasive being 0.3 micron alumina slurried in water.

The pellet was held in place with the axis of the cylinder vertical, by four vertical 10 gage Nichrome wires which were silver soldered 1 1/2 inches above the pellet onto two flattened copper tubes. The pellet was heated to a high temperature by means of an electric current flowing through the Nichrome wires. Power was supplied from a 12-volt 100-ampere-capacity transformer, and controlled with a variable transformer on the high voltage side.

A 1/25 inch Ceramo platinum-10% rhodium thermocouple with a platinum-20% rhodium sheath was welded into the center of the pellet. This was done by cutting a V shaped slot in the side of the pellet near to the bottom. A 0.041 inch hole was drilled axially into the pellet as far as the groove. The thermocouple was inserted into the hole and the groove was filled with platinum rhodium alloy using an electric argon welding unit. The thermocouple led up

ELECTRIAL LEADS

THERMOCOUPLE

SILICONE RUBBER
SEAL

SUPPORT
FITTING

WOVEN GLASS
INSULATION

ROOF OF
APPARATUS

VYCOR GLASS
TUBE

NICHROME WIRE

COOLING COIL

PLATINUM-RHODIUM
PELLET

TARGET SURFACE

1/1 SCALE
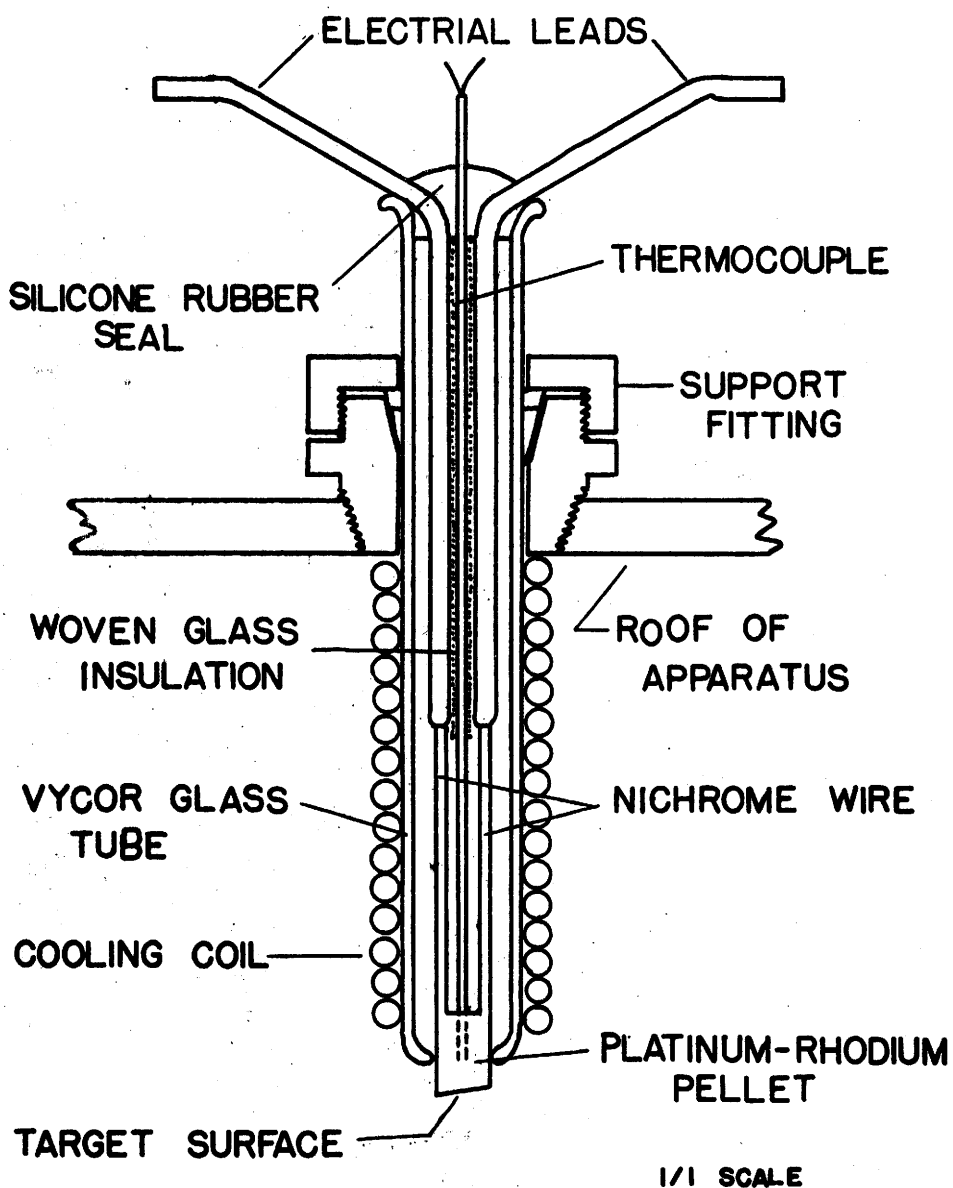
FIG.12 TARGET SURFACE ASSEMBLY

the center between the two pairs of Nichrome wires and out at the top between the copper leads. It was insulated from these leads by a porcelain insulation and a length of woven glass "spaghetti".

The Nichrome wires were insulated with fibrous alumina and the whole unit was enclosed in a 4 1/2 inch long 1/2 inch diameter Vycor glass tube. The pellet projected from the lower end of the tube. The inside diameter of the glass tube at the lower end was reduced by melting until there was very little clearance between the glass and the pellet.

The copper leads and the thermocouple were cemented to the Vycor tube at the top with silicone rubber. This also served to seal off the top of the tube. The thermocouple was encased in rubber up to a terminal block, serving to protect the fine wires. Two large flexible stranded copper wires were silver soldered onto the copper leads a short distance from where they emerge from the Vycor tube. These led to an electrical terminal block mounted on the top of the apparatus.

The Vycor tube was held in place by a 1/2 inch stainless steel Swagelock fitting with teflon ferrules. This fitting was screwed into the roof of the apparatus. Slip between the ferrules and the Vycor tube allowed vertical and rotational adjustment of the target surface position. The heater-target surface assembly was positioned with the polished surface inclined toward the observation

window in the front of the apparatus.

The Vycor tube was firmly enclosed in a 2-inch long cooling coil made with 1/8-inch copper tubing. Tap water, heated to 215-220 degrees F. in a 100 psi steam heat exchanger, was forced at 60 psig through the coil. With vapor flashing in the coil, the external surface temperature of the coil was maintained at close to the boiling point of water at atmospheric pressure. This served to maintain the surrounding vapour temperature at near to saturated conditions by absorbing heat generated by the target surface heater. The circulated water temperature was indicated by a chromel-alumel thermocouple in the tube leading from the top of the heat exchanger. The temperature was controlled using a gate valve on the inlet steam line.

ENCLOSURE

The functions of the enclosure were to support the active components in position, to allow necessary access to these components, to maintain the desired saturated steam environment in the interior and to allow clear visual observation of the interior where necessary.

The enclosure was made up of three parts: the base, the box enclosing the target surface, and the glass pipe connecting the two (Fig. 16).

The base was made up of a 3-inch section of 3-inch inside diameter stainless steel pipe with a 6-inch diameter 7/16-inch thick flange welded on the top end and a large 13 1/4-inch diameter 1/2-inch thick flange welded on the lower end. The bottom end of the pipe was closed off by a 1/2-inch thick, 8 1/4-inch diameter stainless steel base plate.

The drop projector was mounted in the center of the base plate. Holes nearby accommodated the drop former, its height adjustment screw and the water inlet to the base. A 300 watt heating element cemented into the bottom of the base provided heat to boil water in the base and thus to generate the steam atmosphere inside the apparatus. The bottom plate was fastened to the flange above with four 3/8-inch diameter bolts which screwed into the bottom plate. Large 1-inch holes in the flange allowed some lateral adjustment of the relative position of the two. A 1/16-inch thick

teflon gasket insures a leak proof seal between them.

The whole apparatus was suspended in a 12-inch diameter hole in the middle of an 800 pound concrete anti-vibration table. A 1-inch wide steel ring around the edge of the hole contained three levelling screws on which rested the large base flange.

The top 6-inch flange contains two radial holes, one to accommodate the electrical lead to the drop-generator heater and one to allow an optional path for the escape of steam.

A 3-inch nominal diameter, 8-inch long glass pipe connected the base to the top part of the apparatus. The pipe was fastened top and bottom with a standard iron flange and asbestos insert and was gasketed at the top with teflon covered asbestos. The bottom flange around the glass pipe fitted tightly over three steel pins fastened to the top flange of the base and was held in place by bolts which screwed into the pins. This allowed removal of the top part of the apparatus without disturbing the alignment between the drop projector and the top part of the equipment. A thin rubber impregnated paper gasket was used between the glass pipe and the base. This was used to minimize the effect of the tightness of the pin bolts on the alignment. The glass pipe was heated using a flat rubber coated heating tape. This prevented condensation on the inside surface, allowing visual observation of the drop former and drop projector.

The top of the apparatus consisted of a 6-inch diameter 7/16-inch thick circular stainless steel flange to which was fastened a stainless steel box. The box was designed to support the target surface, to allow photography of phenomena occuring at the target surface and to allow insertion of an oil filled pan into which the drop falls when it rebounded from the surface. Provision was made to prevent condensate from interfering with the firing or catching of the drop, and to allow maintainance of a water vapour temperature inside close to the saturation temperature of 100 degrees centigrade.

The amount of heat transferred to the drop during collision was calculated from the change in drop diameter. The drop diameters were measured from a photograph of the drop taken just before collision with the surface and a photograph taken of the drop in the catching pan. It was therefore essential to maintain, in the box, as close to a pure saturated steam atmosphere as possible.

The front of the box consisted of a vertical rectangular plate 4 inches wide, by 4 1/2 inches high, inside dimensions. Near the bottom of the front plate was cut a rectangular slot 3/8-inch high and 3 inches wide. This allowed insertion of the drop catching pan. When the catching pan was not inside, the slot was blocked by a teflon plug. The plug extended 1 3/4 inches into the inside of the box, preventing any condensate falling from the roof of the box from reaching the drop projector below. A 75 watt

cartridge heater element was clamped in a groove in the outside of the front plate just above the slot. This was used to prevent condensation on the inside of the front wall.

A 5/8-inch diameter circular double window was positioned in the center of the front plate. Hot ethylene glycol circulated between the panes in the window prevented condensation on the inside, allowing observation of the target surface directly behind the window.

The sides of the box were constructed of 1/8-inch thick stainless steel plates, 4 1/4-inch wide by 4 1/2-inch high, inside dimensions. A 3 inch by 3 1/4-inch rectangular hole, was cut in one of the sides. This hole was covered by a 1/2-inch stainless steel plate in which was situated an observation hole and two fittings. The observation hole was 2 inches in diameter and was covered by an easily removable brass plate. This allows momentary observation of the interior without major disassembly.

The two fittings in the plate were used to accommodate a gas-temperature probe and a calibration-prefocus rod assembly. The temperature probe, a platinum-rhodium thermocouple, was held in a teflon insert in 1/4-inch "Swagelock" fitting. The thermocouple, made with 0.0005-inch wire, yielded an accurate reading of vapour temperature at its immediate location. The prefocus rod assembly was a device which positioned a small stainless steel rod near the target surface. This rod was used as a reference to prefocus the camera and as a known dimension to scale the photograph.

The support fitting for the rod allowed its temporary removal and its return to the preset location near the surface. The support fitting consisted of a 1/4-inch diameter stainless steel shaft sliding perpendicularly through the side of the box in an extended brass tube. The tube was screwed tightly into the wall of the box. On the outside of the box a brass collar was held on the shaft by a locknut. The collar contained a pin, oriented parallel to the axis of the rod, which fitted tightly into a hole in a flange at the outer end of the brass tube. The actual calibration rod was "L" shaped with one end held by a locknut in a radial holw at the inner end of the stainless steel shaft. The calibration rod was in the same location whenever the pin was seated in the hole. This location could be altered by loosening the locknut in the collar.

The back wall of the box consisted of a 1/2 inch thick stainless steel plate of the same dimensions as the front wall. The light necessary for photography of a drop at the surface entered through a horizontal 3/4 inch inside diameter stainless steel tube passing through the back wall. This tube was held in teflon ferrules in a Swagelock fitting positioned in the back wall directly opposite the viewing window in the front wall.

The tube was 6 1/2 inches long, closed at the outside end by a glass window and at the inner end by a frosted glass window. It was filled with glycerine for the purpose

of extinguishing heat radiation from the light source. The inner end of the tube was positioned approximately 1 inch behind the target surface and was masked with a clip-on copper plate. The plate had a 3/16 inch wide by 1/8 inch high rectangular hole positioned such that the hole was directly behind the target surface when viewed from along the plane of the surface. This reduced the area of the light source, minimizing the error caused by oblique reflection of light at the sides of the drop and calibration rod. The end of the calibration rod was cut off at an angle, with the end face visible from the front. The vertical size dimension of this face was always equal to the true rod diameter, yielding a measure of this reflection error.

The top of the box consisted of a 1/2 inch stainless steel plate 4 inches wide and 4 inches long, inside dimensions. The fitting holding the target surface assembly was positioned in the center, 3/8 inches from the inside of the front plate. The inlet and outlet tubes to the target surface heater cooling coil were sealed together with silicone rubber through a hole in the top. Steam passed out at the top of the box through a 1/2 inch Swagelok fitting near the back corner. Two 75 watt 115 volt cartridge heaters were attached with high thermal conductivity cement to the outside of the top of the box, for use in minimizing condensation on the roof.

The base of the box consisted of a 1/2 inch stainless steel plate. The front part under the target surface was cut away leaving a rectangular hole in the bottom of the box.

The box was gasketted to a mounting plate resting on top of the glass pipe with a 1/16 inch thick teflon gasket and was held in place by four bolts through two exterior mounting brackets positioned at the bottom front corners of side plates. These bolts fitted through slots in the mounting plate cut parallel to the front plane of the box. This allowed sideways adjustment of the position of the box. Elongated holes in the mounting brackets allowed adjustment forward or back. Provision for adjustment was necessary to allow alignment of the target surface and the drop projector.

The joints between the walls of the box were sealed with silicone rubber, applied as a self setting paste immediately before assembly.

During operation a steam atmosphere was maintained inside the equipment. Steam was generated continuously by the boiling of distilled water in the base. The steam flowed up through the apparatus and out through the top of the box, sweeping any air along with it. The steam could be condensed as desired in a glass condenser and the condensate returned by a 1/4 inch stainless steel tube to the base. Provision was made for the addition or drainage of the water from the base.

In order to measure the time period necessary to sweep the apparatus clear of air, a device was constructed to measure the wet bulb temperature in the interior (Fig. 32). This was mounted inside the 1/2-inch side plate on the side of the box. A jet of water from a No. 24 size hypodermic needle formed a water drop on the end of a glass fiber. A ball of 0.0001-inch platinum wire fused onto the end of the fiber helped hold the drop in place. After formation of the drop, a 0.005 inch platinum-rhodium thermocouple was pushed into the drop. The thermocouple indicated the temperature of the drop, equivalent to the wet bulb temperature. Thermocouple conduction error may be neglected with a thermocouple wire of this diameter.

Condensate formed on the inside of the equipment had to be prevented from falling into the drop catching pan or onto the surface of the drop projector. Condensate in the pan could fall from the roof or from the front of the box. In order to prevent this, the front wall was heated by glycol circulated through the window and by the heater above the slot. The power to this heater was regulated such that it was just sufficient to prevent condensation on the lower front wall. An inverted "V" shaped slot milled into the inside of the front surface was effective in deflecting to the side any drops of condensate running down the front wall. A peaked roof made with 0.002-inch thick stainless steel sheet sat on the floor of the box and shielded the catching pan from condensate falling from the back 2/3 of

the roof. Condensation on the roof near the front was largely prevented by the flow of heat from the target surface heater, balancing the loss of heat through the insulation above. This heat input was not sufficient when the surface heater is on low. The additional heat then required was provided by two 115 volt 75-watt cartridge heaters cemented to the top of the box with "Thermon" high thermal conductivity cement. The base of the box and the top of the mounting plate just below was cut and contoured such that all condensate flowed through a hole in the plate and through a 1/4 inch stainless steel tube to a point below the drop projector surface.

It was impossible to prevent all condensate from falling onto the drop projector. Thus during the apparatus heating period the drop projector surface was covered with a small cover which was thrown aside by operation of the piston before an experimental test.

The outside of the equipment was almost completely covered by insulation. The insulation was constructed with cut sections of 1-inch thick rigid "Thurane" foam fastened where necessary with cellulose tape. The top of the box was insulated with loose fiberous alumina insulation held in place by the slabs of foam which extended beyond the top of the box. The glycol and boiling water lines were insulated with strips of cloth. The great inflammability of this insulation necessitated the location of a fire extinguisher nearby.

THE DROP CATCHER

The drop was caught after rebounding from the target surface in a 1 15/16 by 2 inch rectangular glass bottomed pan partially filled with silicone oil (Fig. 14). The pan was cut in a 5 1/8 inch long 2 1/2 inch wide 5/16 inch thick brass plate. This plate was fastened to a handle which clamped against the outside of the front wall of the box, with the plate projecting through into the interior. The plate projected 2 1/8 inches beyond the end of the pan to accommodate a sliding glass cover for the pan. The drop, travelling in a vertical path, passed through a hole in the plate in front of the pan. On hitting the forward inclined target surface it rebounded backward into the pan.

The oil used consisted of a mixture of Dow Corning Silicone fluids: 7 parts 200.20 cs. fluid to 1 part 555 fluid. A mixture is used to obtain a density very close to that of water.

Since the pan had to be removed from the saturated environment in the box before it could be photographed, the drop had to be protected from a decrease in size due to the diffusional loss of water through the oil into the air. This was accomplished by insertion of a glass cover into the oil immediately after the catching pan was removed from the box. The cover rested on four flat glass chips

TEFLON
GASKET

OIL-FILLED GLASS-
BOTTOM PAN

HEATER

GLASS SLIDING COVER

HOLE FOR PASSAGE
OF DROP

GLASS COVER FOR
DROP IN OIL

DOUBLE
GLASS
BOTTOM

1/2 SCALE
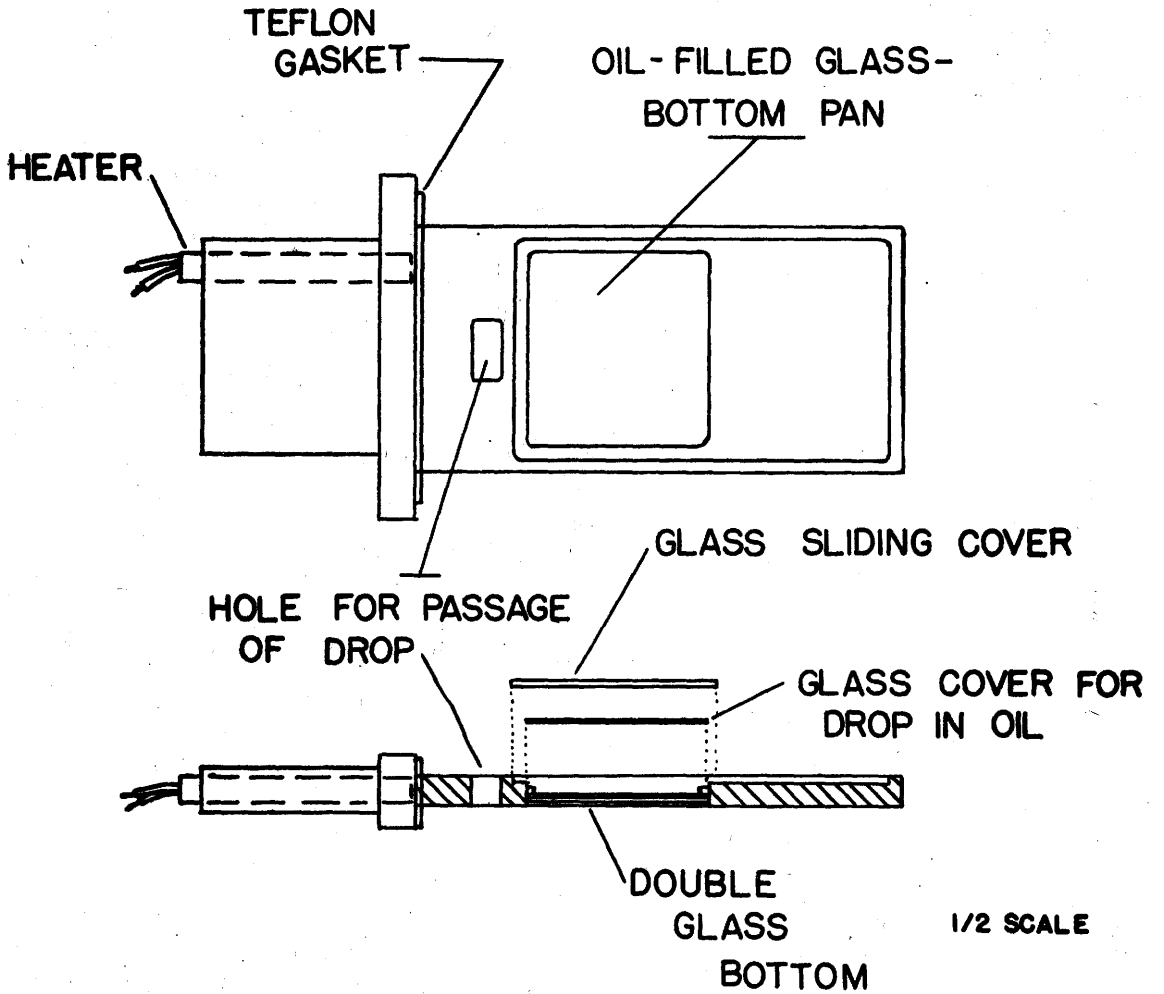
FIG. 14 DROP CATCHER ASSEMBLY

positioned in the corners of the pan, allowing a clearance of 1 millimeter for the drop resting on the bottom of the pan. If the oil was allowed to cool it became supersaturated with water and the drop' had a tendency to increase in size. Cooling was retarded by the two glass covers on the top and by a double window with an air space on the bottom. The drop was prevented from wetting the glass by a coating of translucent silicone rubber applied in a CCl_4 solution and allowed to set.

The rubber solution for coating the glass was prepared by dissolving approximately 5 cc. of General Electric translucent RTV silicone rubber in about 10 cc. of carbon tetrachloride containing about 1 cc. of silicone fluid. A small quantity of the solution was spread over the clean glass bottom of the pan. The glass chips were inserted and also covered with solution. The assembly was then placed in a dust free cupboard until the coating set.

The catcher assembly was heated in an oven to approximately 110 degrees centigrade, before insertion into the box. During its residence in the box its temperature was maintained by a 75 watt 3/8 inch diameter cartridge heater in the handle. The glass cover was heated in the same oven but was not removed until just prior to its insertion into the oil.

The catcher was carried when hot, using a nylon handle which screws into one end.

PHOTOGRAPHY

The drop was photographed with a "Pentax SLI" 35 mm. S.L.R. camera attached to a substage microscope. A photographic eyepiece was used to yield a flat plane of focus. Light was provided by a source and collimating system positioned above the stage. A size reference dimension was obtained using a microscopic scale. A magnefier clipped onto the camera viewer was used for fine focusing. A cable release on the shutter was used to minimuze vibration.

The lens combination used yielded approximately 12 times magnefication on film. It was desirable to keep the degree of magnefication low in order to minimize the time necessary to locate and photograph the drop caught.

Impact of the drop at the target surface was photographed using a Fastax W.F. 4ST16 mm. movie camera operating at a framing rate of approximately 4600 frames per second. One hundred foot rolls of Ansco Versapan negative film were used, and developed with Hyfinol developer in a portable movie film developer. Light for photography was provided by a syncronized stroboscope described in Appendix C. The camera operation is controlled by a Fastax Goose Control unit. A push button switch started the camera. After approximately one second, allowed for camera acceleration, an adjustable event delay timer in the control unit opened the solenoid valve operating the

drop projector and closed a relay in the stroboscope control timer, starting operation of the stroboscope unit. All circuits resumed the off position when a relay in the camera detected the passage of the end of the film past the camera drive mechanism.

The lens system on the camera consisted of a conventional microscope with 1.5 power objective and 7 power Bausch and Lomb-Ultraplane photographic eyepiece. These were mounted at the end of a number of extension tubes and a cross-hair marking attachment. The degree of magnification was adjustable with variation of microscope position. Most of the work was done with a magnification of approximately 5 times. During the later part of the experimental work the microscope was cemented in position with silicone rubber. The aperture of the microscope was adjusted with a ring disc located behind the objective in order to take full advantage of the amount of light to obtain maximum depth of field. Before operation, the camera was focused on the prefocus rod. The location of the rod was set such that, in the correct position, the rod projects slightly into the field of view, thus providing a reference dimension and location in the finished photographic record. Adjustment of the camera position was facilitated by the mounting of a lathe cross fed between the camera and the conventional Fastax mounting tripod.

A time reference on the film was obtained by a neon timing light pulsed by a Fastax crystal oscillator at 100 cycles per second. The camera speed was controlled by a rheostat in the Goose control unit, invariably set at its maximum allowable value of 200 volts. A timer in the Goose control unit stopped the camera in the event of a failure of the relay in the camera.

The spot light used for prefocusing the camera and the stroboscope flash lamp were both held in position on a mounting frame bolted to the table behind the apparatus. The light from the flash lamp was concentrated by a 6 inch diameter 4 inch focal length fresnel lens and a silvered $3\frac{1}{2}$ inch long cone attached to the lamp housing. Directly prior to operation the stroboscope lamp was positioned in place with the end of the cone touching the end of the tube projecting from the back of the box.

Influence of Surface Roughness

An attempt was made to determine superficially the influence of a gross surface roughness. To do this, a reflection micrograph of the highly polished surface was taken with 67 times magnification (Fig. 18). This provides a record of the nature of the surface. The surface was then sanded in many directions with 600 grit silicon carbide. A similar micrograph of this surface was also taken (Fig. 19). The roughened surface was then used in a series of tests to determine the effect of this roughness on the heat transfer process.

Recommendations for Improvement of Experimental Apparatus

1. A new optical system may be designed to make better use of available light allowing an increase in the photographic depth of field.

2. Substitution of a silicone oil for the ethylene glycol, presently being used as a heating fluid for the observation window, will prevent the formation of corrosion products which cloud the glycol. This will necessitate the substitution of metal for the plastic lead tubing.

3. Institution of a separate steam generating system allowing continuous condensate drainage will minimize oil contamination of the interior atmosphere.

4. Elimination of an air leak near the bottom of the drop projector and use of a bottled-gas supply may result in more consistent projector operation.

5. Installation of a small heater on the upper section of the vycor tube enclosing the target surface heater will prevent condensation on the inside of the tube. This condensate forms when the power input to the heater is low and may cause a rapid drop in target surface temperature at any time.

6. Substitution of quartz fibre insulation for the spun alumina insulation about the target surface heater will eliminate a major source of dust in the interior of the apparatus.

7. Installation of a cooling coil around the outside of the drop projector heater will result in a marked reduction in vapour superheat in the interior of the apparatus.

APPENDIX C

The following is a very detailed description of
the operating procedure for the experimental apparatus,
intended as a guide for its operation. A simplified outline
may be found in the "Procedure" section in the main body of
the thesis.

OPERATING PROCEDURE

This section is organized under four headings : -
Preparation for a Series of Tests, Preparation for an
Experimental Run, Test Procedure, and Procedure for Auxiliary
Tests. The first section describes methods of assembly or
preparation of equipment where the procedure is not self-
evident.

For the test procedure itself, a checklist was found
to be absolutely essential in order that no detail be forgotten.
The headings for the checklist are given in the second section.
The apparatus was made of a great many individual components
and thus has low reliability. The operator had always to
be alert to detect and rectify the failure of a component
before it ruined a test run.

PREPARATION FOR A SERIES OF EXPERIMENTS

Target Surface Preparation

The target surface was inspected and cleaned before
each series of experimental runs. In removing the target
surface assembly from the apparatus, care had to be taken
to prevent the surface from becoming marred through contact
with the edge of the retaining fitting. When replacing this
assembly inside the apparatus, the copper cooling coil inside
had to be pushed firmly onto the vycor jacket; otherwise it
projected down past the surface and blocked the light.

When the surface was to be polished after being
marred or scratched, the Vycor jacket was removed and the
pellet-heater unit mounted in cold setting plexiglass. It
was then polished using a series of abrasive papers. It had
to be mounted or a perfectly flat surface could not be obtained.
After polishing, the plastic mount was burned off in a gas
flame. If only minor cleaning and polishing was necessary,
the unit could be left in the Vycor jacket. The hole
between the jacket and the pellet was filled with rubber
cement prior to polishing to prevent the entry of polishing
compound. The surface was then polished with 5 micron and
0.3 micron alumina on wetted lens cleaning tissue. After
polishing, it was washed with distilled water and the rubber
seal removed. Any remaining rubber was burned off in a gas
flame. The surface was then washed with distilled water and

the unit replaced in the apparatus.

In obtaining a roughened surface, the surface was sanded with light pressure in every direction with No. 600 grit silicon carbide paper.

Reflection micrographs were taken of both the smooth (Fig. 18) and the roughened surface (Fig. 19).

The heater wires expanded considerably on heating, such that the level of the surface when hot depended on the heater power input. The target surface had to be near enough to the calibration rod when hot, so that both could be seen in the field of view of the camera. Thus the level of the heater jacket in the Swagelok fitting had to be adjusted by trial according to the surface temperature desired.

Drop Projector Heater Adjustment

The drop projector heater had to be adjusted to the lowest effective power input. If it was too low, the drop on the surface when it became small, would suddenly jump off the surface. If it was too high it added an undesirable excess of superheat to the vapour in the apparatus. Adjustment was made on that basis. The other heater power inputs were adjusted such that they were just sufficient to perform the function of preventing condensation. The correct roof heater adjustment depended on the target surface heater power input. The drop catcher heater was adjusted so as to maintain its temperature at 100 degrees centigrade, as indicated by a thermocouple inserted into a hole in the handle.

Apparatus Alignment

Before operation, it was necessary to align the drop projector, the hole in the drop catcher, the target surface and the calibration-prefocus rod. Alignment of the surface and the drop projector was accomplished through movement of the box at the top of the apparatus on its circular supporting plate underneath, or if necessary, by movement of the base plate under the large flange at the bottom of the apparatus. A drop was placed in the depression at the top of the drop projector using a glass syringe and a needle extended with a long curved length of capillary tubing. The tubing was inserted through the port in the side of the stainless steel box at the top. The drop was allowed to evaporate to a diameter of about one millimeter, at which time it was fired upwards. After loosening the four mounting bolts, the position of the top box was adjusted in successive trials until the projected drop hit the target surface reasonably near to its centre. The location of the point of impact on the surface was observed using a small, angled mirror made by polishing one end of a stainless steel strip and bending this end up. The calibration-prefocus rod was positioned with its end approximately 1/16 inches away from the drop on the surface and with the axis of the rod intersection near to the front edge of the circular area wetted by the drop, roughly 1/4 of a diameter from its front edge. This yielded a best first approximation of the correct position. Further adjustment was made after a trial photograph

of the drop rebounding from the surface. If, on examining the film, the receding drop was in focus but not the approaching drop, then, in order to improve the focus, the prefocus rod had to be moved toward the camera. In accomplishing this, the camera was positioned as in performing an experimental run and was focused on the prefocus rod. The camera was then moved back until the rod was judged to be as much out of focus as was the image of the incoming drop. The position of the rod was then adjusted until again in clear focus. If the receding drop was more out of focus than the approaching drop, a similar procedure was followed, with the camera being moved forward. In projecting a drop with the apparatus cold, the power to the drop projector heater had to be increased to compensate for the increased heat losses.

In order to align the drop catcher, the catcher assembly was placed in the apparatus with the hole through which the drop normally passes blocked with a pane of glass. The catcher was seated firmly against the adjustable stop which was mounted on the front of the apparatus to the right of the slot accommodating the drop catcher. This stop, consisting of an allen screw and a lock nut, was adjusted in successive trials until the projected drop hit the glass in the centre of the hole. The apparatus required realignment only after major disassembly. The joint between the glass pipe and the base was self-aligning, allowing access to the drop former and projector without disturbing the alignment.

Preparation for an Experimental Run

Before turning the apparatus heaters on, the depression in the drop projector was washed with distilled water to remove any dirt on the surface. It was then covered to prevent any dirt from falling condensate from collecting in the depression during the heating period. The drop former was cleaned using caustic solution and distilled water to remove traces of oil.

Before removing the top of the apparatus, the camera and tripod were moved to one side. The viewing lens and lens holder were removed and the light used to illuminate the drop projector was moved to a table nearby. The target surface thermocouple lead was disconnected at the terminal block. The boiling water lines to and from the target surface heater cooling coil were disconnected at the Swagelok fittings near the top of the apparatus. The three bolts, locknuts and washers at the top of the aligning pins on the base of the apparatus were then removed. The top of the apparatus was then lifted clear of the drop former and swung counterclockwise across to the top of the concrete table.

The glycerine in the light conduction tube was checked and replaced if necessary. It had a tendency to turn yellow under the influence of the intense ultra-violet light.

The platinum surface of the depression was sanded lightly with No. 220 grit silicon carbide paper. Following this, it was rubbed with a dry sheet of lens cleaning paper

wound on the end of a pencil. It was then wiped with a damp sheet of the cleaning paper.

The drop former was raised to its maximum height and a small beaker was slipped underneath. It was cleaned by pouring concentrated caustic solution and distilled water over the glass loop. The drop former was then placed with the end of the loop in the depression and the positioning pin at the bottom of the supporting rod in its hole. The tubing was then bent slightly if necessary and the positioning-device height-adjustment screw adjusted from beneath the base of the apparatus until the end of the glass loop just cleared the bottom of the depression. The drop former was then raised and a small circular stainless steel plate was placed across the top of the drop projector. The top of the apparatus was then replaced and the various fittings recon- nected. In tightening the bolts on the aligning pins, every effort was made to tighten them firmly slowly and evenly. This was to minimize the effect of variations in bolt tightness on alignment.

Care was necessary in manipulating the drop former to avoid shorting the electrical connection to the drop- projector heater. It was possible in lifting the drop former to bring its supporting tube into contact with the ungrounded lead to this heater.

Distilled water was then allowed to flow into the base of the apparatus from the funnel connected to the condensate return tube at the left of the apparatus. Any

excess was drained off through the drain tube beneath the apparatus until the water level was just below the lower steam vent. The heater-circulation unit was turned on to circulate hot glycol between the windows. The variable transformers controlling the power input to the base heater, the glass pipe heating tape, the drop projector heater, the roof heater and the front heater were all turned on. The target surface heater control was turned on and set to provide heat sufficient to prevent condensation on the surface. At the end of the heat up period, approximately 1 1/2 hours, the target surface heater control was set to yield the desired surface temperature. The steam to the heat exchanger was turned on along with the water jet on the steam drain vent from the heat exchanger. This water jet served to reduce the amount of steam escaping into the room. The tap water to the heat exchanger and cooling coil was turned on and a check made to ensure that it was flowing properly.

The roof heater control was adjusted with any change in the surface heater control setting such that the heat input was just sufficient to prevent condensation. Approximately two hours were required for the steam atmosphere to fill the entire apparatus, as indicated by the issuance of steam from the top steam vent.

Both drop catching assemblies were cleaned and the glass bottom of each was coated with silicone rubber. The sliding glass covers were cleaned and placed over the pan and both assemblies were placed in the oven at 115 degrees

Centigrade. The two cover glasses were cleaned, treated with anti-wetting agent (General Electric SC-87) and placed in the oven in a folded piece of lens cleaning paper.

The cleaning procedure consisted of washing the oil away with carbon tetrachloride from a wash bottle, followed by scrubbing with a stiff paint brush wetted with a concentrated solution of laboratory glassware detergent. The detergent was rinsed off with distilled water and the surface dried with cleaning tissue. The glass surface was then treated with anti-wetting agent, General Electric SC-87, as follows. One drop was placed on the surface and wiped over the entire surface with cleaning tissue. It was then wiped off until no trace could be observed on the surface. It was then flushed with distilled water and any remaining drops around the side were absorbed onto a wet paint brush. The cleaning process was intended to remove all traces of dust and dirt. Washing with carbon tetrachloride was done in a hood in order to prevent contact with the vapours which are poisonous even in small concentrations.

In preparing the oil, the bottom of a small erlenmeyer flask was covered with about a quarter of an inch of water. The silicon oil was poured in to a depth of about half an inch. The flask was then placed on a little stand in a beaker large enough to allow a cover to be placed over the top without coming in contact with the flask. Distilled water was boiled in the bottom of the beaker for at least one half hour prior to pouring the oil into the drop catching pan.

The chromel-alumel thermocouple in the tube from the heat exchanger and the target surface thermocouple lead were connected to a potentiometer. A mixture of crushed ice and water was placed in a thermos flask containing the thermocouple reference junctions. Both temperature indications were checked to ensure proper operation.

The potential of the boiling water thermocouple was adjusted to between 4.15 and 4.20 mv. by operation the control valve on the steam inlet to the heat exchanger. Only minor adjustment became necessary as the steam flow was turned on or off using a gate valve in the steam line, positioned above the control valve.

The Fastax camera was positioned on the tripod at an angle of 8 1/2 degrees, and focused approximately on the target surface. The tripod was positioned using marks on the floor made for the purpose.

The camera control cables were attached according to instructions outlined in the Fastax manual. Three cables were connected to the camera; the timing marker cable, the 115 volt power cable, and the camera power cable from the Goose control. The sprocket wheel pickup cable was connected from the camera to the pulse amplifier. The stroboscope relay control cable was connected from the stroboscope control timer to the 115 volt plug switched through the event timer in the Goose control.

The push button switch cable was connected to the Goose control and the Goose control power cable was connected to the 115 volt mains. The two filament power switches on the stroboscope were turned on at least 15 minutes prior to operation. The switch on the letdown transformer in the high-power line to the stroboscope was turned off (red button pushed in). The timing sequence switch on the Goose control was set at an indicated 200 volts. The camera run timer was set at 1.5 seconds. The event delay timer was set at 1.25 seconds. The stroboscope control timer was set for a delay of 0.05 seconds and a run time of 0.20 seconds. The three switches on the side of the camera were turned on, completing the preparation of the camera and stroboscope. Further information regarding operation of the stroboscope may be obtained by reference to the stroboscope section, Appendix D.

The telescope was clamped to a vertical rod positioned several feet from the apparatus. It was pointed down toward the drop projector surface at an angle of approximately 39 degrees. A magnifying lens was positioned along the line of sight of the telescope, as close to the drop projector as possible. It was clamped in place using an extended clamp from a nearby rack, and is inclined so as to be perpendicular to the axis of the line of sight of the telescope, as close to the drop projector as possible. The position of both the telescope and lens had to be adjusted until a

satisfactory view was obtained. This was necessary because of irregularities in the glass pipe. This was tested by placing a drop on the surface and allowing it to evaporate under observation to the size to be projected. With the lens and telescope used, 1 division on the scale imposed on the image was roughly equivalent to 100 microns. In attempting to project a drop of a specific size, a delay between starting the camera and projecting the drop must be anticipated. The change in size during this d lay was quite marked and increased with decreasing drop size. The surface of the drop projector was lighted by a spot lamp directed through the magnifying lens, positioned sufficiently to one side so as not to block the line of sight of the telescope.

The micrography apparatus was preset such that a a drop caught in the pan would be nearly in focus when the drop catching assembly was placed on the stage. The reflex camera was loaded with Illford FP3 film and the shutter speed is set to 1/35 of a second.

A 500 milliliter beaker was filled with distilled water and a 1 milliliter glass syringe was placed nearby.

The side port in the top of the apparatus was opened to view the interior and to ensure the absence of condensate from the front part of the roof and the front wall. The calibration rod was checked to ensure its correct position.

TEST PROCEDURE

A 100 foot roll of 16 millimeter film was seated firmly on the top spindle in the Fastax camera with approximately 18 inches of film hanging down. The position of the viewing prism was adjusted into alignment with the camera viewer. The door of the Fastax was then closed. The stroboscope lamp and cable were placed on top of the stroboscope power supply housing and a flood lamp was positioned on the frame behind the apparatus to light the surface for the purpose of focusing the Fastax camera. A Fastax 400 foot balanced loading spool was placed nearby.

The power input to the target surface heater was adjusted to yield the desired temperature.

The beaker containing the prepared oil was removed from the boiling water and allowed to sit on the bench for five minutes in order to allow small drops of water in the oil to settle out. The oil was then poured into the drop catcher to a depth of about 1/8 of an inch. The addition of more oil than necessary was avoided because it tended to spill and contaminate the interior of the apparatus. The glass cover, shoved aside for the addition of the oil, was then slid back over the pan and the catcher allowed to remain in the oven 10 minutes prior to its installation in the apparatus.

The drop former was swung aside and the drop projector piston was operated if necessary to eject the cover aside. The teflon plug was pulled out and replaced, causing any condensate on its surface to fall into the bottom of the apparatus. The drop projector was operated again to remove any water fallen from above. In operating the drop projector, compressed air was turned on and the control regulator adjusted to yield the desired pressure. The button activating the Goose control was depressed starting the timing sequence and activating the event timer which operates the solenoid valve admitting air to the drop projector cylinder. The camera and stroboscope did not operate at this point because neither is turned on. Following operation a toggle valve was closed which shuts off compressed air from the regulator. The water jet ejector was turned on and the ball valve from the compressed air system opened. After a period of about 10 seconds the push button was depressed again, opening the solenoid valve and allowing the drop projector piston to fall into its original position. The toggle and ball valves were then reset to their original position. Before the catcher was placed in the apparatus, the correct positioning of this valve was verified and the set air pressure was recorded on the operation checklist.

Prior to loading the drop catcher, the camera was pivoted aside, the teflon plug was pulled almost all the way out and the drop catcher clamp and a screw driver were positioned nearby. A nylon handle was screwed into a threaded

hole at the end of the drop catcher handle. The drop catcher
was then removed from the oven and carried to the apparatus.
The teflon plug was removed and the glass cover over the drop
catching pan was slid forward. The drop catcher was then
gently inserted into the slot and the side of the handle
section was pushed to the right tight against the set screw.
The clamp was hooked over the two screw studs on the left
hand side and the screw in the clamp was tightened, holding
the drop catcher firmly in place. A check was then made to
insure that the catcher was positioned firmly against the set
screw as the tightening of the screw in the clamp had a ten-
dency to move it away. The plug from the drop catcher heater
was connected to the socket on the end of a cord from a
preset variable transformer. The nylon handle was then
removed, completing the installation of the drop catcher.

The Fastax camera was repositioned in place and the
clamp on the rotating shaft of the tripod was tightened.
The floodlight behind the apparatus was turned on. The camera
was focused on the prefocus rod with the sides of the rod
in exact focus, and the end of the rod just visible in the
field of view. Any necessary adjustments were made using the
height adjustment wheel on the tripod and by the lateral and
front adjustment screws on the lathe crossfeed on which the
camera was mounted. The floodlight was then turned off. The
door of the camera was opened and the film was threaded over
the sprocket wheel and onto the loading reel on the takeup

spindle. Care was necessary to ensure that the camera was not jarred out of focus and that the takeup loading reel was well seated onto the spindle. The door was closed and a check made to ensure that the red light was on at the side' of the camera.

The floodlight was removed from behind the apparatus and the stroboscope lamp housing was screwed onto the frame and pushed into position.

The drop former was then positioned over the depression in the top of the drop projector. A drop was formed by forcing water through the capillary tubing to the drop former using the 1 cc. syringe. A drop which fell off the capillary into the depression was allowed to rest there for approximately 15 seconds. It was then picked off the surface by contacting it with the end of the drop former. The drop former was then moved aside quickly, shaking off the lifted drop. Another drop was then formed and allowed to fall into the bottom of the apparatus. The drop former was then repositioned over the depression.

Care had to be taken not to condense water too quickly. Otherwise air was pulled into the apparatus. This was indicated by the absence of steam flowing from the vent at the top of the apparatus.

Fifteen minutes after the insertion of the drop catcher, a clamp was closed on the tubing leading from the steam outlet at the top of the apparatus. Simultaneously a clamp was opened on the tubing leading from the outlet coming

from the side of the top flange of the base section. This stopped steam flow out the top, allowing it to flow out the bottom. In this way a positive pressure was maintained in the apparatus at all times.

The stroboscope main power switch was turned on followed by the switch on the side of the letdown transformer. A correct voltage reading was verified on a power-supply voltage meter.

A drop was then formed and allowed to fall into the depression. The drop former was swung aside. At this time the target surface thermocouple e.m.f. was measured by a Rubicon potentiometer. The drop on the surface was then observed until it reached nearly the desired diameter, whereupon the push button was depressed starting the controlled sequence of operation of the equipment.

The camera was swung aside and the drop catcher was prepared for removal by connecting the nylon handle, disconnecting the heater connector and removing the clamp. The cover glass was brought from the oven and placed in the oil immediately on removal of the catcher from the apparatus. The sliding glass cover was repositioned over the pan and the catcher quickly transported to the stage of the microscope. A weight was placed on the handle of the catcher to balance it in position. The microscope light was turned on with a green filter in position. The camera shutter was cocked and the microscope focused on a drop. Pictures were taken of all drops in the pan as quickly as possible. The pan was then

scanned completely under the microscope to ensure that no drops were missed. The catcher was then removed from the stage and a picture of a micro scale was taken using an exposure time of 1/8 seconds.

The water in the base of the equipment was then changed to reduce the oil concentration in the base. The steam flow valves were reset and the teflon plug was cleaned and repositioned in the slot. A period of 30 minutes was allowed after steam began to issue from the top of the apparatus before commencing another test run.

The drop catcher was drained of oil, cleaned and prepared as previously. The drop catcher required 30 minutes in the oven to reach the required temperature.

When shutting down the apparatus both the target surface heater and the drop projector heater were left on low in order to prevent condensation on them. The water was not drained from the base until some time after shutting off the base heater. Otherwise the temperature in the base rose enough to melt the special composition solder on the drop former support.

OPERATION CHECKLIST

Switches, Steam, Water On.

Oil, Catcher Ready.

Base Water Changed.

Temperature Measurement Set.

Camera, Stroboscope Ready.

Drop Observation Setup Adjusted.

Cooling Water Temperature O.K.

Oil in Catcher.

Microphotography Set.

Target Surface Power Set.

Interior Check.

Drop Projector Operation O.K.

Valves Set, Record Pressure.

Load Catcher.

Focus, Load Camera, Position Stroboscope.

Clean Projector Surface.

Steam Vent.

Stroboscope Voltage On.

Drop On.

Drop Former Out of Way.

Preset Potentiometer to Surface Temperature.

Fire Circuits.

Stroboscope Voltage Off.

Read, Record Surface Temperature.

Photograph Drops Caught.

PHOTOGRAPHIC FILM PROCESSING

The 16 millimeter movie film was developed in a
Land F Portable Cine Processor obtained from the Superior
Bulk Film Co., 442 North Wells St., Chicago 10, Illinois,
U.S.A. The light, available for the development of reversal
film, was removed and the drive gear ratio was changed from
1:1 to 2:1, increasing the contact time to 200 seconds
for a 3 roller tank and 140 seconds for a 2 roller tank.

The machine was troublesome in operation. The mylar
leader tape was carefully tightened before operation, but
even then the film occasionally rode off the drive wheels,
jammed and broke. The friction slip drive on the takeup
spool was occasionally troublesome and corrosion inside
due to fixer contact was extensive and will necessitate
periodic repairs. On arrival many of the cans leaked slightly
and had to be repaired. On the whole, no complaint can be
made, as the unit was much more economical than others
available and the availability of such a processor on hand
was found to be essential for this type of study. Later
modifications eliminated most of the difficulty.

One gallon of developer was divided between the first
two tanks. Hyfinol developer was used, manufactured as a
dry powder in cans by the Ansco (General Analine and Film,
439-447 E. Illinois St., Chicago, Illinois 60611, U.S.A.)
and widely available. This yielded a development time of
approximately 5 minutes. It is not possible to give an

exact development time, because contact with the developer is intermittent. After development of 100 feet of film, 150 milliliters of Acufine replenisher were added to each tank. The developer was replaced after development of 700 feet of film. The tank no. 3 contained 1.25 liters of stop bath and tank nos. 4,5, and 6 contained Ansco "Rapa-fix" fixer. The fixer in the fourth tank was replaced when indicated by cloudiness (underfixing) in the developed film. Fixer from the 4th tank was added to the 5th, and fixer from the 5th to the 6th, after the fixer in the 6th tank had been discarded, improving the utilization of the fixer. The seventh, ninth and tenth tanks contained distilled wash water. The eighth tank contained Kodak Hypo eliminator solution which was replaced at the same time as the developer.

Care was necessary in threading the machine in order to ensure that the emulsion side of the film passing through was always facing out in going over the spools. Otherwise a dirty film resulted, which was impossible to clean.

Prior to developing, the solutions in tanks No. 1 and 2 were heated or cooled as necessary to 30 degrees centigrade. The solutions in the tanks increased in temperature during operation of the processor.

The 35 millimeter film from the microscope camera was developed for 4 1/2 minutes in a developing tank using "Acufine" developer. After development, was the tank washed out with water and then fixer solution was put in the tank for the specified length of time. The temperature of the

solutions was not critical, although, in order to obtain maximum acutance or line sharpness an effort was made to ensure that they were at approximately the same temperature.

The developer solution was replenished with 15 millileters of "Acufine" replenisher solution after each roll of film was developed. One gallon of developer was sufficient to develop 60 rolls of film.

The developer solution was placed in air tight bottles when not in use as it deteriorated by oxidation very rapidly, especially when at the high temperatures in the continuous processor.

The continuous processor remains threaded all the time as the film being developed remained between two lengths of mylar tape. To load the film, one of the lengths of tape was wound onto the feed reel. One end of the film was stapled onto the end of the tape with the emulsion side facing in and the film overlapping the tape. All the lights were turned out and the complete film was wound onto the reel from the Fastax takeup reel. Fifty feet of film was then wound onto a prepared 50 foot size spool (until it was filled), and the film was then broken. The film on the 50 foot spool was then wound onto the original 100 foot reel. The end of this film was fastened with tape and the reel placed in the original can for later use in a normal speed camera. The lights were turned on and a second exposed length of film was stapled on, emulsion side in with the leading end overlapping. The procedure for stripping off the front 50 feet

was repeated, and the end of the tape leading through the processor was then stapled onto the end of the second film. The feed spool rotated clockwise as the film passed into the machine. The tape was pulled taut completing preparation for operation.

APPENDIX D

Description and Operating Instructions

for the Operation of the High-Power High-Frequency Stroboscope

in Synchronization with the Fastax Motionpicture Camera

192

Acknowledgement

Function and Application

The function of the stroboscope was to generate a series of very high intensity pulses of light of very short duration in synchronization with a Fastax motion camera running at approximately 4600 frames per second. With a flash duration of 3 microseconds, it decreased the exposure time by a factor of about 15. This resulted in an appreciable increase in the clarity of the image when photographing a moving object. With a flash energy of 2 joules per flash and operating in synchronization at a frequency of 4.6 kilocycles, it provided the same amount of light per frame (photograph) as would be provided by a 45 kilowatt continuous light source. Since the fastax exposure time per frame was only 1/5 the frame period, most of the output from a continuous source would not be usable.

The high intensity and compact size of this light source made it particularly useful for micrographic work. Since the image velocity equals the product of the object velocity and the magnification, a short exposure time with its stopping action was important. The brightness of the light allowed the use of a slow film with good line definition and allowed a small lens aperture with a consequent increase in the depth field.

The unit was applied in this study for the shadow photography of the impact of small drops on a hot surface. It is expected to find wide application in the future study of a wide variety small scale dynamic phenomena.

charged again by the flow of power from the main bank and through the RL shunt across the lamp. Because of energy storage in the charging choke, the voltage on the discharge capacitor was increased over that on the main capacitor bank. The hold-off diode functioned to prevent this charge from leaking back.

The frequency of such a circuit was limited by the time allowed for the thyratron to deionize. If the thyratron for any reason failed to deionize it began to conduct continuously. The circuit was then protected by three special fuses in the main power switch. These will blow inside a few seconds, providing adequate protection for all components.

A reduction in the thyratron heater voltage from the specified 6.3 volts was necessary in order to reduce the deionization time to a sufficiently low value. This decrease reduced the temperature of a lithium hydride reservoir, reducing the hydrogen pressure in the tube. Forced air cooling stabilized the thermal balance irrespective of air currents in the room. Reduction of the hydrogen pressure also reduced the current carrying capacity of the tube, excessive reduction causing erratic operation and, eventually preventing ionization entirely. Consequently the voltage was adjusted up or down until satisfactory operation was obtained. This was accomplished by changing the input taps on the two series connected filament transformers.

Since the characteristics of the tube changed with age, periodic adjustment was necessary.

The magnetic pickup in the Fastax camera consisted of an iron spool with a point at one end and a magnet attached to the other. A coil of fine copper wire was wound on the spool, with the ungrounded leads passing back to a pulse amplifier. During camera operation an iron piece passed the pointed end of the pickup every frame interval. This disturbed the magnetic field about the bar, inducing a voltage across the coil of about 100 millivolts. This voltage was fed to the pulse amplifier, which fires when the voltage from the coil reacted a certain level. The output pulse, a 150 volt spike of several microseconds duration, was sufficient to ionize the thyratron, causing the lamp to flash. The position of thepickup in the camera was adjusted by trial until satisfactory synchronization was obtained.

A variation in frequency due to magnetic inhomogeneity of the Fastax sprocket wheel led to the addition of a cup shaped extension on the side of the wheel. Precisely spaced slots in the side of the cup serves to drive the pickup.

The pulse amplifier consisted of a conventional trigger circuit. It required an input of not less that 100 millivolts of approximately sine wave form. Special features included a high voltage filament transformer on the output tube and a high voltage output capacitor. It was

grounded only at the thyratron cathode in order to minimize the effect of pickup. (Fig. 35).

A voltage regulating transformer was placed in the 110 volt input to the unit in order to stabilize the supply for the pulse amplifier.

Large resistances composed of a number of small resistors connected in series shunt the high voltage to ground at the main bank and at the discharge capacitor. These serve to allow the high voltage to bleed off after operation. The main bank resistor was also used as a connection point for the meter indicating the voltage on the main capacitor bank.

POWER INPUT
3 PHASE, 575V.

FLASH
LAMP

FASTAX
CAMERA

250Ω

TRANSFORMER
575/150,200,250 V.

IOM IOM—ON EACH RECTIFIER

1.0 H

0.5 H

500Ω

866A

0.1μF

+7KV

12μF

450μH

5C22

20M

100M

50Ω

7K

PANEL
METER

TRANSFORMERS
230V/9KV-0-9KV

872A

TIMING
CIRCUITS

TRIGGER
PULSE
GENERATOR
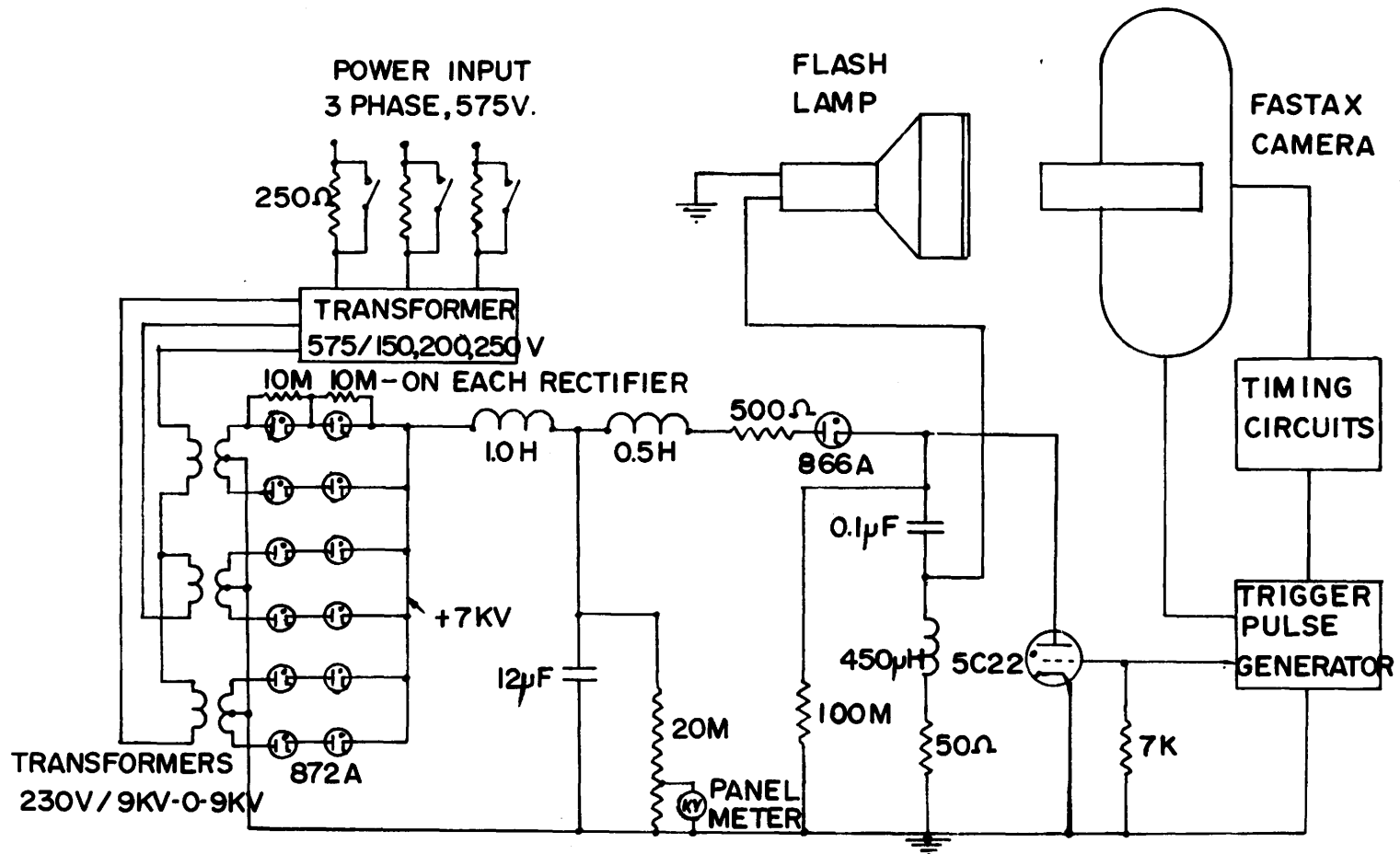
FIG.34   STROBOSCOPE   CIRCUIT   DIAGRAM
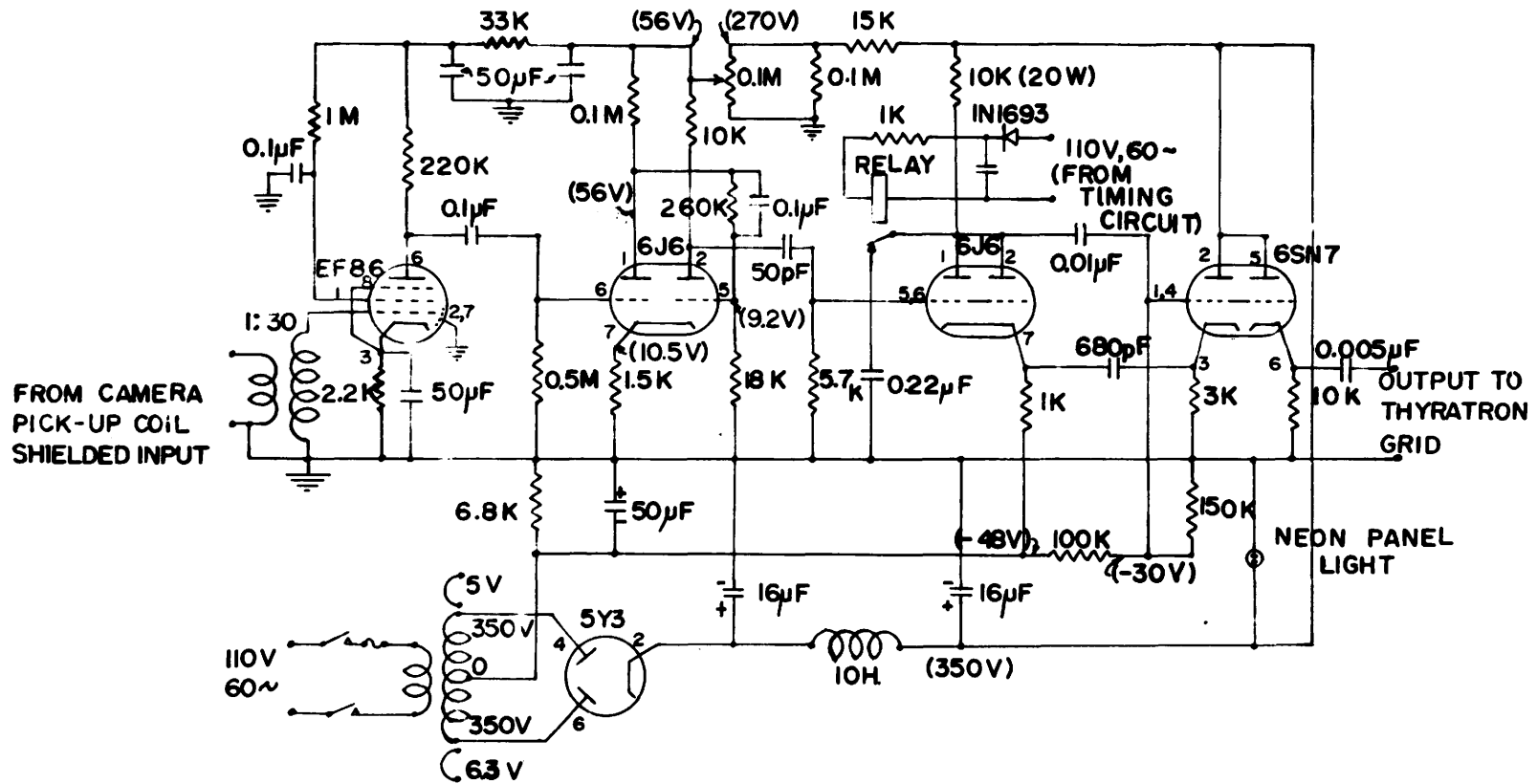
FIG. 35   STROBOSCOPE   PULSE   AMPLIFIER

CIRCUIT   DIAGRAM

FIGURE 36

115 VAC

15K STEPS   560Ω
150Ω   150Ω 1K
2N2161
4MFD oil   27Ω   SCR C20B

15K STEPS   560Ω
150Ω   150Ω 1K
2N2161
4MFD oil   27Ω   SCR C20B

POTTER BRUMFIELD KHP17D11

115 VAC OUT
115 VAC
1021   40Ω   24VDC
100 MFD   100 MFD

STROBOSCOPE DELAY AND DURATION CONTROL TIMER

RUN AND DELAY
0.005 TO 0.50 SEC. IN STEPS OF 0.05
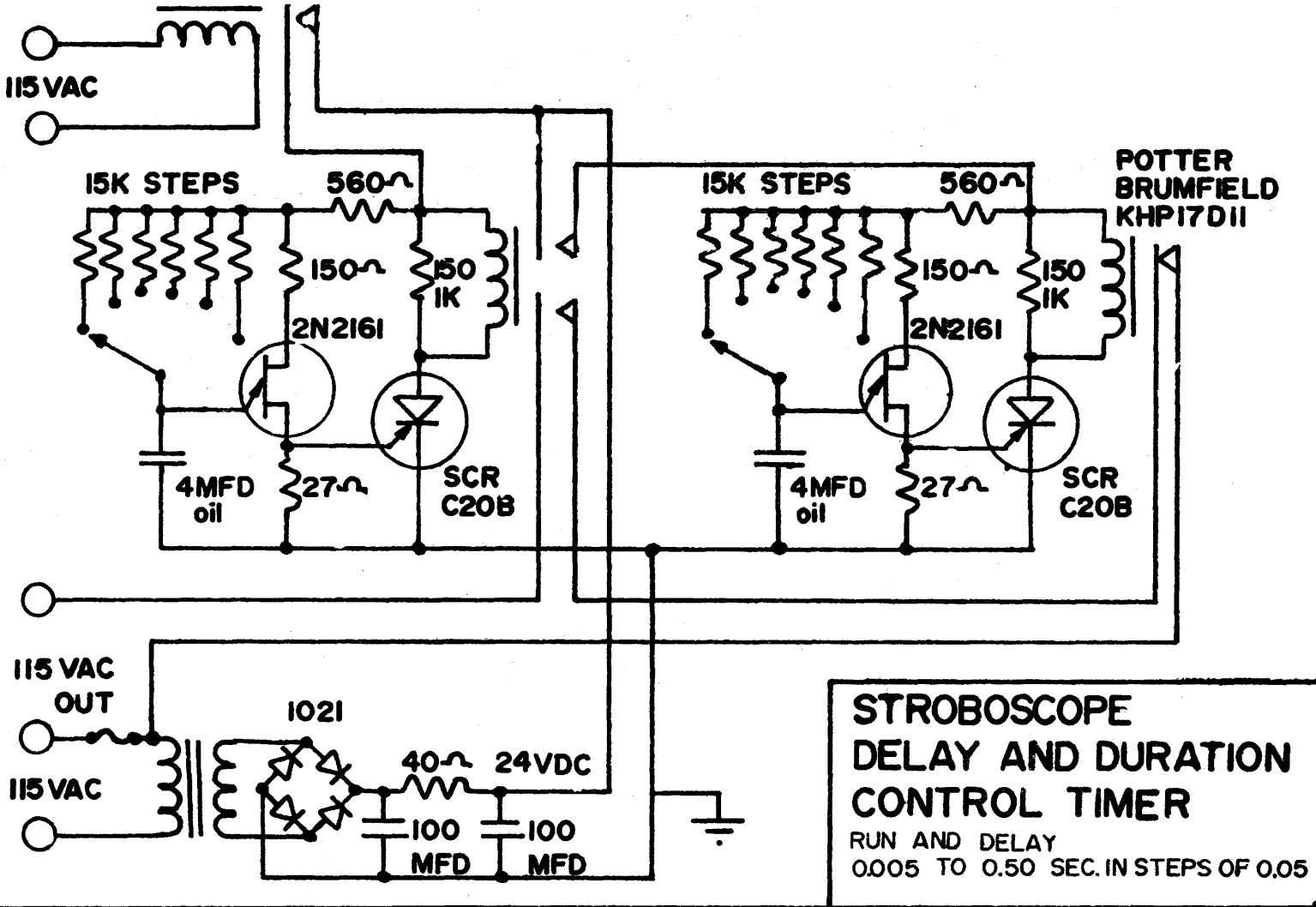
Efforts to operate the unit met with little success until realization of the importance of reducing the thyratron heater-reservoir voltage below its specified value. A later attempt to use a thyratron with a separate reservoir heater proved unsuccessful. Performance of the thyratron proved erratic until it was enclosed and cooled by a blower.

Synchronization of the camera with the stroboscope was obtained initially using a magnetic pickup on the teeth of the Fastax sprocket wheel. Variations in timing due to magnetic nonhomogeneity in the sprocket wheel were eliminated by the addition of an extension on the side of the sprocket wheel. Some jitter was encountered due to pulse feedback into the input. This was overcome by removing all ground connections but one on the pickup-pulse amplifier circuit. The pulse amplifier had a tendency to fail on occasion due to high voltage feedback into the output tube. The frequency of failure was reduced by the insertion of a HV isolation filament transformer on the output tube.

The construction of the stroboscope resulted in a considerable saving in cost over that required to purchase a commercially available unit. A considerable saving in time could have resulted if complete specifications and instructions had been available prior to construction.

Component Specification and Source

Main Power Supply Fuses

Fusetron FRS 2½ Dual-element Bussmann Mfg. Division, McGraw-Edison Co., St. Louis 7, Mo. U.S.A. Local Supplier Dosco Electric, Hamilton.

Letdown Transformer

3 Phase autotransformer: 1 input 550 volts, output taps 150, 200, 250 volts, Rated 12 kilowatts. Hammond Transformer Manf. Co., Guelph, Ontario.

High Voltage Transformers

Single Phase Transformer: input 230 volts, output plus 9000, zero, minus 9000 volts. Manufactured by Canadian General Electric. Supplied as U.S. Government Surplus by Scientific Specialties Div., P.O. Box 141, El Cerrito, California.

High Voltage Lead Wire

Canada Wire and Cable GTO 15. Stranded wire with polyethylene and PVC insulation. Rated 15000 volts. Supplied by Northern Electric, Hamilton.

High Voltage Rectifiers

872A Mercury Vapor Rectifiers. Filament 5 volts, 7.5 amps. Caps: Safety Plate Grip SPP-9 N.R.C. Inc. Bases: E.F. Johnson Co. No. 123-211-100. All supplied by Zentronics, Hamilton. Filament transformers Audio Development Co. No. A5699A and General Electric 7477922 Stock No. TF-210,

all rated at 10 KV isolation. Filament transformers supplied as surplus from Lectronic Research Laboratories, 715 Arch St., Philadelphia 6, Pa., U.S.A.

Hold-off Diode

866A Mercury Vapor Reactifier Filament 2.5 volts, 5 amperes. Tube, cap and base supplied by Zentronics, Hamilton. Filament transformer Kenyon No. S-10694. Insulation 15 KV test supplied as surplus from Lectronic Research Laboratories, 715 Arch St., Philadelphia 6, Pa., U.S.A.

Shunt Resistor on Main Bank

Series connection of 20 of 470K two watt resistors mounted on an insulator board.

Voltage Meter

Is connected in series with a variable resistor and carbon resistor across the last 470K resistor in the main bank shunt resistor. The meter is a Triplett Model 420 0-100 D.C. microamperes. The variable resistor is adjusted such that 10 KV on the main bank yields a reading of 100 microamperes. A Techtronic Oscilloscope with a high voltage probe was used in adjusting the calibration. The materials were obtained from Zentronics, Hamilton.

Discharge Capacitor

0.1 microfarad 10%, 15KV working voltage, noninductive Dubilier Nitrogol made in England. Supplier Ernest Turner Electrical Instruments Limited, Chittern Works, High Wycome, Bucks, England.

Hydrogen Thyratron

5C22 hydrogen filled tube. Filament 6.3 volts 10 amperes. Base and tube supplied by Lectronic Research Laboratories 715 Arch Street Philadelphia 6, Pa., U.S.A. Filament transformers American Transformer Co. Filament Transformer Spec. No. 26395 Rated 35 KV. Two units: outputs in series input 110 volts and 220 volts - taps selected to yield desired output voltage. Supplier Lectronic Research Laboratories.

Flash Lamp, Lamp Housing and Lead Cable

The flash tube is a small bore quartz tube filled with xenon under high pressure. It is specially designed to yield a short flash time (2-3 microseconds). It has a rating of 4 kilowatt seconds, the maximum power dissipation at any one time. Any excess over this will reduce the life of the lamp. The complete unit was supplied by Ernest Turner Electrical Instruments Ltd., High Wycombe, Bucks, England.

Pulse Amplifier

The pulse amplifier was designed and built at McMaster University using components from local suppliers.

Stroboscope Troubleshooting

If the stroboscope fails to operate properly check all connections to ensure that they are made and secure. Check also to ensure that all switches are properly positioned and that all controls are adjusted to their desired values. If a stroboscope unit ffailure is indicated, attempt to achieve satisfactory operation by carrying out the following steps. With each operation stand with hand on the main power switch, ready to turn off if continuous conduction is indicated by a loud hum and a bright blue glow in the tubes, which does not cease when the lamp stops operating. Proceed with great caution.

     a. Check fuses.

     b. Disconnect thyratron at top and turn on power to check function of power supply.

     c. Replace flash lamp and try operation.

     d. Substitute new tubes in pulse amplifier.

     e. Change thyratron heater voltage from 5.5 to 6.3 volts in steps of about 0.2 with successive trials.

     f. Substitute new thyratron and repeat part e.

     g. Seek further assistance.

A screw driver placed across the terminals of the discharge capacitor when the meter indicates that most of the charge has dissipated through the shunt resistors will ensure that no charge remains on the high voltage supply. The voltage

of each of the thyratron filament transformers may be
increased by connecting the input leads to terminals
closer together. The power to these transformers may be
turned off using the two switches on the front of the power
supply.

The life of the lamp is limited, perhaps to as far
as 50,000 flashes. If the intensity starts to drop off as
evidenced by a fading in density of the photographs, the
first action taken should be to note the effect of substituting
a new lamp. Yellowing of the glycerol in the light conduction
tube could also cause a drop in light intensity so that
this possibility should be investigated.

Stroboscope Operating Instructions

1. Become completely familiar with the operating instructions
   and design of the stroboscope before attempting to
   operate. Exercise extreme care as the voltages involved
   are lethal. The lamp is a source of intense ultraviolet
   radiation and as such can cause burns and eye damage.

2. Turn on power to tube heaters and pulse amplifier.
   To accomplish this, plug the 110 volt and 220 volt into
   their respective wall sockets and turn on the three
   toggle switches on the front of the chassis. Leave
   on at least 15 minutes before turning on the high
   voltage power.

3. Connect the trigger signal input cable to the left hand
   coaxial plug on the front of the trigger pulse amplifier.
   Although no extensive testing has been done it is expected
   that the stroboscope will trigger satisfactorily on a
   signal of about 100 millivolts and which approximates
   a sine wave in form. The upper limit of frequency is
   probably in the order of 8 kilocycles per second.

4. The pulses from the amplifier do not reach the thyratron
   unless a 110 volt AC signal is fed in at the two pole
   connector on the front of the pulse amplifier. This
   may be operated through the event timer on the camera
   control and should be set such that the number of
   flashes at any one time does not exceed 2000. The pulses

are fed from the amplifier to the thyratron through a coaxial cable connected to the coaxial connectors on the right side of the pulse amplifier and on the front of the main chassis.

5. Set the timers controlling the delay and duration of operation to yield the minimum usable time of operation. The life of the lamp decreases rapidly with increased loading. At 1000 flashes per run (4 kilojoules loading) the expected life is 100 runs ($1.30 per run). The life of the lamp will be more than proportionately greater with a decrease in loading. Aging of the lamps is marked by a falling off in flash intensity.

6. Check the basement switch to ensure that the 550 volt power is on in the Chemical Engineering wing (3 position switch positioned vertically up). If the switch is in the down position check with the Metallurgy department before changing. Check to ensure that the jumper bars on the saturable core reactors are disconnected. If necessary disconnect bars with switch locked in the off (horizontal) position. Before turning on power check to ensure that all concerned are aware of the live voltage on the AST reactor heater banks. Turn on the switch on the saturable core reactor housing after a check to ensure that the switch in room A214 is off (down position) (lock combination 35-14-45).

7. Before turning on stroboscope power check to ensure
    that the switch on the side of the let down transformer
    if off (red button depressed). Turn on main switch
    and the switch on the side of the transformer. Check
    the meter on the front of the chassis to see if the volt-
    age is on. Do not leave the high voltage on any longer
    that necessary as the life of the capacitors under load
    is limited.

APPENDIX E   CALCULATION OF DROPLET EVAPORATION LOSS

CAUSED BY VAPOUR SUPERHEAT

Any superheat in the vapour in the top of the apparatus will cause partial evaporation of the drop during its travel from the target surface to the drop catching pan. Since the objective is to measure the amount of evaporation due solely to surface contact, this will result in an error. The magnitude of this error may be estimated as follows.

A 300 micron water drop will settle in air at a terminal velocity of approximately 30 feet per second (13). The drop rebounds from the surface at a velocity of approximately 2 feet per second and will accelerate as it travels toward the catcher pan. The Nusselt number for evaporation of the drop is given by the expression

$$\frac{hD}{k} = 2.0 + 0.6 \ (\text{Re})^{1/2} \ (\text{Pr})^{1/3}$$

The residence time in the superheated vapour is proportional to the inverse of the velocity. The Nusselt number, as given by the above equation, is a much weaker function of velocity. Therefore, the higher the velocity of travel over the fixed distance between the surface and the catcher, the less will be the amount of evaporation.

Assume that a velocity of 2 feet per second is maintained by the drop. The residence time of the drop in travelling two inches from the target surface to the oil

pan will be approximately 1/12 seconds.

For a 300 micron drop travelling in saturated steam at 2 feet per second.

$$Re \ = \ 9.12$$

$$Pr \ = \ 1.06$$

$$\frac{hD}{k} \ = 3.85$$

Total volume evaporated = <u>Total Heat Transferred.</u> Assuming 10 degrees Fahrenheit of superheat, the volume percent evaporation will equal

$$\frac{100 \triangle V_{ol}}{V_{ol}} = \frac{1200 \ k \triangle Tt}{\rho \ \lambda \ D^2} \quad \frac{hD}{k}$$

$$= \ 0.3\%$$

Generally the amount of superheat will be less than this. Vapour temperature measurements taken indicated that the amount of superheat was less than 3 degrees when the steam was vented from the bottom of the apparatus.

In conclusion, therefore, it may be stated that the error due to this influence is small compared to other errors.

APPENDIX F   VAPOUR FLOW AND HEAT TRANSFER BENEATH THE DROP

A drop sitting in film boiling on a hot surface is separated from the surface by a vapour film. If it is assumed that the film thickness is uniform,and that heat transfer is by conduction across the film from a surface at uniform temperature, then it is possible to write and solve the coupled partial differential equations describing both the heat transfer from the surface and the flow of vapour from the drop. This was accomplished by other workers (4). In this case, by the use of a digital computer for the numerical solution of the equations, a more accurate solution was obtained.

A computer program was prepared to solve numerically the set of ordinary non linear differential equations arising from the transformation by the method of similarity of the partial differential equations describing flow underneath a drop sitting in film boiling on a hot surface. The transformation used was identical to that of Baumeister, Hamill, Schwartz and Schoessow (4), the object being to obtain numerical results more accurate than those which they obtained using an analog computer. The equations were solved using a 4th. order Runge-Kutta-Gill routine available on the computer. The transformed equations were as follows : -

$$(\phi')^2 - 2\phi\phi'' = 1 + \phi'''$$

$$2\phi\phi' = -\psi' - \phi''$$

where

$$F(Z) = \frac{4\nu}{a}\,\psi(\xi)$$

$$f(Z) = \sqrt{a\nu}\;\phi(\xi)$$

$$\xi = \sqrt{\frac{a}{\nu}}\;Z$$

The similarity transformations were

$$\omega = -2 f(Z)$$

$$u = r f'(Z)$$

$$P' = \frac{1}{2}\,a^2\,\frac{\rho}{g_c}\left(r_0^2 - r^2 + f(Z)\right)$$

These were made on the governing partial differential
equations as follows : -

$$u \frac{\partial u}{\partial r} + w \frac{\partial u}{\partial z} = -\frac{gc}{\rho} \frac{\partial P}{\partial r} + \nu \left(\frac{\partial^2 u}{\partial r^2} + \frac{1}{r} \frac{\partial u}{\partial r} - \frac{u}{r^2} + \frac{\partial^2 u}{\partial z^2} \right)$$

$$u \frac{\partial w}{\partial r} + w \frac{\partial w}{\partial z} = -\frac{gc}{\rho} \frac{\partial P}{\partial z} + \nu \left(\frac{\partial^2 w}{\partial r^2} + \frac{1}{r} \frac{\partial w}{\partial r} + \frac{\partial^2 w}{\partial z^2} \right)$$

The marching solution of the ordinary differential
equations was advanced from the initial conditions : -

$$\zeta = 0, \quad \phi = 0, \quad \phi' = 0, \quad \psi = 0$$

by incrementing on ζ , referred to as DEL in the program
output, after specifying ϕ''. The number of iterations,
found to be sufficient, was usually 150. The results are
tabulated in table A for the end boundary condition at which
$\phi' = 0.0$

TABLE A

ϕ	ϕ''	ζ (DEL)	ψ	$\phi''(0)$
0.00008	-0.05000	0.0998	0.00000	0.05
0.00067	-0.09999	0.2000	0.00000	0.10
0.00225	-0.14994	0.3000	-0.00001	0.15
0.00533	-0.19974	0.4001	-0.00005	0.20
0.01042	-0.24922	0.5007	-0.00009	0.25
0.01803	-0.2989	0.6009	-0.00032	0.30
0.02866	-0.3478	0.7019	-0.00082	0.35
0.04287	-0.39566	0.8037	-0.00183	0.40
0.06123	-0.44217	0.9066	-0.00375	0.45
0.8434	-0.48677	1.0137	-0.00711	0.50

The following correlation was obtained by Baumeister, Hamill, Schwartz and Schoessow (9) for use in obtaining a closed solution for a heat transfer coefficient : -

$$\text{at } \phi' = 0, \qquad \phi = 0.086\, \zeta^3$$

The following correlation was obtained from the data in Table A using a computor library program : -

	Correlation	Standard Error of Estimate Squared
at $\phi' = 0$	$\phi = 0.0815\, \zeta^3$	0.78×10^{-7} on 14 DF.
	$\phi'' = 0.4871\, \zeta$	0.13×10^{-4} on 12 DF.

APPENDIX G   ECCENTRICITY OF THE DROP DUE TO AERODYNAMIC FORCES

A measurement of drop size is made from photographs of the drop before it strikes the hot surface. In so doing it is assumed that the drop is spherical and that variations in measurements taken in different directions will vary under a random influence of minor drop vibration and lack of image clarity. Aerodynamic forces on the moving drop could, however, cause a directionally biased error if not acounted for.

These forces will cause the drop to be other than perfectly spherical. Analysis of the degree of distortion was made on the assumption that the distorted shape was a spheroid with its axis in the direction of motion (14).

The fineness ratio, h, of the spheroid is the ratio of the length of the axis in the direction of motion to the diameter perpendicular to it. It was given by Hughes and Gilliland (14) as a function of

$$\psi_2 = (Re)^{2.35}/Su.$$

where
$$Su = \frac{g\sigma\, d\, \rho_o}{\mu_o^2}$$

$$Re = \frac{dV\rho_o}{\mu_o}$$

For a 500 micron water drop travelling in steam at 5 feet per second,

$$Su = \frac{(32.2)(58.9)(0.005)(2.2481)(10^{-6})}{(26.83)(0.0125)(0.0125)(6.72)(6.72)(10^{-8})}$$

$$= 11240.$$

$$Re = \frac{(0.05)(5.0)}{(26.83)(0.0125)(6.72)(10^{-4})(2.54)(12)} = 36.3$$

$$\psi_2 = \frac{(36.3)^{2.35}}{11240} = 0.41$$

From table 1, part C   h = 0.9987

Eccentricity = 0.2%

The variation in measured drop size due to vibration and lack of image clarity was much larger than this. This error was therefore neglected.

Appendix H   The Rate of Loss of Drop Superheat

It is quite likely that the drop left the target surface after impact in a superheated condition. If the drop did not lose this superheat before entering the oil then the assumption that the amount of evaporation is equivalent to the amount of heat transfer would not be valid.

The following calculation indicates that if the drop surface is maintained at the saturation temperature, then over 95 percent of the superheat present on leaving the surface would be dissipated by conduction alone in the 1/12 second of travel to the drop catching pan. The previous assumption is therefore assumed to be valid.

Degree of Loss of Superheat

$$Q_o = C_p \, \frac{\pi D^3}{6} (T_o - T_\infty) \qquad \text{for a sphere} \qquad (30)$$

For a drop of constant temperature the Biot modulus is infinity.

Ratio of Final/Initial Superheat	$\dfrac{a'\theta}{r_o^2}$
0.29	0.01
0.60	0.05
0.77	0.10
0.95	0.25

Thermal Diffusivity $\qquad a' = 0.001553/(0.95)^2 \quad cm^2/sec.$

$$\theta = 1/12 \ sec.$$

Therefore $\quad \dfrac{a\theta}{r_o^2} = 0.359 \quad$ for a 200 micron drop.

Therefore, more than 95 percent of the superheat in the drop is lost before the drop reaches the catching pan.

Appendix I   Error in Measuring Drop Diameter due to
Gravity Deformation in the Oil

The change in diameter of a drop sitting on a non-wetted surface due to gravity deformation was calculated in an approximate manner. The objective was to determine whether or not there was appreciable error in assuming that the drop was spherical instead of flattened at the bottom in measuring the diameter and calculating the volume from it.

If the drop is assumed to remain spherical except for a flattened portion at the bottom, then the product of the pressure inside the drop due to surface tension and the area of the flattened portion must equal the weight of the drop less any boyant force upon the drop. Equating the volume of drops resting and not resting on the surface, it is possible to derive equations relating the diameter of one to the other.

The equations, derived as described, are as follows : -

$$z = \overset{*}{A}(x^3 y)^{1/2} \quad ....(1)$$

$$H = y - (y^2 - z^2)^{1/2} \quad ...(2)$$

$$8(y^3 - x^3) = H(H^2 + 3\overset{*}{A}{}^2) \quad ...(3)$$

$$\overset{*}{A} = \left(\frac{2\rho}{3\sigma}\right)^{1/2}$$
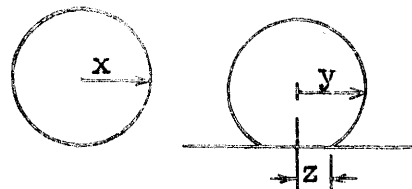
Knowing x, ρ and σ, it is possible to solve for y. The results for a 1000 micron drop are tabulated as follows : -

$\dfrac{\rho}{\sigma}\left(\dfrac{gm}{dyne\ cm^2}\right)$	y(microns)
0.005	1000.07
0.010	1000.28
0.020	1001.11
0.050	1007.56
0.100	1035.87

The silicone oil used has a specific gravity between 1.1 and 1.0. The water-silicone oil interfacial tension was more than 10 dynes/cm. Therefore ρ/σ would be less than 0.01 and the error in assuming the apparent diameter equal to the true diameter is negligible.

APPENDIX J   <u>Estimation of Error in the Measurement</u>

<u>of Surface Temperature</u>

The platinum-rhodium thermocouple used to measure

the target surface temperature was welded into the middle

of the pellet, approximately 1/16 of an inch below the metal

surface. Since the pellet was heated from above the thermocouple

indicated a temperature above the true surface temperature.

It is difficult to estimate ⟨⟩ the convective heat transfer

from the surface. Using a formula given by McAdams for a

heated surface facing down in air (3), a rough estimate of

the heat transfer coefficient at 500°F. may be obtained :

$$h = 0.12 \ (\Delta t/L)^{0.25}$$

$$= 0.7 \ \text{Btu/hr.sq.ft.}°F.$$

A coefficient for heat transfer by radiation may

be estimated from Fig. 28-8 of Bennett and Myers (31),

as being approximately 4 Btu/hr.sq.ft.°F. The thermal

conductivity of platinum-rhodium is approximately 15

Btu/hr.ft.°F. Therefore, the thermocouple error at 500°F., $\Delta t'$,

may be estimated as follows : -

$$\frac{kA \ \Delta t'}{L} = hA \ \Delta t$$

$$\Delta t' = \frac{h \ \Delta t h}{K}$$

$$h = 4.0 + 0.7 = 4.7$$

$$\text{Error,} \quad t' \quad = \frac{(4.7)(500-212)}{(16)(12)(15)} \quad = 0.47°\text{F}.$$

The error in temperature measurement is not large enough to be considered significant, even at the higher temperature where the radiant heat transfer coefficient will be ten times as large.

APPENDIX K   SURFACE TENSION MEASUREMENTS

Surface tension measurements were made using the Pendant Drop method (19, 20). A drop was suspended from the end of a 1/8 inch stainless steel tube inside the apparatus in a steam atmosphere. The 1/8 inch tube was mounted in a 1/2 inch stainless steel tube passing through the fitting in the roof of the apparatus which normally accommodated the target surface assembly. The mask was removed from the end of the light conduction tube, and the tube was moved back as far from the window as possible. Light for photography was provided by a 300 watt flood lamp positioned 6 inches from the outside end of the light conduction tube. The drop was photographed through the window using a 55mm. lens on a 60mm. extension tube, with a 35mm. Pentax S.V.1 camera body. Magnification was nearly unity. Kodak Improved Panatomic X was used with a lens opening of f/1.4 and a shutter speed of 1/125 seconds. This is a superior film for this application because of its high contrast and antihalation properties.

A drop was formed at the end of the 1/8 inch tube by injection of water from a leak proof glass syringe through a 3/4 stainless steel capillary tube soldered into the top 1/8 inch tube. The apparatus heater settings were as described previously, but no water was circulated through the target surface heater cooling coil.

A sample of condensed water, characteristic of the interior atmosphere, was obtained by drawing steam into the syringe and allowing it to condense until a sufficient sample was obtained. Surface tension measurements for distilled water were obtained by filling the syringe with distilled water from the tap. Measurements with distilled water were taken only after every effort had been made to cleanse the interior of all traces of silicone oil.

Six measurements of surface tension were obtained from separate photographs for condensed water and for distilled water according to the method of Fordham (19). Small droplets of oil were observed in the condensed water. The experimental results are shown in Table VIII. Using a Students "t" test, there was no significant difference in surface tension between the condensed water and the distilled water at the 90 percent level of significance. The degree of magnification on the film was obtained from a measurement of the outside diameter of the 1/8 inch tube.

The mean value of surface tension 60.9 dynes per centimeter compares with a value of 58.9 dynes per centimeter obtained from the literature (13). The technique used in these measurements was not sufficiently refined to warrant any conclusions regarding this difference, especially on consideration of the well known fact that very small concentrations of impurities may have a very large effect on surface tension. One may however, conclude that the presence of a small quantity of silicone oil in water does not have a large effect on its surface tension.

Table VIII   Surface Tension Measurements

A. Sample of Condensate from the Interior of the Apparatus

Frame Number	d_e(cm)	d_s(cm)	Surface Tension
1	0.3661	0.3114	60.7
2	0.3664	0.3100	61.5
3	0.3686	0.3139	61.2
5	0.3691	0.3171	59.9
6	0.3730	0.3205	61.2
7	0.3698	0.3158	61.1
		Mean	60.93
		S.D.	0.52

B. Sample of Distilled Water form Tap

Frame Number	d_e(cm)	d_s(cm)	Surface Tension
10	0.3713	0.3210	59.6
12	0.3725	0.3205	60.9
13	0.3727	0.3198	61.4
14	0.3688	0.3151	60.7
15	0.3749	0.3234	61.2
16	0.3754	0.3224	62.0
		Mean	60.97
		S.D.	0.74

Water Density 0.95838 gm./cc.

Image Magnification 0.9654

Test of the Significance of Difference

Pooled estimate of the standard deviation of means

$$\bar{S}(X) = 0.698$$

$$S \cdot t = \frac{60.97 - 60.93}{0.698(1/6 + 1/6)} = 0.10$$

$$S \cdot t_{0.9,10} = 0.129$$

Therefore, if one assumes no difference between the means, the probability of being wrong in the assumption is less than 10%.

SAMPLE CALCULATION OF SURFACE TENSION

Measurements of Width of Image of 1/8 inch tube:

   0.1276, 0.1278, 0.1278, 0.1279, 0.1274.   Mean 0.1279

Measurements by Micrometer of Diameter of 1/8 inch tube:

   0.1238, 0.1235, 0.1234, 0.1230, 0.1236.   Mean 0.12346

For Frame 1

$$d_e = (0.1493 \times 0.12346 \times 2.54)/(0.12788)$$

$$= 0.3661 \text{ cm.}$$

$$d_s = (0.1270 \times 0.12346 \times 2.54)/(0.12788)$$

$$= 0.3114 \text{ cm.}$$

$$S = d_s/d_e = (0.3114)/(0.3661) = 0.8501$$

From Fordham (19)

Surface Tension $= 980.667 \times 0.95838 \times (0.3661)^2 \times 0.482$

$= 60.7$ dynes per centimeter.

APPENDIX L   COMPUTER PROGRAMS

The computer programs in Fortran IV used during the course of this study are presented in the following section. The program for the solution of the model of the drop collision is preceeded by an abbreviated outline of the logic flow, intended to aid in its interpretation.

Logic Flow of Program for Solution of

the Model of Drop Collision Dynamics

Read Constants, Drop Diameter, Weber Number.

Calculate the Sum of the Initial Surface and Kinetic Energy

(23)   Set Counter I = 0, Time = 0.

(100)   Increment I = I + 1, Time (I) = Time (I - 1) + DT.

(7)   Set Search Limits for Tabular Body thickness, A.

         Set A(I) = Lower Limit.

(SUBR)   Calculate Radius of Tabular Body, R (I) (equation 1).

(SUBR)   Calculate and Sum all terms in the Energy Balance
         (equation 2).

(219)   Increment A (I).

(SUBR)   Calculate R (I) (equation 1).

(SUBR)   Calculate and Sum all terms in the Energy Balance
         (equation 2).

         Multiply the last two values of the sum of terms

         together (RNO). If Multiple is not negative return

         to (219).

(30)   If Multiple is negative perform Fibonacci Search on

         A(I) between the last two values to best approximate

         a root value of A(I) yielding a zero Sum of all terms

         in the Energy Balance (equation 2).

         Calculate, R(I).

         Calculate Force of Impact, F(I).

         Calculate the Rate of Change of A(I) with time.

Calculate the Coefficient for Heat Transfer from the surface (equation 3).

(6)   Calculate the total heat transfer during the time interval, QDROP.

Calculate Total Heat Transferred, QTOTAL(I) = QTOTAL(I-1)
+ QDROP.

Calculate Film Thickness, FILM(I) (equation 4).

(43)   Test Is Tabular Body Energy equal to Initial Total Energy.

If not return to (100), I = I + 1, Time (I) = Time (I-1)
+ DT.

Calculate the Maximum Pressure under the Impacting Drop (equation 5).

(200)   Calculate Percent Change in Diameter from Total Heat Transferred.

Calculate dimensionless values of R(I), A(I), F(I), Time (I).

(75)   Interpolate to obtain values for R, A, F for even values of Time.

Output.

```
C     MODEL OF DROP COLLISION DYNAMICS
C
C
C
C        NOMENCLATURE
C     PHYSICAL CONSTANTS
C     GC - GRAVITATIONAL CONSTANT IN GM.CM./DYNE CM.SQ.
C     LAMBDA-LATENT HEAT IN CALORIES PER GRAM
C     RHO--LIQUID DENSITY IN GRAMS PER MILLILETER
C     RHOV-DENSITY OF VAPOUR IN GRAMS PER MILLILETER
C     CPV-VAPOUR HEAT CAPACITY IN GRAM CALORIES PER GRAM DEGREE C.
C     THRMCV-THERMAL CONDUCTIVITY OF VAPOUR IN CAL/SEC.CM.DEG C.
C     MU- VAPOUR VISCOSITY IN GRAMS PER CM. SEC.
C
C     VARIABLES
C     D-DIAMETER OF APPROACHING DROP IN CENTIMETERS
C     V-VELOCITY OF APPROACHING DROP IN CENTIMETERS PER SECOND
C     RUN-REFERENCE NUMBER
C     WEBER-WEBER NUMBER
C     R(I) IS RADIUS OF UNDERSIDE OF DROP IN CENTIMETERS
C     A(I) IS THICKNESS OF TABULAR BODY IN CENTIMETERS
C     F(I) IS FORCE ACROSS VAPOUR FILM IN DYNES
C     TIME(I) IS TIME FROM DROP CONTACT WITH SURFACE IN SECONDS
C     HSURF- H.T. COEFFICIENT FOR  CONDUCTION FROM TARGET SURFACE
C       IN GRAM CALORIES PER SECOND SQ CEM. DEGREE CENTIGRADE
C     TDIFF-TEMPERATURE DIFFERENCE BETWEEN SURFACE AND DROP IN DEG. C.
C     QTOTAL-HEAT TRANSFERRED TO DROP UP TO TIME(I)
C     PEVAP-PERCENT CHANGE IN DIAMETER DUE TO EVAPOURATION
C     FILM-FILM THICKNESS IN CM.
C
      REAL LAMBDA
      REAL MU
      DIMENSION A(300),TIME(300),R(300),DADT(300),F(300)
      DIMENSION HSURF(300),TDIFF(300),QTOTAL(300),FILM(300)
      DIMENSION FF(30),VA(11),ALPH(10)
      DIMENSION VEL(300)
      COMMON RHO,GC,V,PI,D,SIGMA,CST,JKL,CA,CB,CC,CD,CE,CF,CG,CH,CI,CJ,
     1TABSEI,DA,DT,LAMBDA,THRMCV,TDIFF,F,CPV,RHOV,RR,ESUM,MU,BD,SL5,PD,
     2VREF,FC
      PI=3.14159
      GC=1.0
      CST=(3.14159/12.)+(1./3.)-(3.14159*3.14159/64.)
      SIGMA=58.9
      RHO=.95838
      RHOV=(453.59)/(10000.0*30.52*2.8317)
      MU=0.015/100.0
      LAMBDA=970.3*0.5556
      CPV=0.46
      THRMCV=(0.021*251.98*9.0)/(3600.0*2.54*12.0*5.0)
      CA=PI/8.0
      CB=(CA**2)-(1.0/6.0)
      CE=SIGMA*PI
```

```
      CF=PI*RHO/4.0
      READ(5,970) NJ,LIMIT,LIMIT2,ANOI
C     NJ IS THE NUMBER OF SETS OF INPUT DATA (NO. OF RUNS)
C     ANOI IS THE NUMBER OF D/V INCREMENTS FOR THE ITERATION
      KL=0
      DO 78 LJ=1,NJ
      READ(5,971) RUN,D,WEBER
      READ(5,777) DTEMP
  777 FORMAT(F15.5)
      V=SQRT((     SIGMA*WEBER)/(D*RHO))
      BD=PI*V*RHO/GC
      EC=PI*(D**3)/6.0
C
C     SOLUTION OF PART ONE OF MODEL
C
      CC=PI*D*SIGMA
      CD=((RHO*V*V)/(2.0*GC))*(PI/3.0)
C     CALCULATION OF TIME INCREMENT
      DT=D/(ANOI*V)
C     CALCULATE INITIAL TOTAL SURFACE PLUS KENETIC ENERGY OF DROP
      TESTC=PI*D*D*SIGMA+RHO*V*V*PI*(D**3.0)/(12.0*GC)
C
C     DEFINE FIBONACCI SERIES UP TO F(30)
      FF(1)=1.0
      FF(2)=2.0
      DO 10 LLL=3,30
   10 FF(LLL)=FF(LLL-1)+FF(LLL-2)
      CNA=(0.163*4.0*GC/PI)**0.25
      CNB=RHOV*(THRMCV**3.0)/MU
      CNC=CNB*LAMBDA
      CND=CNB*0.5*CPV
      HFCF=(LAMBDA-CPV*DTEMP)/(LAMBDA+0.5*CPV*DTEMP)
C
   23 I=0
      TIME(1)=0.0
      PMAX=0.0
  100 I=I+1
      TDIFF(I)=DTEMP
      IF(I.EQ.1) GO TO 5
      TIME(I)=TIME(I-1)+DT
      DA=A(I-1)
      GO TO 7
    5 TIME(I)=DT
      DA=0.0
    7 CONTINUE
C     SET SEARCH LIMITS FOR A(I)
      X0=0.000001
      IF(I.GT.3) X0=0.75*A(I-1)
      XN=D-V*TIME(I)
      IF(XN.LE.0.0) GO TO 3
    2 QC=XN+V*TIME(I)
```

```
      UC=QC*QC*(1.5*D-QC)
      TERM=XN*XN*CB+UC/(3.0*XN)
C
C     ROOT VALUES ARE ALL DETERMINATE EXCEPT THE TERMINAL VALUE AT TIM
C      EQUAL TO VT-A, BUT SELECTED TRIAL VALUES OF A USED AS BOUNDARIE
C      ON THE ROOT FINDING ROUTINE MAY PRODUCE INDETERMINATE TERMS
C      ZERO AND NEGATIVE TESTS ARE INCLUDED TO AVOID INDETERMINATE TER
C
      IF(TERM.GT.0.0) GO TO 3
      XN=XN-0.00001
      GO TO 2
    3 YO=FN(XO,TIME(I),DADT(I))
      IF(YO.GT.0.0) GO TO 308
      GO TO 219
  308 WRITE(6,963)
      IF(XO.LE.0.00001) GO TO 307
      XO=0.000001
      GO TO 3
  307 WRITE(6,961)
C
C     FIBONACCI SEARCH
C
  219 XR=XO
      YR=YO
      XO=XO+0.0001
      IF(XO.GE.XN) GO TO 220
      YO=FN(XO,TIME(I),DADT(I))
      RNO=YR*YO
      IF(RNO.LT.0.0) GO TO 221
      GO TO 219
  220 XO=XN
  221 XN=XO
      XO=XR
      YO=ABS(FN(XO,TIME(I),DADT(I)))
      YN=ABS(FN(XN,TIME(I),DADT(I)))
      S=(XN-XO)*(FF(LIMIT-1)/FF(LIMIT))
      X1=XN-S
      X2=XO+S
      Y1=ABS(FN(X1,TIME(I),DADT(I)))
      Y2=ABS(FN(X2,TIME(I),DADT(I)))
      LL=LIMIT-2
      DO 30 NOFIB=1,LL
      IF(Y1.GE.Y2) GO TO 20
      XN=X2
      YN=Y2
      X2=X1
      Y2=Y1
      X1=XO+(XN-X2)
      Y1=ABS(FN(X1,TIME(I),DADT(I)))
      IF(X1.LT.X2) GO TO 30
      XX=X1
```

```
      YY=Y1
      X1=X2
      Y1=Y2
      X2=XX
      Y2=YY
      GO TO 30
   20 X0=X1
      Y0=Y1
      X1=X2
      Y1=Y2
      X2=XN-(X1-X0)
      Y2=ABS(FN(X2,TIME(I),DADT(I)))
      IF(X1.LT.X2) GO TO 30
      XX=X1
      YY=Y1
      X1=X2
      Y1=Y2
      X2=XX
      Y2=YY
   30 CONTINUE
      A(I)=(X1+X2)/2.0
      Y2=ABS(FN(A(I),TIME(I),DADT(I)))
      F(I)=CH
      RRRR=(A(I)*A(I)*CB
     1+((V*TIME(I)+A(I))**2)*(1.5*D-V*TIME(I)-A(I))/(3.0*A(I)))
      IF(RRRR.LE.0.0) R(I)=0.0
      IF(RRRR.LE.0.0) GO TO 43
      R(I)=-(PI*A(I)/8.0)+RRRR**0.5
C
C
C     CALCULATION OF HEAT TRANSFER AND PERCENT EVAPORATION
C     ASSUMING UNIFORM VAPOUR FILM THICKNESS AND TEMP. DIFF.
C
      CNE=(CNC/TDIFF(I)+CND)*F(I)
      IF(CNE.LE.0.0) HSURF(I)=0.0
      IF(CNE.LE.0.0) GO TO 6
      HSURF(I)=(CNA/R(I))*((CNE)**0.25)
    6 QSURF=HSURF(I)*2.0*PI*R(I)*R(I)*TDIFF(I)
      QDROP=QSURF*HFCF
      IF(I.EQ.1) QTOTAL(I)=QDROP*DT
      IF(I.GT.1) QTOTAL(I)=QTOTAL(I-1)+QDROP*DT
      CHID=1.0/(1.0+CPV*TDIFF(I)/(3.0*LAMBDA))
      FILM(I)=THRMCV*CHID/HSURF(I)
   43 CONTINUE
      RR=R(I)
      ESUM=SL5
      TEST=PI*SIGMA*(2.0*R(I)*R(I)+PI*A(I)*R(I)+A(I)*A(I)-(V*TIME(I)+
     1A(I))*(D-V*TIME(I)-A(I)))-ESUM
C     TEST DOES SURFACE ENERGY OF TABULAR BODY EQUAL INITIAL ENERGY
      IF(TEST.LT.TESTC) GO TO 100
      IEND=I
C
```

```
C      CALCULATION OF MAXIMUM PRESSURE UNDER IMPACTING DROP
C      IN POUNDS PER SQUARE INCH ABSOLUTE
C      ASSUMING PARABOLIC PRESSURE DISTRIBUTION UNDER DROP
       DO 200 I=1,IEND
       PC=14.696+(2.0*1.4504*F(I))/(PI*R(I)*R(I)*100000.0)
       IF(PC.LE.PMAX) GO TO 731
       II=I
       PMAX=PC
  731 CONTINUE
  200   CONTINUE
C
C      PERCENT CHANGE IN DIAMETER FOR SMALL CHANGES IN DIAMETER
       DVOLEQ=QTOTAL(IEND)/(LAMBDA*RHO)
       PEVAP=(200.0*DVOLEQ)/(PI*(D**3.0))
C
C      DIMENSIONALIZATION OF VARIABLES
C
       AG=(D-A(IEND))/(V*D)
       FG=RHO*D*D*V*V
       DO 37 I=1,IEND
       TIME(I)=TIME(I)/TIME(IEND)
       R(I)=R(I)/D
       A(I)=A(I)/D
       F(I)=F(I)/FG
   37 CONTINUE
       WRITE(6,956)
       WRITE(6,143) RUN,WEBER
C
       WRITE(6,954)
       WRITE(6,948)
C
C      LINEAR INTERPOLATION ROUTINE
C
       TTIM=0.0
       I=0
   75 TTIM=TTIM+0.1
   76 I=I+1
       IF(TIME(I).GE.TTIM) GO TO 77
       GO TO 76
   77 TPROD=(TTIM-TIME(I-1))/(TIME(I)-TIME(I-1))
       CAA=A(I-1)+TPROD*(A(I)-A(I-1))
       CRR=R(I-1)+TPROD*(R(I)-R(I-1))
       CFF=F(I-1)+TPROD*(F(I)-F(I-1))
       WRITE(6,949) I,TTIM,CRR,CAA,CFF
       IF(TTIM.GT.0.99) GO TO 22
       GO TO 75
   22 CONTINUE
       WRITE(6,968) II,PMAX
       WRITE(6,975)
       WRITE(6,976) (I,FILM(I),HSURF(I),I=1,IEND,10)
       WRITE(6,954)
```

```
      WRITE(6,141)PEVAP
      STEMP=212.0+DTEMP*9.0/5.0
      WRITE(6,983) STEMP
      WRITE(6,112)
C
C
   78 CONTINUE
   99 STOP
C
C
  112 FORMAT(1H1)
  141 FORMAT(3X,27HPERCENT CHANGE IN DIAMETER=,F8.4///)
  142 FORMAT(25X,8HDVCDTI=,E20.7/)
  143 FORMAT(2X,11HRUN NUMBER ,F10.1,5X,20HWEBER NUMBER EQUALS ,F10.5//)
  355 FORMAT(8F10.5)
  356 FORMAT(F15.5)
  900 FORMAT(2F10.5,2I5)
  948 FORMAT(3X,1HI,10X,
     1                     7HTIME(I),15X,4HR(I),16X,4HA(I),16X,4HF(I))
  949 FORMAT(I5,5E20.7)
  950 FORMAT(5E20.7)
  951 FORMAT(//I10,E20.7)
  952 FORMAT(6E20.7)
  954 FORMAT(//)
  955 FORMAT(20X,2I10)
  956 FORMAT(////)
  957 FORMAT(5E20.7,I10)
  958 FORMAT(2E20.7)
  961 FORMAT(1X,1H*)
  962 FORMAT(1X,2H**)
  963 FORMAT(1X,3H***)
  968 FORMAT(2H0 ,I5,5X,5HPMAX=,F10.4,2X,4HPSIA//)
  970 FORMAT(3I10,F10.5)
  971 FORMAT(3F15.5)
  975 FORMAT(3X,1HI,6X,20HFILM THICKNESS (CM.),6X,5HHSURF,/)
  976 FORMAT(I5,2E20.7)
  983 FORMAT(3X,20HSURFACE TEMPERATURE=,F10.1,2X,18HDEGREES FAHRENHEIT)
      END




      FUNCTION FN(A,TIME,DADT)
      DIMENSION TDIFF(300),F(300)
      REAL LAMBDA
      REAL MU
      COMMON RHO,GC,V,PI,D,SIGMA,CSI,JKL,CA,CB,CC,CD,CE,CF,CG,CH,CI,CJ,
     1TABSEI,DA,DT,LAMBDA,THRMCV,IDIFF,F,CPV,RHOV,RR,ESUM,MU,BD,SL5,PD,
     2VREF,EC
```

```
      QC=V*TIME+A
      SC=D-QC
      UC=QC*QC*(1.5*D-QC)
      DADT=(A-DA)/DT
C     SC AND A MUST ALWAYS BE GREATER THAN ZERO
   21 RRRR=(A*A*CB+(UC/(3.0*A)))
      IF(RRRR.GT.0.0) GO TO 85
      R=0.0
      GO TO 86
   85 R=-CA*A+SQRT(RRRR)
      IF(R.LE.0.0) R=0.0
   86 CONTINUE
      SL1=QC*CC
      SL2=CD*UC
      SL3=CE*(2.0*R*R+PI*A*R+A*A-QC*SC)
      IF(SC.GT.0.0) GO TO 88
      SL4=0.0
      Q=DADT
      RSQ=QC*SC
      P=RSQ*(V+Q)
      GO TO 87
   88 Q=DADT
      RSQ=QC*SC
      P=RSQ*(V+Q)
      S=R+(A/3.0)
      THETA=R**2
      IF(THETA.GT.RSQ) GO TO 84
      SL4=(CF/(4.0*A))*((THETA*V)**2)
      GO TO 87
   84 CONTINUE
      SL4=(CF/A)*((((RSQ*V)**2)/4.0)+P*P*ALOG(S/SQRT(RSQ))-P*Q*(S*S-RSQ
     1+Q*Q*(((S**4)-RSQ*RSQ)/4.0))
   87 CONTINUE
      F(I)=BD*P
      CH=F(I)
      IF(F(I).LE.0.0) FD=0.0
      IF(F(I).LE.0.0) GO TO 90
      TRI=1.0/(1.0-CPV*TDIFF(I)/(6.0*LAMBDA))
      BC=0.48714
      FD=(4.0*BC/3.0)*(((4.0*PI*MU*THRMCV*TRI*IDIFF(I)*(F(I)**3   ))/
     1(0.172*LAMBDA*GC*RHOV))**0.25)
      CJ=RSQ
   90 SL5=(R-RR)*FD+ESUM
      FN=SL1+SL2-SL3-SL4+SL5
      RETURN
      END
```

242

```
C     SOLUTION OF SIMILARITY TRANSFORMED EQUATIONS FOR
C              FLOW OF VAPOUR UNDERNEATH DROP
C
      PROGRAM ASSEMBLED BY W.F.PETRYSCHUK
C
C     INPUT INFORMATION
C     CARD ONE- NUMBER OF CASES FORMAT (10I8)
C     CARD TWO- 5, NO. OF OUTPUTS LT 500, NO. OF ITERAIIONS
C     BETWEEN OUTPUTS    FORMAT(10I8)
C     CARD THREE D2PHI(0), DEL STEP LENGTH   FORMAT(2F10.5)
C
C     OUTPUT INFORMATION
C     DEL,PHI,DPHI,PSI,DEL*PHI, AS TITLED ON OUTPUT
C
      DIMENSION Y(5,500),YI(10),YY(5),YK(5)
      EXTERNAL F
      READ(5,999) NCASE
      DO 2 KPROB=1,NCASE
      READ (5,999) N1,N2,N3
      DO 3 I=1,5
    3 YI(I)=0.0
      READ(5,998) YI(3),H
      WRITE(6,996) KPROB,NCASE,YI(3)
      CALL RKG(F,Y,N1,N2,N3,YI,H)
      DO 1 J=1,N2
      Z=Y(K,J)*Y(1,J)
    1 WRITE(6,997) Y(5,J),Y(1,J),Y(2,J) ,Y(3,J)
    2 CONTINUE
      STOP
  999 FORMAT(10I8)
  998 FORMAT(5F10.5)
  997 FORMAT(25X,F20.4,4F20.5)
  996 FORMAT(1H1,50X,19HTHIS IS CASE NUMBER,I3,2X,2HOF,I3/29H
     1    INITIAL CONDITION FOR D2PHI,F8.4//40X,3HDEL,17X,3HPHI,
     216X,4HDPHI,14X,5HDDPHI)
      END



      SUBROUTINE F(YY,YK)
      DIMENSION YY(5),YK(5)
      IF(YK(1).LT.(-.1)) GO TO 1
      YK(1)=YY(2)
      YK(2)=YY(3)
      YK(3)=YY(2)**2-2.0*YY(1)*YY(3)-1.0
      YK(4)=-YY(3)-2.0*YY(1)*YY(2)
      YK(5)=1.0
    1 RETURN
      END
```

243

```
C     PROGRAM FOR COMPUTATION OF TOTAL HEAT TRANSFER AND EQUIVALENT
C     VOLUME OF LIQUID EVAPOURATED FOR TRANSIENT DIRECT CONTACT
C     HEAT TRANSFER USING SEMI INFINITE MODEL
C
C     DROP OF WATER AT 212 DEG F
C     THERMAL PROPERTIES IN GRAM CALORIE CENTIMETER UNITS
C
      REAL LAMBDA,KL,KS,LVOL
      KL=0.001553
      KS=0.093
      ALPHAL=0.001553/(0.95*0.95)
      ALPHAS=0.093/(20.5*0.036)
      LAMBDA=539.55
      READ(5,906) J
      DO 50 N=1,J
      READ(5,900) TO,TBOIL,DTIME,TIMLIM
      READ(5,904) F,D
C
      AREA=3.14159*F*(D**2)/4.0
      DVOL=3.14159*(D**3)/6.0
      TSURF=(TO-TBOIL)/(1.0+(KL/KS)*SQRT(ALPHAS/ALPHAL))+TBOIL
      WRITE(6,905)
      WRITE(6,901) TSURF,TO
      WRITE(6,907) D,F
C
      TIME=0.0
      TDIFF=TSURF-TBOIL
      CONST=3.14159*ALPHAL
      WRITE(6,902)
   10 TIME=TIME+DTIME
      QTOTAL=2.0*KL*TDIFF*SQRT(TIME/CONST)
      LVOL=QTOTAL*AREA/LAMBDA
      PEVAP=LVOL*100.0/DVOL
      DELD=1.0-(1.0-LVOL/DVOL)**0.333333
      DELD=100.0*DELD
      WRITE(6,903) QTOTAL,PEVAP,TIME,DELD
      IF(TIME.LE.TIMLIM) GO TO 10
   50 CONTINUE
      STOP
  900 FORMAT(4F15.5)
  901 FORMAT(3X,13HSURFACE TEMP=,F15.5,3X,11HMETAL TEMP=,F15.5/)
  902 FORMAT(12X,18HTOTAL HT/UNIT AREA,13X,9HPCT.EVAP.,17X,4HTIME,
     119X,9HPCT. DD/D,/)
  903 FORMAT(10X,F15.5,10X,F15.5,10X,F15.5,10X,F15.5)
  904 FORMAT(2F15.5)
  905 FORMAT(1H1)
  906 FORMAT(I5)
  907 FORMAT(3X,11HDROP DIAM.=,F10.5,5X,27HFRACTION OF CSA IN CONTACT=,
     1F10.5/)
      END
```

```
C     ANALYSIS OF DATA FROM EXPERIMENTS ON DROPLET BOUNCE OFF A PLATE
C
C     THE PROGRAM IS DESIGNED TO CALCULATE THREE RESULTS FROM ONE SET
C     OF EXPERIMENTAL MEASUREMENTS- THE MEAN AND THE TWO 95 PERCENT
C     CONFIDENCE LIMITS CALCULATED FROM THE EXPERIMENTAL DATA.
C
C         INPUT VARIABLES DEFINED
C     RN-EXPERIMENT NUMBER (DECIMAL NUMBER)
C     THREE EXPERIMENT NUMBERS ARE USED FOR EACH SET OF MEASUREMENTS
C     TEMP IS THE MEASURED TARGET SURFACE TEMPERATURE IN DEGREES F.
C     PRESS IS THE DROP PROJECTOR AIR PRESSURE IN PSIG.
C     APF-DROP ADVANCE PER FRAME ON FILM IN INCHES
C     F IS THE FRAME FREQUENCY IN FRAMES PER SECOND
C     SPRAYD(N) IS THE ESTIMATED AVERAGE DIAMETER OF SPRAY DROPS
C     SPRAY(N) IS THE NUMBER OF SPRAY DROPS LOST
C     L IS THE NUMBER OF DROPS CAUGHT
C     ALPHA IS AN INPUT CONTROL NUMBER(DECIMAL NUMBER)
C     DAF- DROP DIAMETER ON FILM IN INCHES
C     CDF-DIAMETER OF IMAGE OF CAUGHT DROP IN INCHES
C     PROGRAM ACCOMMODATES A MAXIMUM OF FIVE CAUGHT DROPS
C     CR-ACTUAL DIAMETER OF CALIBRATION ROD IN INCHES
C     CSF-SIZE ON FILM OF 0.020 SECTION OF MICROSCALE IN INCHES
C     A MAXIMUM OF 200 EXPERIMENTS CAN BE HANDLED AT ONE TIME
C     M IS THE TOTAL NUMBER OF EXPERIMENTS TO BE CALCULATED AT THIS TIME
C             CALCULATED VARIABLES DEFINED
C     DA(I) IN MICRONS--APPROACH DIAMETER
C     V(I) IN FT/SEC --APPROACH VELOCITY
C     CD(I,N) IN MICRONS--DIAMETER OF DROPS CAUGHT
C     EQCD(I) IN MICRONS--VOLUME EQUIV. DIAM. OF ALL DROPS CAUGHT
C     PERCT DIFF IS THE DIFFERENCE BETWEEN THE DROP DIAMETER
C     APPROACH AND THE COMBINED DIAMETER OFTHE DROPS CAUGHT PLUS
C     ESTIMATED SPRAY LOSS, EXPRESSED AS A PERCENTAGE OF THE DIAMETER
C     ON APPROACH
C     WEB(I)--WEBER NUMBER
C     REN(I)-- REYNOLDS NUMBER
C     DMOM IS DROP MOMENTUM IN GM.CM./SEC.
C     TEMP-SURFACE TEMPERATURE IN DEGREES FAHRENHEIT
C     PRESS-DROP PROJECTOR AIR PRESSURE IN PSIG
C
C         LIQUID PROPERTIES
C     VISC-VISCOSITY IN CENTIPOISE
C     SIGMA= SURFACE TENSION IN DYNES/CENTIMETER
C     RHO-DENSITY IN GRAMS/CUBIC CENTIMETER
C
C             PROGRAM FOLLOWS
      DIMENSION CDF(350,5),RN(350),TEMP(350),PRESS(350)
      DIMENSION DAF(350),APF(350),F(350),CR(350),CRF(350),CSF(350)
      DIMENSION DA(350),V(350),CD(350,5) ,EQCD(350),WEB(350),REN(350)
      DIMENSION TAU(350),SPRAYD(350),SPRAYN(350)
      DO 88 I=1,350
      RN(I)=0.0
      SPRAYD(I)=0.0
```

```
      SPRAYN(I)=0.0
      DAF(I)=0.0
      CD(I,1)=0.0
      CD(I,2)=0.0
      CD(I,3)=0.0
   88 CONTINUE
      READ (5,999) M,VISC,SIGMA,RHO
      DO 100 I=1,M,3
      READ(5,998) RN(I),RN(I+1),RN(I+2),TEMP(I),PRESS(I)
      READ(5,998) APF(I),F(I),SPRAYN(I),SPRAYD(I)
      READ(5,998)DAF(I),DAF(I+1),DAF(I+2)
      READ(5,999)L,ALPHA
      WRITE(6,223) RN(I),APF(I),DAF(I),ALPHA,L
  223 FORMAT(4F15.5,I5)
C     IF CAUGHT DROP UNIFORM SET ALPHA=2.0 AND INPUT ONE SET OF
C     CAUGHT DROP DIAMETERS
C     IF CAUGHT DROP NOT UNIFORM SET ALPHA=0.0 AND INPUT THREE SETS OF
C     CAUGHT DROP DIAMETERS
      IF(L.LE.1) L=1
      READ(5,998)(CDF(I,N),N=1,L)
      IF(ALPHA.GE.1.0) GO TO 37
      READ(5,998)(CDF(I+1,N),N=1,L)
      READ(5,998)(CDF(I+2,N),N=1,L)
   35 READ(5,998)CR(I),CSF(I),CRF(I)
      GO TO 38
   37 DO 48 JJ=1,L
      CDF(I+1,JJ)=CDF(I,JJ)
      CDF(I+2,JJ)=CDF(I,JJ)
   48 CONTINUE
      GO TO 35
   38 CONTINUE
      WRITE(6,223) CDF(I,1),CDF(I+1,1),CDF(I+2,1),CR(I),I
      DO 22 KK=1,2
      LL=I+KK
      TEMP(LL)=TEMP(I)
      PRESS(LL)=PRESS(I)
      SPRAYN(LL)=SPRAYN(I)
      SPRAYD(LL)=SPRAYD(I)
      CSF(LL)=CSF(I)
      APF(LL)=APF(I)
      F(LL)=F(I)
      CR(LL)=CR(I)
      CRF(LL)=CRF(I)
   22 CONTINUE
      NN=L+1
      KL=I+2
      DO 10 K=I,KL
      IF(SPRAYN(K).LE.0.1) GO TO 5
      CDF(K,NN )=(SPRAYN(K)*((SPRAYD(K))**3))**0.333333
      GO TO 6
    5 CDF(K,NN)=0.0
```

```
    6 CONTINUE
      SUM=0.0
      DO 20 MM=1,NN
      CD(K,MM)=CDF(K,MM)*508.0/CSF(K)
      SUM=SUM+((CD(K,MM))**3.0)
   20 CONTINUE
      IF(SUM.LE.0.0) GO TO 4
      EQCD(K)=(SUM)**0.333333
      GO TO 10
    4 EQCD(K)=0.0
   10 CONTINUE
  100 CONTINUE
      DO 55 I=1,M
      DA(I)= DAF(I)*CR(I)*25400./CRF(I)
      V(I)=APF(I)*CR(I)*F(I)/(CRF(I)*12.0)
      WEB(I)=(144.0*2.54*2.54*RHO*DA(I)*V(I)*V(I))/(10000.0*SIGMA)
      REN(I)=(144.*2.54**2* DA(I))*V(I)*RHO)/(6.72*453.59* VISC)
      TAU(I)=3.14159*(((RHO*(DA(I)**3.0))/(16.0*SIGMA))**0.5)
      TAU(I)=TAU(I)/1000000.0
   55 CONTINUE
      I=0
      DO 400 II=1,M,10
      WRITE(6,995)
      DO 500 J=1,10
      WRITE(6,994)
      DO 600 K=1,3
      N=K+(J-1)*3+(II-1)*3
      I=I+1
      DIFF = (DA(I) - EQCD(I))*100.0/DA(I)
      WRITE(6,997) RN(I),DA(I),V(I),EQCD(I),DIFF,
     1 CD(I,1),CD(I,2),CD(I,3),WEB(I),REN(I),TEMP(I),PRESS(I),TAU(I)
      IF(N.GE.M) GO TO 401
  600 CONTINUE
  500 CONTINUE
      WRITE(6,994)
  400 CONTINUE
  401 WRITE(6,994)
      WRITE(6,992)
      STOP
  992 FORMAT(1H1)
  994 FORMAT(3X,128(1H-)/)
  995 FORMAT(1H1,3X,3HRUN,7X,6HAPPRCH,8H  APPRCH,10H VOL-EQUIV,3X,
     1 5HPRCNT,15X,8HDIAMETER,12X,5HWEBER,6X,8HREYNOLDS
     9,3X,4HTEMP,8X,5HPRESS,5X,3HTAU/4X,3HNO.,8X,
     2 5HDIAM.,4X,4HVEL.,5X,5HDIAM.,4X,4HDIFF,16X,6HCAUGHT,12X,
     3 6HNUMBER,6X,6HNUMBER//)
  997 FORMAT(2X,F6.1,F10.1,F8.1,F11.1,F9.1,3F9.1,F13.5,F13.0,F8.1,F12.1,
     1F12.5)
  998 FORMAT(5F15.5)
  999 FORMAT(I5,3F15.5)
      END
```

```
C     ROUTINE FOR CALCULATION OF DIAMETER MEASUREMENT MEAN AND
C     95 PERCENT CONFIDENCE LIMIT USING ONE SIDED STUDENTS T TEST
C
C     READ IN T VALUES FOR 1 TO 25 DEGREES OF FREEDOM FOR 95 PERCENT
C     CONFIDENCE LIMIT
      DIMENSION T(50),DATA(50)
      REAL MEAN
      READ(5,999)(T(N),N=1,25 )
C
C     READ J, NUMBER OF SETS OF READINGS
      READ(5,998) J
      WRITE(6,997)
      DO 10 I=1,J
C     READ L, RUN NUMBER AND M, NUMBER OF READINGS
      READ(5,998) L,M
      READ(5,999)(DATA(N),N=1,M)
      SUM=0.0
      DO 20 N=1,M
      SUM=SUM+DATA(N)
   20 CONTINUE
      A=M
      MEAN=SUM/A
      S=0.0
      DO 30 N=1,M
      S=S+(DATA(N)-MEAN)**2
   30 CONTINUE
      SXBAR=SQRT(S/(A*(A-1.0)))
C     SXBAR IS THE ESTIMATE OF THE STANDARD DEVIATION OF READING MEANS
      TTEST=T(M-1)
      CLIM=TTEST*SXBAR
      H=MEAN+CLIM
      P=MEAN-CLIM
      WRITE(6,500) L,M
      WRITE(6,501) MEAN,H,P,SXBAR
      WRITE(7,988) P,MEAN,H
   10 CONTINUE
      WRITE(6,997)
      STOP
  988 FORMAT(3F15.5)
  997 FORMAT(1H1)
  998 FORMAT(10I8)
  999 FORMAT(10F8.5)
  500 FORMAT(2X,8HRUN NO. ,I5,2X,I5,9H READINGS)
  501 FORMAT(2X,5HMEAN=,F10.4,2X,2HH=,F10.4,2X,2HL=,F10.4,2X,
     16HSXBAR=,F10.4//)
      END
```

```
C     CALCULATION OF LINEAR REGRESSION CONSTANTS AND
C     CORRELATION COEFFICIENTS FOR TWO SIMULTANEOUS DATA SETS
C
      DIMENSION X(100),Y(100),Z(100)
      READ(5,900) N,ANO
      READ(5,901)(Y(I),X(I),Z(I),I=1,N)
      A=0.0
      B=0.0
      C=0.0
      D=0.0
      E=0.0
      F=0.0
      G=0.0
      BA=0.0
C
      DO 10 I=1,N
      A=A+Y(I)
      B=B+X(I)
      C=C+Z(I)
      D=D+X(I)**2
      E=E+Z(I)**2
      BA=BA+Y(I)**2
      F=F+X(I)*Y(I)
      G=G+Z(I)*Y(I)
   10 CONTINUE
C
      H=D-(B**2)/ANO
      HZ=E-(C**2)/ANO
      AA=F-A*B/ANO
      AZ=G-A*C/ANO
      XBAR=B/ANO
      YBAR=A/ANO
      ZBAR=C/ANO
      COEFZ=AZ/HZ
      COEFX=AA/H
      CONSTZ=YBAR-COEFZ*ZBAR
      CONSTX=YBAR-COEFX*XBAR
      BB=BA-(A**2)/ANO
      RX=AA/SQRT(H*BB)
      RZ=AZ/SQRT(HZ*BB)
C
      WRITE(6,902) CONSTX,COEFX,RX
      WRITE(6,902) CONSTZ,COEFZ,RZ
      STOP
  900 FORMAT(I5,F10.5)
  901 FORMAT(3F15.5)
  902 FORMAT(3X,2HA=,F20.7,5X,2HB=,F20.7,5X,2HR=,F20.7/)
      END
```

APPENDIX M   Nomenclature

A	Thickness of the tabular body of fluid formed on collision (cm.).
AEND	Thickness of the tabular body of fluid at the end of the impact period (cm.).
AREA	Area of contact between the Drop Liquid and the Target Surface (sq.cm.).
a	Proportionality constant (1/sec.).
a'	Thermal diffusivity sq.cm./sec.).
Cp	Specific Heat at Constant Pressure (cal./gm°C.).
D	Drop Diameter (cm.).
d	Height of spherical segment (cm.).
de	Maximum diameter of pendant drop in horizontal direction (cm.).
ds	Diameter of pendant drop in the horizontal direction a distance de from the bottom of the drop.
$\triangle$ E	Energy contribution due to shear stress (dyne cm.)
F	Force with which the impacting drop pushes on the surface (dynes).
g	Gravitational acceleration (cm./sec.^{2}).
g_c	Gravitational constant (gm.cm./dyne sec.^{2}).
h	Heat transfer coefficient (cal./sec.cm.^{2}°C.).
k	Thermal conductivity of the vapour (cal./cm.sec.°C.).
K	Thermal conductivity of the vapour(cal./cm.sec°C.).
KL	Thermal conductivity of the drop liquid (cal./cm.sec.°C.).
KS	Thermal conductivity of the target surface material (cal./cm.sec.°C.).
	Distance from the top of the drop to the surface (cm.).
P	Manipulation variable (cm.^{3}/sec.).
P'	Pressure in the vapour film (dynes/sq.cm.).
Pr	Prandtl Number for the Drop in the Steam Atmosphere.
Q	Rate of change of A with time (cm./sec.).
Q_o	Total Heat Loss from the drop in travelling from thetarget surface to the surface of the oil (cal.).

Q'	Total Heat Transferred to the drop at a time t after impact with the surface (cal.).
r	Radial distance (cm.).
$\curlywedge$	Radial distance to the line of contact between the drop and the upper surface of the tabular body (cm.).
r_o	Drop radius (cm.).
R	Radius of the circular area of the tabular body of fluid adjacent to the surface (cm.).
Re	Reynolds Number for the Drop Falling in a Steam Atmosphere.
S	Distance A or R (cm.).
S·t	Value of Students t (statistical test).
t	Time after drop contact with the target surface (sec.).
t'	Error in surface temperature measurement (°C.).
T_s	Constant Interface Temperature (°C.).
T_m	Bulk Temperature of the Target Surface (°C.).
T_L	Bulk Temperature of the Drop Liquid (°C.).
T_R	Dimensionless Time (sec.).
T_o	Initial Average Drop Temperature on rebound (°C.).
T_{oo}	Average Drop Temperature as the drop enters the oil (°C.).
$\triangle T$	Temperature Difference between the surface and the drop (°C.).
U	Radial Velocity of fluid in the tabular body (cm/sec)
U'	Radial Velocity of fluid in the tabular body at r = (cm./sec.).
u	Vapour Velocity in the radial direction (cm/sec)
V	Drop Velocity (cm./sec.).
VOL	Volume of the Drop (ml.).
V_A	Approach Velocity of the Drop (cm./sec.).
V_R	Recession Velocity of the Drop (cm./sec.).
w	Vapour Velocity in the axial direction (cm/sec).
z	Axial Distance from the surface (cm.).

Greek Letters

$\propto$	Proportionality Constant (1/sec.).
$\propto_s$	Thermal Diffusivity of the Surface Material (sq.cm./sec.).
$\propto_L$	Thermal Diffusivity of the Drop Liquid(sq.cm./sec.).
δ	Vapour Film Thickness (cm.)
σ	Drop Liquid - Vapour Surface Tension(dynes/cm.).
$\wedge$	Sensible Heat Correction Factor.
λ	Drop Liquid Latent Heat (cal./gm.).
π	Constant = 3.14159
ϕ, ϕ', ϕ''	Dimensionless transformation Variables (4).
ψ, ψ'	Dimensionless transformation Variables (4).
ρ	Drop liquid density (gm./cc.)
ρ_g	Drop-liquid vapour density (gm./cc.).
ρ_o	Vapour density (gm./cc.).
μ_a	Drop liquid viscosity (gm./cm.sec).
μ_g	Drop-liquid vapour viscosity (gm./cm.sec.)
μ_o	Vapour viscosity (gm./cm.sec.)
ν	Kinematic viscosity (sq.cm./sec.).
τ_r	Surface Shear Stress (dynes/sq.cm.).
ζ	Dimensionless coordinate.
θ	Time of Travel of the Drop from the Target surface to the oil (sec.).

APPENDIX N   Equipment and Material Details

(Sources of Supply Given Where of Interest)

Substage Microscope: Officine Galileo No. 125418 with liquid source.

Supplier of Lamps for Microscope:

Microscope Lenses: Objective: Bausch and Lamb 48 mm. n.a. 0.08.

Eyepiece: Bausch and Lamb low Ultraplane.

Camera: Pentax Sia, Serial No. 670701 used with a Pentax microscope adaptor and a Pentax magnifier clipped to the eyepiece.

Film: Illford FP 3 100 ASA tungsten light. 35 mm. Purchased in 100 foot rolls and loaded in 30 exposure lengths from a daylight loader into Pentax casettes.

Silicone Oil: Dow Corning Silicone fluid: mixture 7 parts 200 fluid (20 cs.) and 1 part 555 fluid. Available from Dow Corning Silicones Limited, 1 Tippet Road., Downsview P.O., Toronto, Ontario.

Silicone Rubber: General Electric RTV 108 - Translucent. Available from local wholesale electrical appliance dealers.

Oven: Labline Natural circulation oven, 3 1/2 cubic foot size, 1200 watts. For supplier details see McMaster University Chem. Eng. reference number 78.

Film Measuring Microscope: Hilger and Watts Engineers Microscope Unit C, Serial Number 97972, England. For supplier details see McMaster University Eng. Gen. ref. no. 10022.

Air Pressure Filter Regulator: Conoflow Model FH 2051, 0-125 psig. regulation. Supplier Baker Instruments Limited, 185 Davenport Rd., Toronto 5, Ontario.

Air Pressure Gauge: Wekster - 0-60 psig., 1 psi. subdivision.
        Air calibrated. 6 inch face.
        For supplier details see McMaster Chem. Eng. Ref.
        No. 114.

Variable Transformers : -

Target Heater Control: Amertran Serial Number N.P. 32322.
        Input 115 V., 15 amps; output 0-150 V., 30 amperes.

Other Heaters controlled using form 1 KVA Superior Electric
        "Powerstate" and two 200 VA Ohurite Cat. VT-2F
        variable transformers.

Target Heater Transformer: Ignal Transformer. Wires for
        output 12 V., 100 amperes.
        Supplied by Lectronic Research Laboratories, 715
        Arch St., Philadelphia 6, Pa., U.S.A.

Spot Lamp: Burton Medio-Quip Co. Model 1200, 100 watts.
        Supplied by Fisher Scientific, 184 Railside Rd.,
        Don Mills, Ontario.

Telescope: Griffin and George Ltd., London England.
        Standard cathetometer telescope with 1 1/2 inch
        objective extension and modification for scaled
        graticule.

Solenoid Valve: Asco 1/8 inch orifice 1/4 inch pipe connections
        Cat. No. 826222. Rated differential pressure, 130 psi.
        Supplier: Davis Automatic Controls Limited
        4251 Dundas St., W., Toronto 18, Ontario.

Glycol Circulating Unit: Haake Model Fe, Serial No. 621730
        Contact thermometer (thermostat) 0-100°C., Heater 500
        watts capacity.
        Supplied by Fisher Scientific, 184 Railside Rd.,
        Don Mills, Ontario.

Heater Units: Cartridge Heaters: 75 watts, 120 volts
        3/8" diameter Cat. No. C203.
        Base Heater: 500 watts. 3 inch radius, circular
                        loop, Steel Sheath.
        Supplied by the Canadian Chromalox Company Ltd.,
        210 Rescale Blvd., Rexdale P.O., Toronto, Ontario.

Viewing Window Glasses:: 3/4 diameter X 1/8 inch thick
circular optical quality discs.
Supplied by Swift Lubricator Company, Elmyra,
N.Y., U.S.A.

Drop Catcher Glass: Optically flat 3 1/4 x 4 lantan slide
glass cut with a carbide tip tool and ground with
emery paper (on metallurgical polishing set).

SC-87 Drysil Anti Wetting Agent (Dimethyl-dichloro-silane)
obtained from the Industrial Products Department,
Canadian General Electric, 940 Lansdowne Ave.,
Toronto 4, Ontario.

High Speed Motion Picture Camera: Fastax WF4ST, Serial
No. 416 ST3. Controlled by Fastax Goose Control
Unit Model WF-358 Ser. No. 1339. Time marking on
film obtained using Wollensak Pulse Generator.
Source: Minnesota Mining and Manufacturing Co.,
Revere-Wollensak Division,
850 Hudson Avenue,
Rochester, N.Y., U.S.A.

Thermocouple Wire:

Target Surface: 6 inch length, 1/25 inch OD Ceramo PT-20%
Rh Sheath.
Pt-10% Rh thermocouple 36 gauge wire.
Supplier, Thermo Electric (Canada) Ltd.,
Brampton, Ontario.

TABLES OF DATA

255

Table I - Experimental Measurements

Surface Temperature (°F)	Drop Diameter (microns)	Drop Velocity (feet/second)	Measured Percent Change in Diameter	Weber Number	Reynolds Number	Experimental Reference Number
323	501	4.1	-4.4	12.6	2110	187
331	432	4.1	-4.7	11.0	1820	184
333	540	4.5	+0.2	16.6	2500	185
334	415	4.0	-2.7	10.1	1720	186
336	392	3.4	-0.3	6.9	1380	182
337	393	7.1	-7.8	29.5	2860	262
341	462	3.9	+0.1	10.4	1840	183
344	291	6.3	+1.1	17.6	1900	259
355	492	3.4	-0.7	8.6	1730	196
357	344	7.0	-1.0	25.6	2490	261
362	680	4.9	-0.7	25.0	3450	205
364	346	6.3	-4.2	20.9	2260	267
366	358	5.0	0.0	13.4	1830	298
366	348	5.7	+2.3	17.1	2040	299
367	705	5.1	+2.2	27.2	3700	209

Table I - Continued

Surface Temperature (°F)	Drop Diameter (micron)	Drop Velocity (feet/second)	Measured Percent Change in Diameter	Weber Number	Reynolds Number	Experimental Reference Number
367	536	8.5	-2.6	57.8	4660	300
368	687	4.4	-2.0	19.8	3090	203
368	665	5.3	-0.2	28.4	3640	206
369	617	4.4	+0.7	18.4	2820	208
373						269
373	686	5.2	-4.3	28.5	3700	204
374	601	4.0	+0.2	14.7	2500	207
374	373	6.7	-2.9	25.7	2590	270
375	589	4.3	+2.6	16.1	2580	202
375	491	4.7	-0.2	16.0	2350	210
378	537	4.5	-2.4	16.7	2510	211
378	668	4.1	+0.5	16.6	2790	213
380	359	6.6	-1.2	23.6	2440	260
392	462	2.5	-0.8	4.4	1200	175
392	352	6.7	-6.6	24.2	2450	263

Table I - Continued

Surface Temperature (°F)	Drop Diameter (micron)	Drop Velocity (feet/second)	Measured Percent Change in Diameter	Weber Number	Reynolds Number	Experimental Reference Number
394	375	4.3	-3.0	10.6	1670	264
395	372	7.5	-2.9	31.5	2870	252
398	550	4.4	-0.9	16.1	2500	177
400	468	3.8	-0.5	10.2	1830	174
401	447	2.2	-0.7	3.4	1030	176
403	493	3.5	0.0	9.1	1772	179
404	581	4.4	-19.3	16.9	2620	172
407	521	4.4	-1.1	14.1	2350	171
408	457	4.1	-6.8	11.6	1930	170
408	494	4.0	+0.7	11.9	2030	178
408	361	5.7	-1.9	17.5	2110	255
409	418	5.6	+0.2	19.9	2420	290
410	392	6.4	-0.5	24.6	2600	291
410	372	4.7	-0.3	12.2	1790	292
410	338	5.2	-2.2	13.6	1790	254

Table I - Continued

Surface Temperature (°F)	Drop Diameter (micron)	Drop Velocity (feet/second)	Measured Percent Change in Diameter	Weber Number	Reynolds Number	Experimental Reference Number
410	458	6.3	-3.3	27.2	2960	293
410	375	6.6	-7.0	25.0	2560	294
413	351	5.2	-5.5	14.4	1880	253
438	549	8.2	-6.0	55.2	4610	235
445	643	4.5	-0.8	19.8	2990	240
446	462	3.0	-0.9	6.2	1420	245
450	394	5.2	-3.5	15.9	2100	287
454	309	6.6	-7.9	20.6	2110	284
455	632	5.6	-3.1	30.2	4660	239
456	477	4.1	+0.2	12.0	2010	241
457	325	5.9	-11.1	16.9	1970	283
460	316	4.5	-2.0	9.7	1470	250
462	435	4.2	+0.2	11.7	1890	242
463	313	4.9	-3.0	11.3	1570	251
466	581	5.9	-0.2	30.3	3520	230

Table I - Continued

Surface Temperature (°F)	Drop Diameter (microns)	Drop Velocity (feet/second)	Measured Percent Change in Diameter	Weber Number	Reynolds Number	Experimental Reference Number
469	527	7.6	-4.7	46.0	4130	232
470	576	4.5	+0.8	17.3	2640	234
471	323	6.5	-3.6	20.8	2170	249
472	494	6.4	+0.8	30.8	3270	231
479	523	7.9	-6.2	49.3	4250	233
494	329	6.3	-10.2	19.5	2120	295
513	337	7.1	-17.3	25.8	2470	296
515	376	4.2	- 1.0	9.9	1620	297
523	477	4.6	+1.6	15.5	2280	144
523	355	5.3	-1.0	15.0	1930	279
525	445	2.6	-1.9	4.5	1190	135
525	556	4.4	+1.6	16.0	2490	140
526	702	4.7	-4.3	23.6	3410	147
527	565	6.9	+0.9	40.2	3990	227
528	674	4.9	+2.1	24.2	3380	148

Table I - Continued

Surface Temperature (°F)	Drop Diameter (microns)	Drop Velocity (feet/second)	Measured Percent Change in Diameter	Weber Number	Reynolds Number	Experimental Reference Number
533	588	4.1	-0.6	15.2	2510	138
533	570	3.3	+0.7	9.3	1930	225
534	514	2.6	+0.7	5.1	1360	137
539	561	4.4	-0.8	16.5	2550	149
539	606	5.9	+1.5	31.4	3660	220
539	575	6.4	+0.7	35.6	3790	226
541	546	4.2	-0.6	14.4	2350	150
544	551	4.2	-1.1	14.3	2360	152
547	534	8.3	-0.8	55.8	4570	229
687	652	4.8	-1.3	22.6	3220	166
691	525	4.3	-0.4	14.7	2330	165
692	613	4.2	+0.7	16.5	2670	164
702	572	4.2	+0.2	15.0	2460	169
704	545	4.5	-1.1	16.5	2520	167
705	595	4.4	+0.6	17.1	2670	161

Table I - Continued

Surface Temperature (°F)	Drop Diameter (microns)	Drop Velocity (feet/second)	Measured Percent Change in Diameter	Weber Number	Reynolds Number	Experimental Reference Number
705	525	4.3	-0.8	14.9	2350	168
709	584	3.3	-0.3	9.8	2010	162
713	622	4.7	+0.7	20.1	3030	156
713	596	3.1	-0.8	8.8	1920	163
714	671	4.9	-0.6	24.8	3420	159
725	568	4.3	-0.9	15.9	2520	160
872	556	3.7	-0.6	11.2	2090	194
880	536	2.0	+0.4	3.1	1090	193
890	384	7.5	+0.1	32.2	2950	273
895	317	6.0	-0.8	17.1	1950	275
895	329	5.0	+3.6	12.6	1710	278
898	302	5.5	+1.2	13.9	1720	277

Table II – <u>The Percent Change in Diameter during the Initial
Impact Period for a 400 Micron Drop, calculated using
the Dynamics and Vapour Film Heat Transfer Models.</u>

Surface Temperature	Percent Change in Diameter	Weber Number
260	0.004	2
400	0.012	2
600	0.017	2
800	0.020	2
1200	0.021	2
260	0.005	10
400	0.014	10
600	0.021	10
800	0.025	10
1200	0.026	10
260	0.005	30
400	0.014	30
600	0.020	30
800	0.024	30
1200	0.024	30

Table III - <u>Typical Calculated Deformation of a Drop during</u> <u>Impact, obtained by solution of the Impact</u> <u>Dynamics Model.</u>

Weber Number 10, Drop Size 400 microns, Surface Temperature 500°F

Dimensionless Time $(TV/CD-AEND)$	Radius in Contact (R/D)	Thickness of Tabular Body (A/D)	Force of Impact (F/ D^2V^2)	Film Thickness (microns)
0.1	0.29	0.01	0.89	-
0.2	0.37	0.16	1.50	6.5
0.3	0.40	0.23	1.75	-
0.4	0.42	0.30	1.70	7.2
0.5	0.43	0.36	1.44	-
0.6	0.42	0.40	1.09	8.0
0.7	0.41	0.44	0.70	-
0.8	0.42	0.45	0.39	9.8
0.9	0.42	0.46	0.17	-
1.0	0.42	0.46	0.00	-

Table IV - <u>Radius of the Area of the Drop in Contact with the Surface and Thickness of the Tabular Body at the End of the Impact Period, tabulated in order of increasing Weber Number, calculated using the Impact Dynamics Model.</u>

Weber Number	R/D	A/D
0.05	0.119	0.820
0.1	0.162	0.760
1.0	0.419	0.460
2.0	0.552	0.350
5.0	0.808	0.210
10.0	1.081	0.130
15.0	1.252	0.100
20.0	1.412	0.080
30.0	1.806	0.050

266

Table V - <u>Calculated Averages of Experimental Measurements</u>
<u>of Drop Diameter Change on Impact with a Hot</u>
<u>Surface</u>.

| Surface Temperature (°F) | | Percent Change in Diameter | | |
Range	Mean	Mean	Standard Deviation	Number of Measurements
323-341	333	-2.00	2.23	6
344-380	367	-1.23	2.50	19
438-479	461	-2.04	2.43	14
523-547	533	+0.19	2.01	16
687-725	705	-0.33	0.72	12
872-898	888	+0.65	1.62	6

Table VI - <u>Illustration of the Relation Between Drop
Diameter and Percent Change in Diameter
due to Evaporation During the Impact Period,
as Derived using the Impact Dynamics and
Vapour Film Heat Transfer Models.</u>

Weber Number 10

Surface Temperature (°F)	Percent Change in Diameter	
	For a 10 Micron Drop	For a 400 Micron Drop
260	0.008	0.005
300	0.014	0.009
400	0.022	0.014
500	0.028	0.018
600	0.036	0.021
700	0.039	0.024
800	0.041	0.025
1200	0.040	0.026

Table VII - Maximum Value of Pressure Beneath Impacting
             Drops Calculated at Intervals of Dimensionless
             Time Using Impact Dynamics and Vapour Film
             Heat Transfer Models.

Drop Diameter (Microns)	Surface Temperature (°F)	Maximum Pressure (psig)	Time Calculated	Total Number of Iterations
10	260	175	(44/79)	79
10	400	168	(44/79)	79
10	500	168	(44/79)	79
10	600	206	(1/78)	78
10	700	261	(1/78)	78
10	800	330	(1/78)	78
400	260	0.305	(10/54)	54
400	400	0.305	(11/54)	54
400	500	0.303	(11/54)	54
400	600	0.303	(11/54)	54
400	700	0.303	(10/54)	54
400	800	0.303	(11/54)	54

Table IX - <u>Typical Calculated Values of Confidence Limits</u>
<u>on Experimental Measurements of Change in</u>
<u>Diameter on Impact.</u>

Drop Diameter (Microns)	Measured Percent Change in Diameter	95 Percent Confidence Limit	Number of Measurements of Diameter before Impact	Experimental Reference Number
501	-4.1	-4.0 to -4.6	7	187
540	0.2	-0.7 to 0.9	10	185
462	-0.1	-0.4 to 0.2	18	183
343	-1.0	-1.1 to -0.8	12	261
358	0.0	-0.4 to 0.3	24	298
601	0.2	-0.6 to 1.0	9	207
687	-2.0	-2.8 to -1.3	12	203
492	-0.7	-1.8 to 0.5	12	196
705	2.2	1.0 to 3.5	6	209
523	-6.2	-4.8 to -7.5	14	233
359	-1.2	-1.6 to -0.9	12	260
384	0.1	0.5 to -0.3	6	273